ADTEC

Final Technical Report
Contract No. AF 30(602)-3495

HIGH POWER FERRITE PHASE SHIFTER

October, 1965

ADVANCED TECHNOLOGY CORPORATION

1830 YORK ROAD TIMONIUM, MARYLAND

HIGH POWER FERRITE PHASE SHIFTER

Prepared for

Rome Air Development Center
Air Force Systems Command
United States Air Force
Griffiss Air Force Base
New York

Final Technical Report
Contract No. AF 30(602)-3495
ARPA Order No 550
Program Code No 4730

October 1965

ADVANCED TECHNOLOGY CORPORATION
1830 York Road
Timonium, Maryland

Project Engineer: Frederick L. Wentworth

ABSTRACT

Theoretical estimates of phase shifter performance as a function of material parameters are presented by examining the results obtained from the small perturbation model used by Button and Lax and from the fully ferrite loaded, parallel plane waveguide model used by Suhl and Walker. The extension of Suhl's theory on nonlinear effects at high power by Fletcher and Silence is applied to relate the material parameters and operating frequency to the magnetic field required to avoid high power subsidiary resonance effects. Experiments designed to demonstrate the relationship of phase shift and loss characteristics to material parameters and configuration for longitudinally magnetized ferrites in rectangular waveguide are described. Polycrystalline ferrites with both cubic and hexagonal structures are examined. Of the hexagonal materials, both uniaxial and planar types with oriented anisotropy fields are discussed. The experimental work leading to the growth of extremely large single crystals of lithium ferrite and their electrical and magnetic properties are reported. Experiments which reduced the linewidth of lithium ferrite samples by heat treatment and polishing are described. High power tests to 100 kw peak are reported for waveguide configurations containing (1) single crystal lithium ferrite; (2) polycrystalline cubic structure, nickel ferrite; and (3) polycrystalline hexagonal structure nickel-cobalt "W" ferrite with its magnetic anisotropy oriented parallel to the applied magnetic field. These high power tests demonstrate that the nonlinear high power effects can be avoided by operating at magnetic fields above ferrimagnetic resonance as prescribed by Fletcher and Silence.

TABLE OF CONTENTS

LIST OF ILLUSTRATIONS

LIST OF ILLUSTRATIONS (Continued)

LIST OF ILLUSTRATIONS (Continued)

I. INTRODUCTION

The contractor has proposed to develop a high power, 360° reciprocal ferrite phase shifter for both C- and X-bands having the capability of handling a peak power of 100 kilowatts, and an average power of 1 kilowatt with less than a 1 db loss. The approach for achieving a high power capability (the fundamental goal) was to avoid the familiar low field subsidiary resonance losses by operating at magnetic fields above ferrimagnetic resonance.

When the ferrite material originally proposed for the phase shifters proved to be unsatisfactory due to excessive loss in the region above resonance, the program emphasis was shifted toward selecting a satisfactory ferrite. In this task all of the available ferrite materials potentially acceptable for the two frequency bands were examined.

In the Semiannual Technical Report which documents the first half of the program it was concluded from both theoretical and experimental investigations that none of the available polycrystalline ferrites would be satisfactory. The theory specified a material property of narrow ferromagnetic linewidth as a principal requirement for achieving the desired phase shifter figure of merit. It was determined, at that time, that linewidths on the order of 10 oersteds would be needed; consequently, the emphasis during the second half of the program was directed toward evaluating the properties of very narrow linewidth ferrites.

The work during the second period has resulted in a refined definition of the material requirements for high power phase shifters. A discussion on the selection of a ferrite from theoretical considerations is given in Section II. In the following four sections the experimental work which was used to demonstrate various aspects of the theory is discussed and in the final section the conclusions are drawn for the whole program.

II. THEORETICAL CONSIDERATIONS IN SELECTING A FERRITE FOR A PHASE SHIFTER

Ferrites can be used to introduce a phase shift in a transmission line because they have a variable permeability. The functional dependence of this permeability can be found by considering the equation of motion of the total magnetization in the ferrite,

$$\dot{\vec{M}} = \gamma(\vec{M} \times \vec{H}_{eff}) - \frac{a}{|\vec{M}|}(\vec{M} \times \dot{\vec{M}}), \tag{1}$$

where the last term is the Landau-Lifshitz damping term to the first power in the damping factor a. This equation has been solved[1] for the x-componer of magnetization (m_x) induced by the RF magnetic field in a longitudinally magnetized ferrite rod:

$$4\pi m_x = \frac{\omega_m\left[-j\omega h_y + (\omega_r + \frac{j}{T})\, h_x\right]}{\left[\omega_r + \frac{j}{T}\right]^2 - \omega^2}, \tag{2}$$

where

$$\omega_m = \gamma 4\pi M_s$$

$$\omega_r = \gamma\left[H_o + H_a + 2\pi M_s\right]$$

$$\frac{1}{T} = \frac{\gamma \Delta H}{2}$$

ω = RF frequency,

and

$4\pi M_s$ = saturation magnetization of the ferrite,

ΔH = linewidth of the ferrite,

H_a = anisotropy field (oriented in the direction of the applied field)

---

1. See Appendix A of the Semiannual Technical Report on this Contract. In rectangular waveguide x and y are directions along the wide and narrow dimensions, respectively, and z is the direction of propagation.

H_o = applied dc magnetic field in the z direction,

h_x, h_y = components of the RF magnetic field.

The induced magnetization is related to the RF magnetic field through the susceptibility tensor $[\chi]$,

$$\vec{m} = [\chi] \cdot \vec{h} , \tag{3}$$

where

$$[\chi] = \begin{bmatrix} \chi_{xx} & \chi_{xy} & 0 \\ \chi_{yx} & \chi_{yy} & 0 \\ 0 & 0 & 0 \end{bmatrix} . \tag{4}$$

Equation 3 can be expanded to find the x-component of the magnetization,

$$4\pi m_x = \chi_{xx} h_x + \chi_{xy} h_y , \tag{5}$$

in gaussian units. Comparing Equations 2 and 5 yields the magnetic susceptibility in terms of material parameters, operating frequency, and applied field:

$$\chi_{xx} = \frac{\omega_m(\omega_r + \frac{j}{T})}{[\omega_r + \frac{j}{T}]^2 - \omega^2} , \tag{6}$$

and

$$-\chi_{xy} = \frac{j\omega_m\omega}{[\omega_r + \frac{j}{T}]^2 - \omega^2} \tag{7}$$

Equations 6 and 7 can be simplified,

$$\chi_{xx} = \frac{\omega_m(\omega_r + \frac{j}{T})}{\omega_r^2 - \omega^2 - \frac{1}{T^2} + 2j\frac{\omega_r}{T}} , \tag{8}$$

and

$$-\chi_{xy} = \frac{j\omega_m \omega}{\omega_r^2 - \omega^2 - \frac{1}{T^2} + 2j\frac{\omega_r}{T}} \tag{9}$$

Both the diagonal and off-diagonal components of the susceptibility tensor are complex, and the real and imaginary parts can be found by rationalization of Equations 8 and 9:

$$\chi_{xx} = \chi'_{xx} - j\chi''_{xx} , \tag{10}$$

$$\chi'_{xx} = \frac{\omega_m \omega_r (\omega_r^2 + \frac{1}{T^2} - \omega^2)}{[\omega_r^2 - \omega^2 - \frac{1}{T^2}]^2 + 4\frac{\omega_r^2}{T^2}} \tag{11}$$

$$\chi''_{xx} = \frac{\frac{\omega_m}{T}(\omega_r^2 + \omega^2 + \frac{1}{T^2})}{[\omega_r^2 - \omega^2 - \frac{1}{T^2}]^2 + 4\frac{\omega_r^2}{T^2}} \tag{12}$$

and

$$-\chi_{xy} = \chi'_{xy} + j\chi''_{xy} , \tag{13}$$

$$\chi'_{xy} = \frac{2\omega_m \omega \frac{\omega_r}{T}}{[\omega_r^2 - \omega^2 - \frac{1}{T^2}]^2 + 4\frac{\omega_r^2}{T^2}} \tag{14}$$

$$\chi''_{xy} = \frac{\omega_m \omega [\omega_r^2 - \omega^2 - \frac{1}{T^2}]}{[\omega_r^2 - \omega^2 - \frac{1}{T^2}]^2 + 4\frac{\omega_r^2}{T^2}} \tag{15}$$

A solution of Equation 1 for m_y would show that the susceptibility tensor is anti-symmetric with equal diagonal components:

$$\chi_{xx} = \chi_{yy},$$

$$\chi_{xy} = -\chi_{yx}.$$

The equations for the susceptibility have been found to be more useful when expressed in terms of the dimensionless quantities ω_r/ω, ω_m/ω, and ωT.

$$\chi'_{xx} = \frac{\omega_m}{\omega} \frac{\left(\frac{\omega_r}{\omega}\right)\left[\left(\frac{\omega_r}{\omega}\right)^2 + \left(\frac{1}{\omega T}\right)^2 - 1\right]}{\Delta}, \tag{16}$$

$$\chi''_{xx} = \frac{\omega_m}{\omega} \frac{\left(\frac{1}{\omega T}\right)\left[\left(\frac{\omega_r}{\omega}\right)^2 + \left(\frac{1}{\omega T}\right)^2 + 1\right]}{\Delta}, \tag{17}$$

$$\chi'_{xy} = \frac{\omega_m}{\omega} \frac{2\left(\frac{\omega_r}{\omega}\right)\left(\frac{1}{\omega T}\right)}{\Delta}, \tag{18}$$

$$\chi''_{xy} = \frac{\omega_m}{\omega} \frac{\left[\left(\frac{\omega_r}{\omega}\right)^2 - \left(\frac{1}{\omega T}\right)^2 - 1\right]}{\Delta}, \tag{19}$$

where

$$\Delta = \left[\left(\frac{\omega_r}{\omega}\right)^2 - \left(\frac{1}{\omega T}\right)^2 - 1\right]^2 + 4\left(\frac{\omega_r}{\omega}\right)^2\left(\frac{1}{\omega T}\right)^2. \tag{20}$$

The permeability tensor is given in the usual notation of electrodymanics by

$$[\mu] = \begin{vmatrix} \mu & -j\kappa & 0 \\ j\kappa & \mu & 0 \\ 0 & 0 & 1 \end{vmatrix}, \tag{21}$$

where the permeability is complex and is related to the susceptibility as,

$$\mu = 1 + \chi_{xx}, \tag{22}$$

and

$$j\kappa = -\chi_{xy} . \tag{23}$$

The permeability can be written in terms of the material parameters of the ferrite by using Equations 16, 17, 18, and 19 where:

$$\mu = \mu' - j\mu'', \tag{24}$$

$$\mu' = 1 + \chi'_{xx}, \tag{25}$$

$$\mu'' = \chi''_{xx} \tag{26}$$

and

$$\kappa = \kappa' - j\kappa'', \tag{27}$$

$$\kappa' = \chi''_{xy}, \tag{28}$$

$$\kappa'' = \chi'_{xy}. \tag{29}$$

For a given set of ferrite material properties ($4\pi M_s$, ΔH, H_a), one can use the derived expressions to compute the permeability as a function of frequency (ω) and applied field (H_o). However, to predict the operation of a phase shifter requires a knowledge of how the permeability enters into the propagation constant and hence a knowledge of the field structure in the ferrite. The principle interest on this program has been in ferrites with cross sections small compared to their length and longitudinally magnetized in rectangular waveguide. An exact solution of Maxwell's equations for this boundary value problem has not been found. Our effort has not been to solve this problem, but rather to formulate some estimates of phase shifter performance as a function of material parameters by examining two conditions for which the boundary value problems have been solved. These are the cases, (1) of a ferrite in rectangular waveguide when the ferrite represents a small perturbation to the ordinary waveguide mode, and (2) a parallel plane waveguide fully filled with ferrite.

If the ferrite cross section is very small compared to the height and width of the waveguide, the fields in the loaded waveguide are not

essentially different from the unloaded fields. Hence, if the unloaded waveguide would propagate the dominant TE_{10} mode, the loaded guide can be considered to also propagate the TE_{10} mode. This will be referred to as the small perturbation model. It should be pointed out that the ferrite cross section required in practical devices, i.e., large enough to achieve a reasonable phase shift per unit length, does not in general satisfy this requirement. As the cross section increases from some infinitesmal value to some real value, one finds that Maxwell's equations do not separate into two independent solutions associated with pure TE and TM type modes. They are complicated hybrid modes, containing both electric and magnetic components in the direction of propagation. When the small perturbation technique is used, considering only the TE_{10} mode to propagate, one can proceed in a manner similar to that used by Button and Lax[2] and assume that the h_y component of the RF magnetic field is zero and that the off-diagonal components of the susceptibility tensor contribute no effect. Thus, Equation 5 reduces to

$$4\pi m_x = \chi h_x. \tag{30}$$

The permeability tensor is therefore diagonal, with the components of the complex permeability given by Equations 25 and 26. In order to facilitate the examination of many different ferrites, Equations 16 and 17 have been used to construct a set of generalized curves which are given in Figures 1 through 4.

Phase shifter performance is best studied by examining figure of merit. This is defined as the ratio of phase shift to insertion loss and is proportional to $\frac{\Delta\mu'}{\mu''}$ in regions where magnetic losses are much greater than dielectric loss. As one moves far from magnetic resonance, μ'' tends toward zero and the actual observed loss is purely electric in origin. Since for a given frequency the dielectric loss is a constant over

---

2. K. Button and B. Lax, Microwave Ferrites and Ferrimagnetics, McGraw-Hill Book Company, Inc., New York, p. 349; New York.

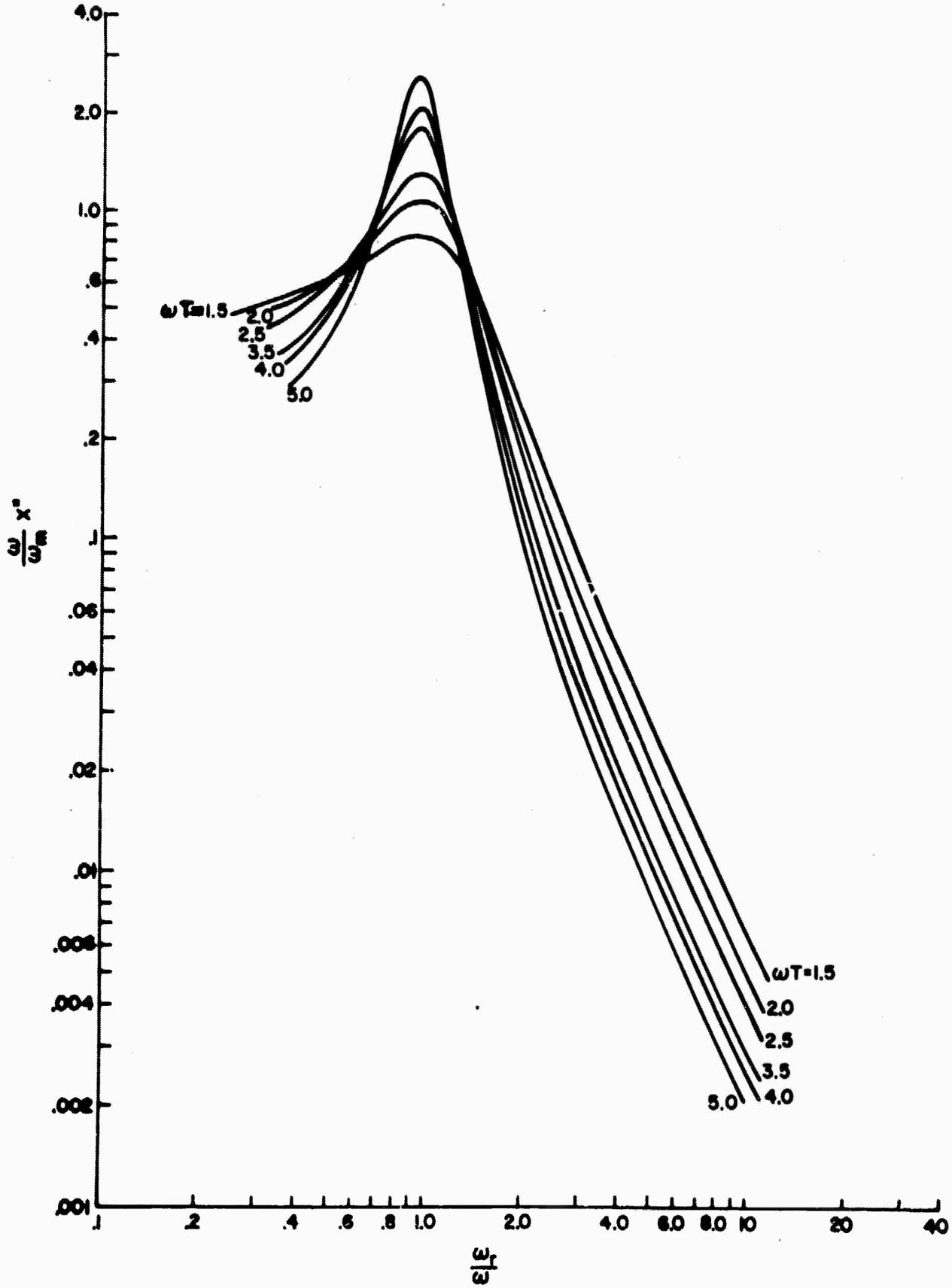

FIG. 1 - GENERALIZED CURVES OF X" AS A FUNCTION OF $\frac{\omega_r}{\omega}$ AND ωT FOR A LONGITUDINALLY MAGNETIZED FERRITE ROD.

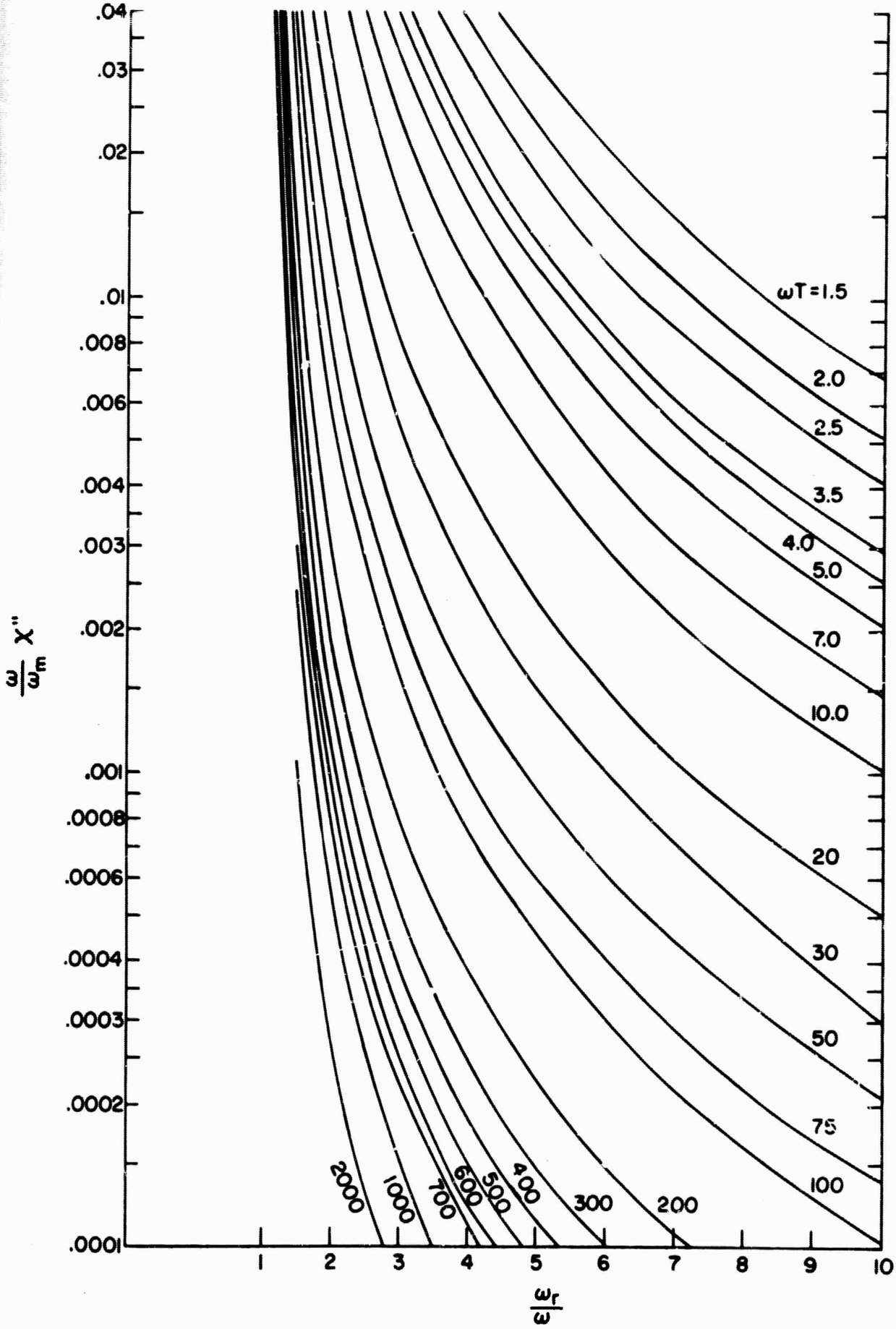

FIG. 2 - GENERALIZED CURVES OF χ'' AS A FUNCTION OF $\frac{\omega_r}{\omega}$ AND ωT FOR A LONGITUDINALLY MAGNETIZED FERRITE ROD.

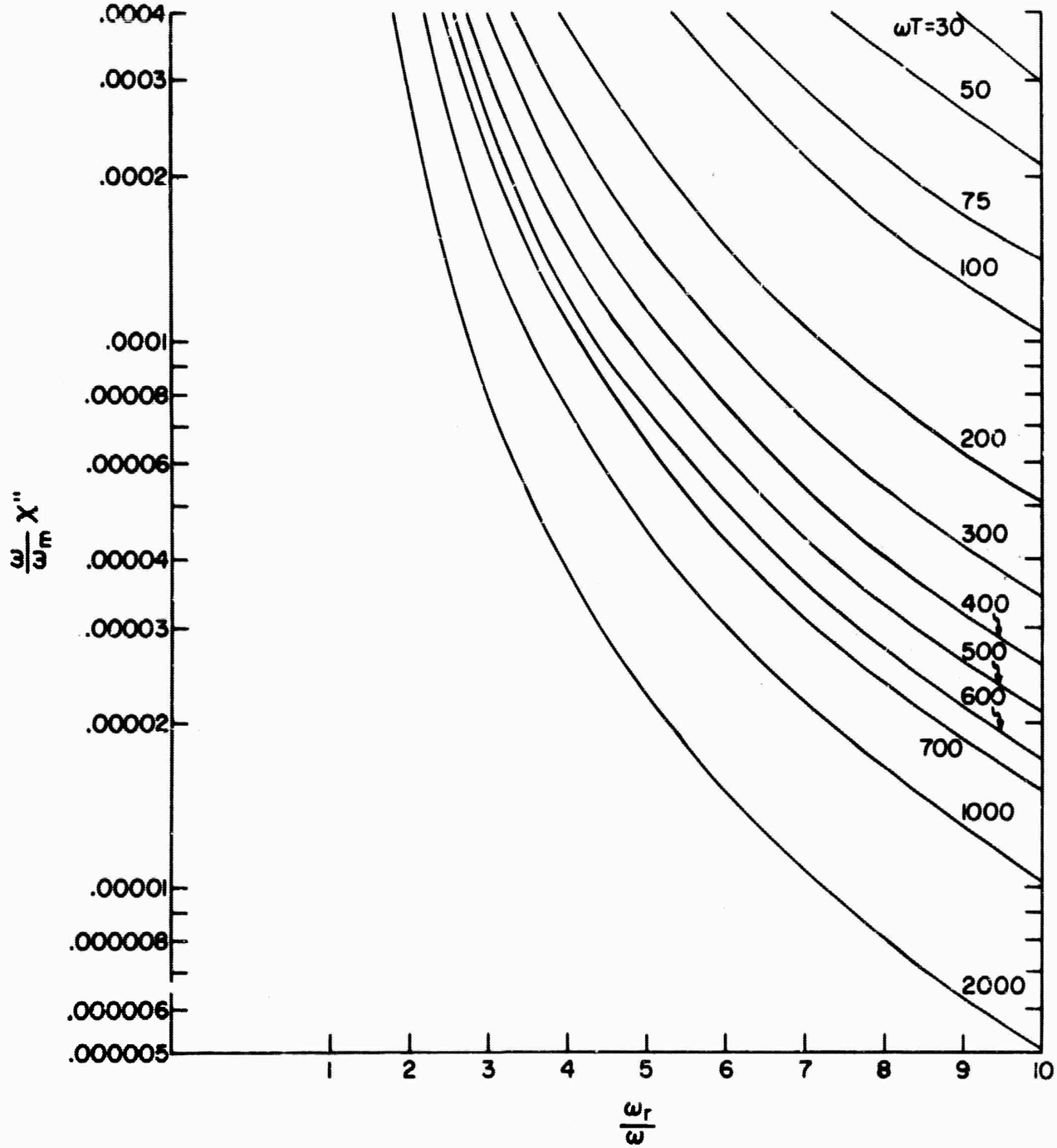

FIG. 3 -GENERALIZED CURVES OF χ'' AS A FUNCTION OF $\frac{\omega_r}{\omega}$ AND ωT FOR A LONGITUDINALLY MAGNETIZED FERRITE ROD.

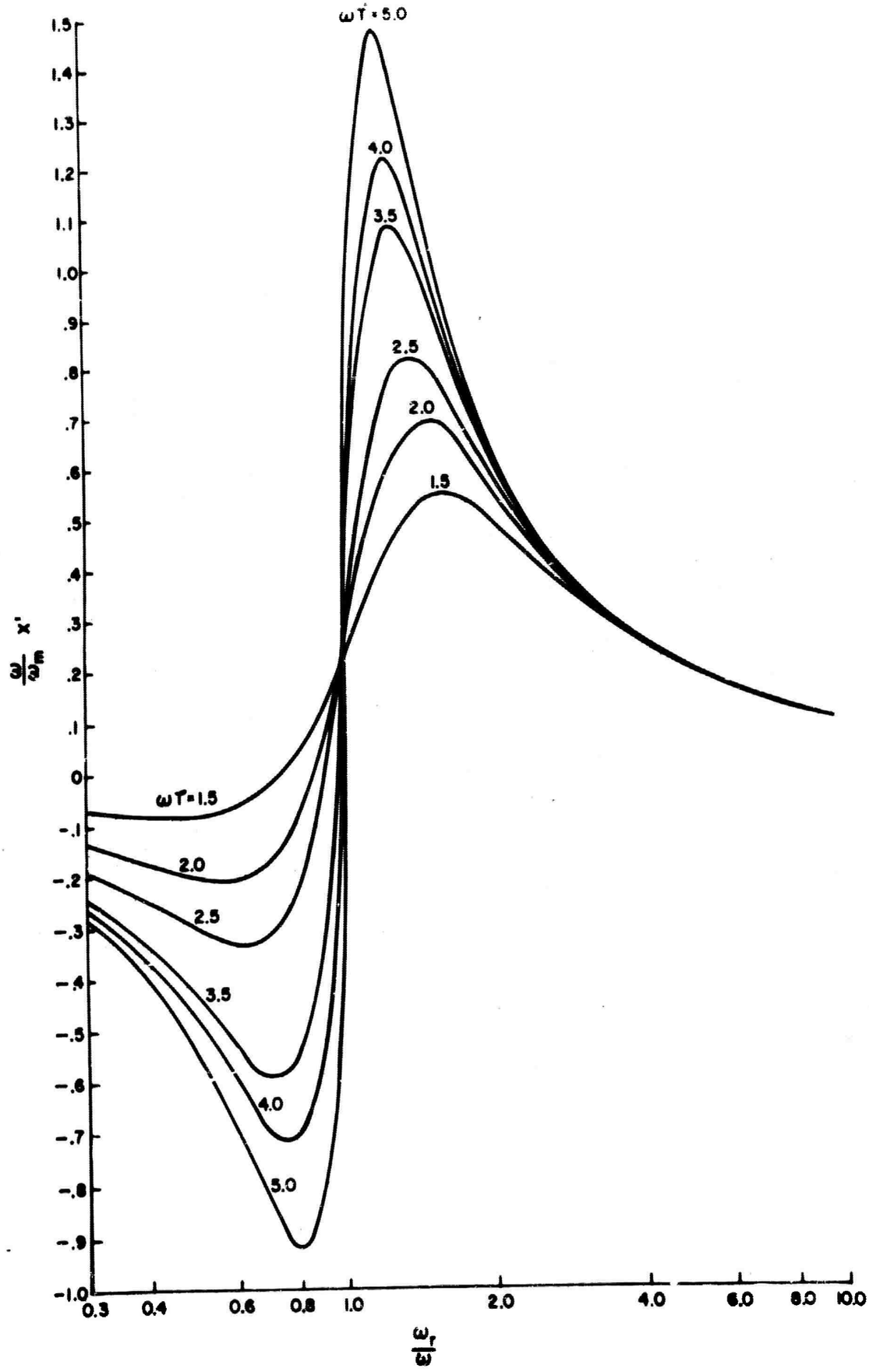

FIG. 4 –GENERALIZED CURVES OF X' AS A FUNCTION OF $\frac{\omega_r}{\omega}$ AND ωT FOR A LONGITUDINALLY MAGNETIZED FERRITE ROD

the range of operation, the optimum operating conditions will still correspond to the largest value of $\frac{\Delta\mu'}{\mu''}$, where $\Delta\mu'$ is the change in μ' over some range of applied field and μ'' is assigned the largest value in this range which corresponds to the largest observed insertion loss. In this program the region of interest is after magnetic saturation and at magnetic fields above resonance; thus, the performance analysis will be confined to that region.

The generalized curves have been used to construct curves of μ' and μ'' versus applied magnetic field (H_o). Some of these curves are given in Figures 5 through 10 for which the saturation magnetization is constant ($4\pi M_s$ = 3500 gauss) but the linewidth (ΔH) and anisotropy field (H_a) vary. Fictitious negative values of H_o have been allowed in order to display the resonant curve shape.

The effect of a variation of the anisotropy field can be seen in a comparison of Figures 5 and 6. As the anisotropy field changes from 11.2 koe to 3.5 koe, with the other material parameters held constant, there is no substantial change in the figure of merit ($\frac{\Delta\mu'}{\mu''}$) for an applied field variation from 0 to 1000 oersteds. The principle effect is a shift in the value of magnetic field for resonance in the subject configuration because the effective field in ferrite is the sum of the applied field and the anisotropy field. The state of resonance is defined when μ'', and therefore χ'', is a maximum and it occurs approximately when,

$$\omega_r^2 = \omega^2 + \frac{1}{T^2} , \tag{31}$$

or

$$\gamma^2 \left[H_o + H_a + 2\pi M_s\right]^2 = (2\pi f)^2 + \frac{\gamma^2 (\Delta H)^2}{4} . \tag{32}$$

For a given application, the optimum value of anisotropy field is that which allows operation on the desired portion of the μ' and μ'' curves for minimum values of applied field and thus minimum driver power requirements.

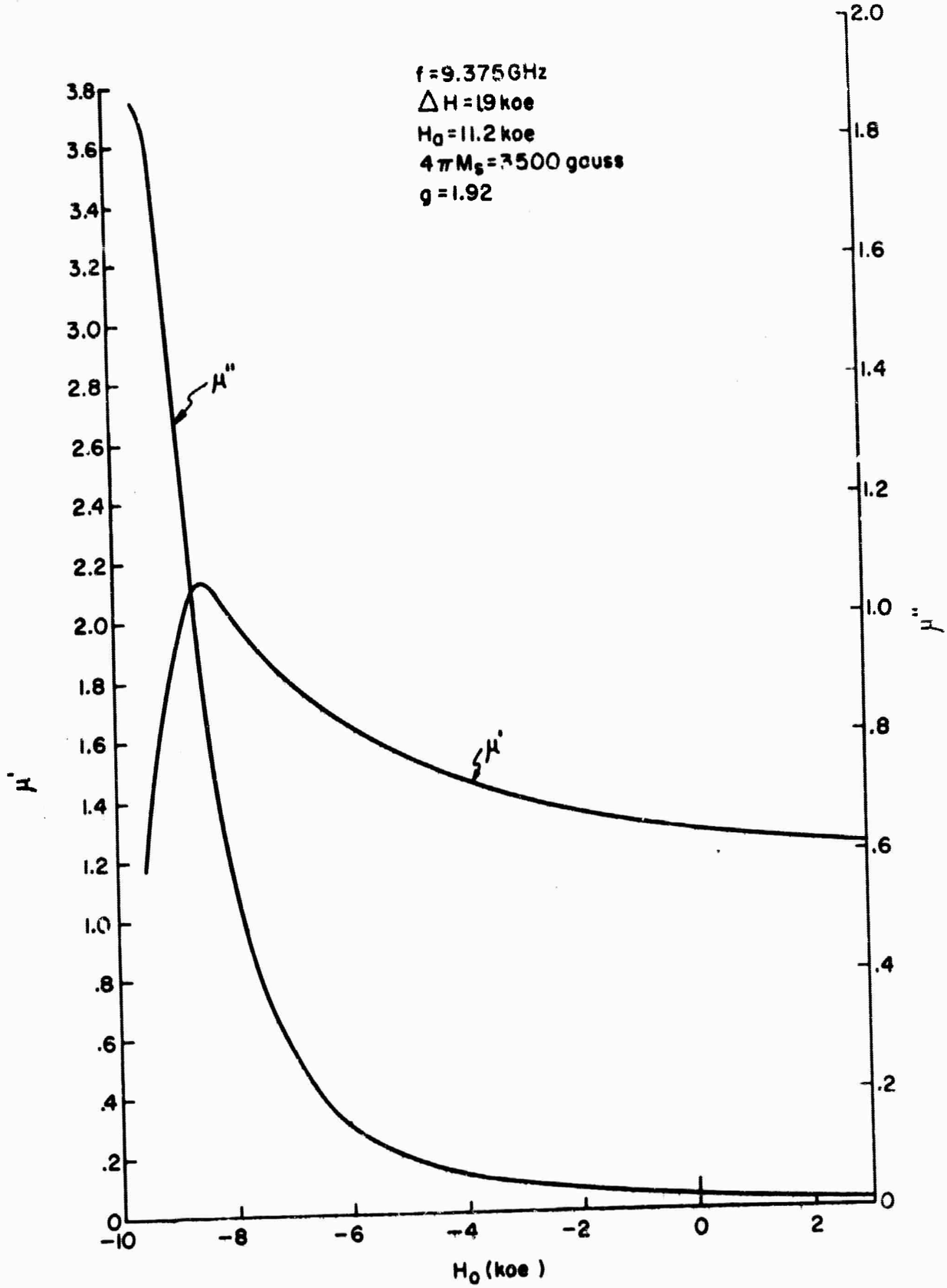

FIG. 5 $-\mu'$ AND μ'' vs APPLIED FIELD, H_0=11.2 koe AND ΔH=1.9 koe

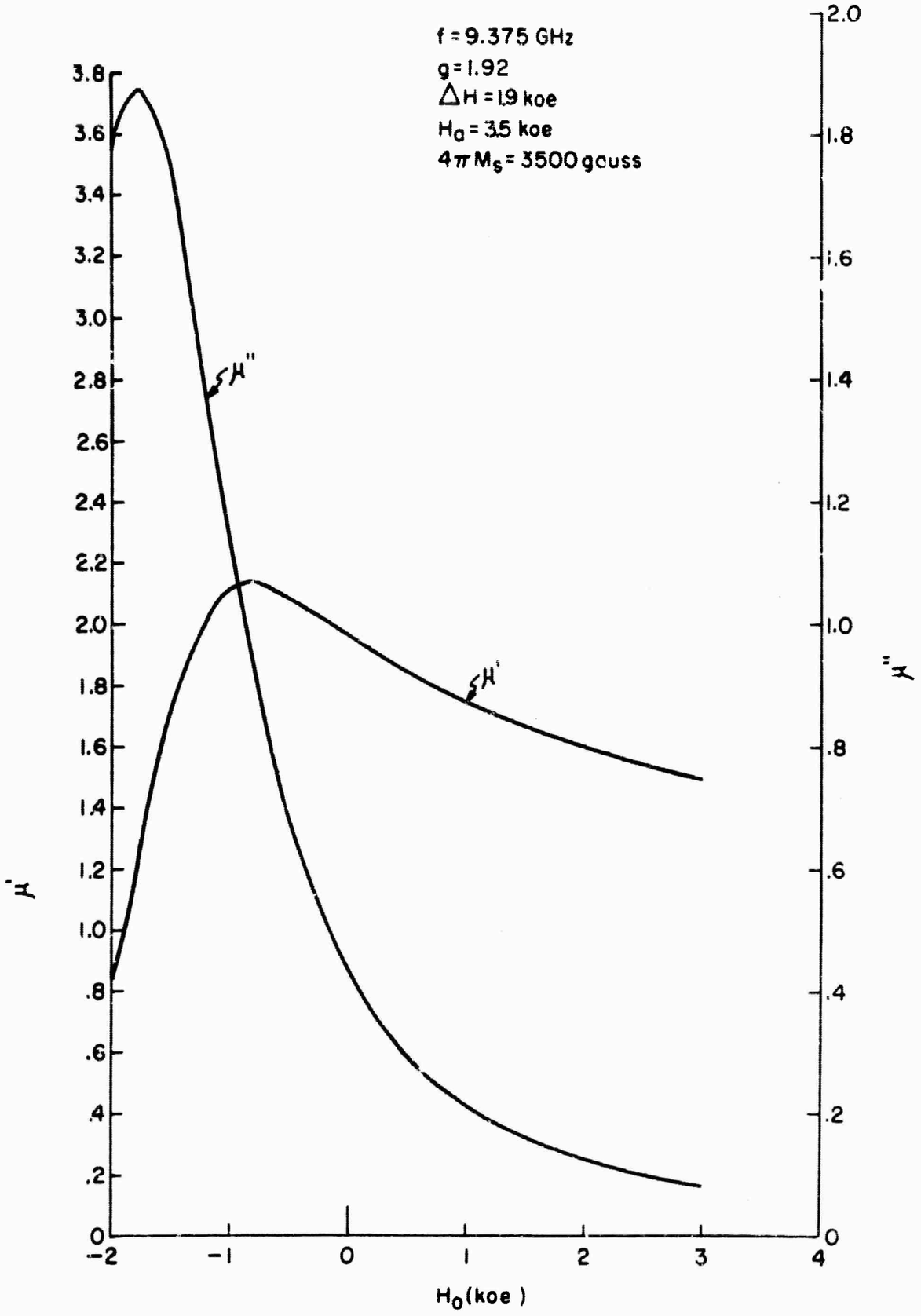

FIG. 6 $-\mu'$ AND μ'' vs APPLIED FIELD, $H_0 = 3.5$ koe AND $\Delta H = 1.9$ koe

Similar considerations can be applied to the saturation moment ($4\pi M_s$). Once the ferrite is saturated, $4\pi M_s$ is independent of the applied field. The equation for the figure of merit can be written,

$$F.M. = \frac{\Delta\mu'}{\mu''} = \frac{\Delta(1+\chi')}{\chi''} = \frac{\Delta\chi'}{\chi''} , \tag{33}$$

where

$$\frac{\Delta\chi'}{\chi''} = \frac{\partial\chi'}{\partial H_o} \frac{\Delta H_o}{\chi''} . \tag{34}$$

Both χ' and χ'' are proportional to $\frac{\omega_m}{\omega}$ which is independent of H_o and therefore can be factored out of the equation for figure of merit. The saturation moment consequently only enters Equation 34 through the expression

$$\omega_r = \gamma [H_o + H_a + 2\pi M_s] , \tag{35}$$

in Equations 16 and 17, and as a result, the figure of merit changes very little with M_s. The principle effect is that the magnetic field for resonance changes and is proportional with changes in M_s.

The most important material parameter affecting the figure of merit is linewidth. Its influence can be studied by comparing $\frac{\Delta\mu'}{\mu''}$ in Figures 7, 8, 9, and 10. For an applied field variation from 0 to 1000 oersteds the corresponding figures of merit for linewidths of ΔH = 2000, 1000, 500, and 100 oersteds are seen to be $\frac{\Delta\mu'}{\mu''}$ = 0.81, 1.60, 3.20, and 16.53, respectively ($\frac{\Delta\mu'}{\mu''}$ is given in radians per neper and can be converted to degrees per db through multiplication by 6.6). In general, the figure of merit is inversely proportional to the linewidth. This relationship holds for applied fields greater than several linewidths from resonance. Figure 4 shows that, for $\omega_r/\omega > 3.5$, χ' and therefore $\Delta\chi'$, is independent of ωT and hence independent of linewidth since,

$$\omega T = \frac{2\omega}{\gamma\Delta H} . \tag{36}$$

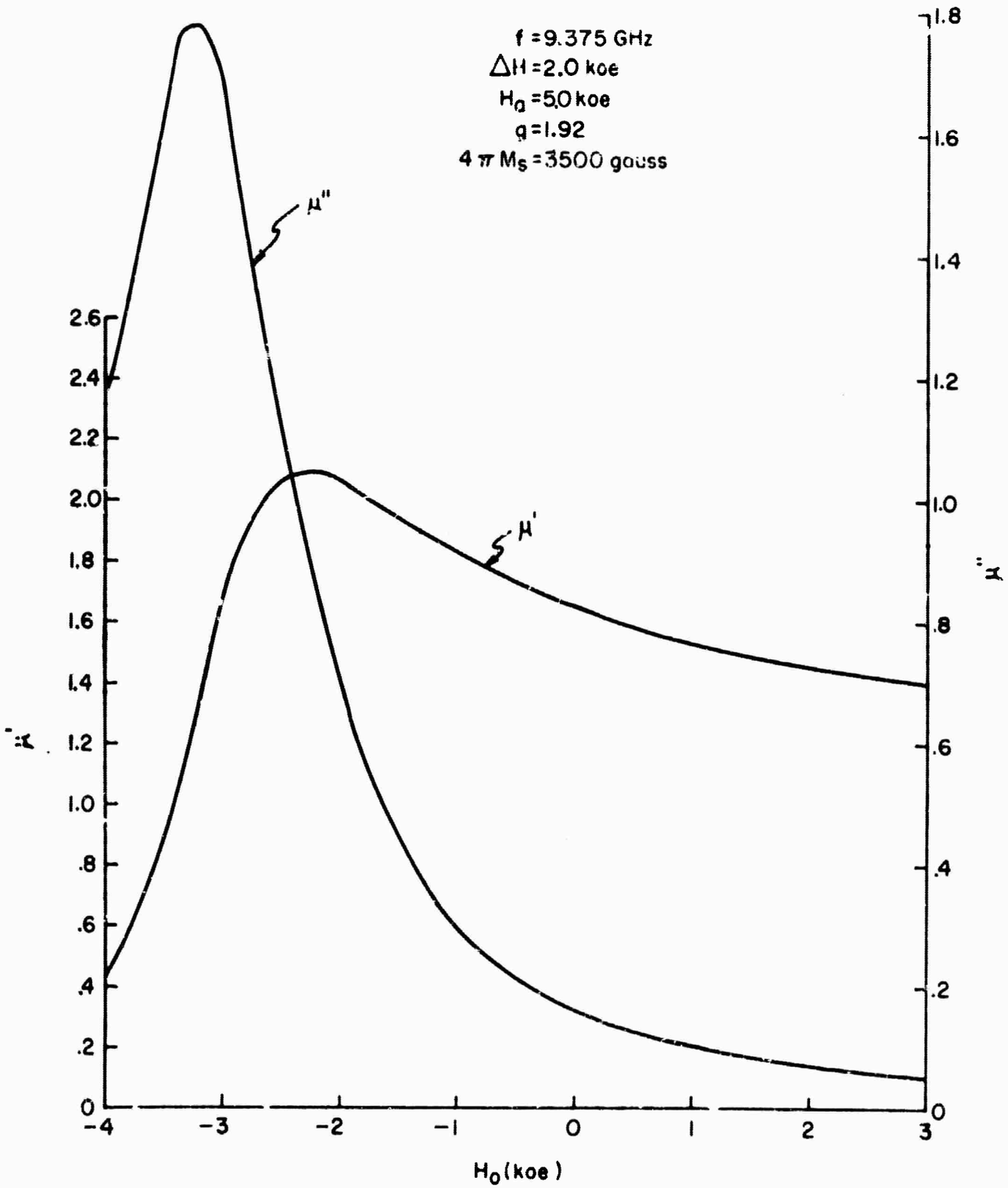

FIG. 7 μ' AND μ'' vs APPLIED FIELD, H_c = 5.0 koe AND ΔH = 2.0 koe

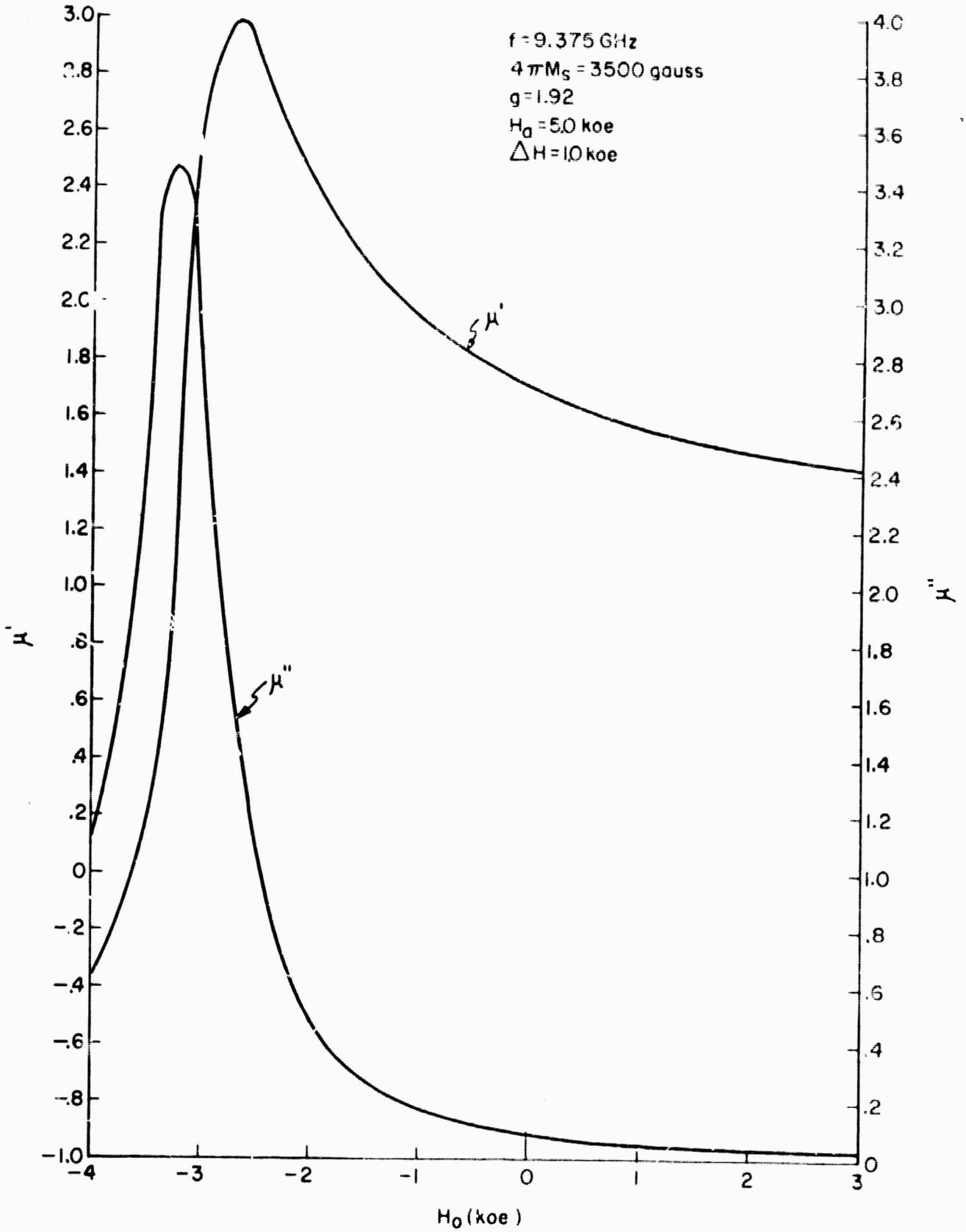

FIG. 8 $-\mu'$ AND μ'' vs APPLIED FIELD, $H_a = 5.0$ koe AND $\Delta H = 1.0$ koe

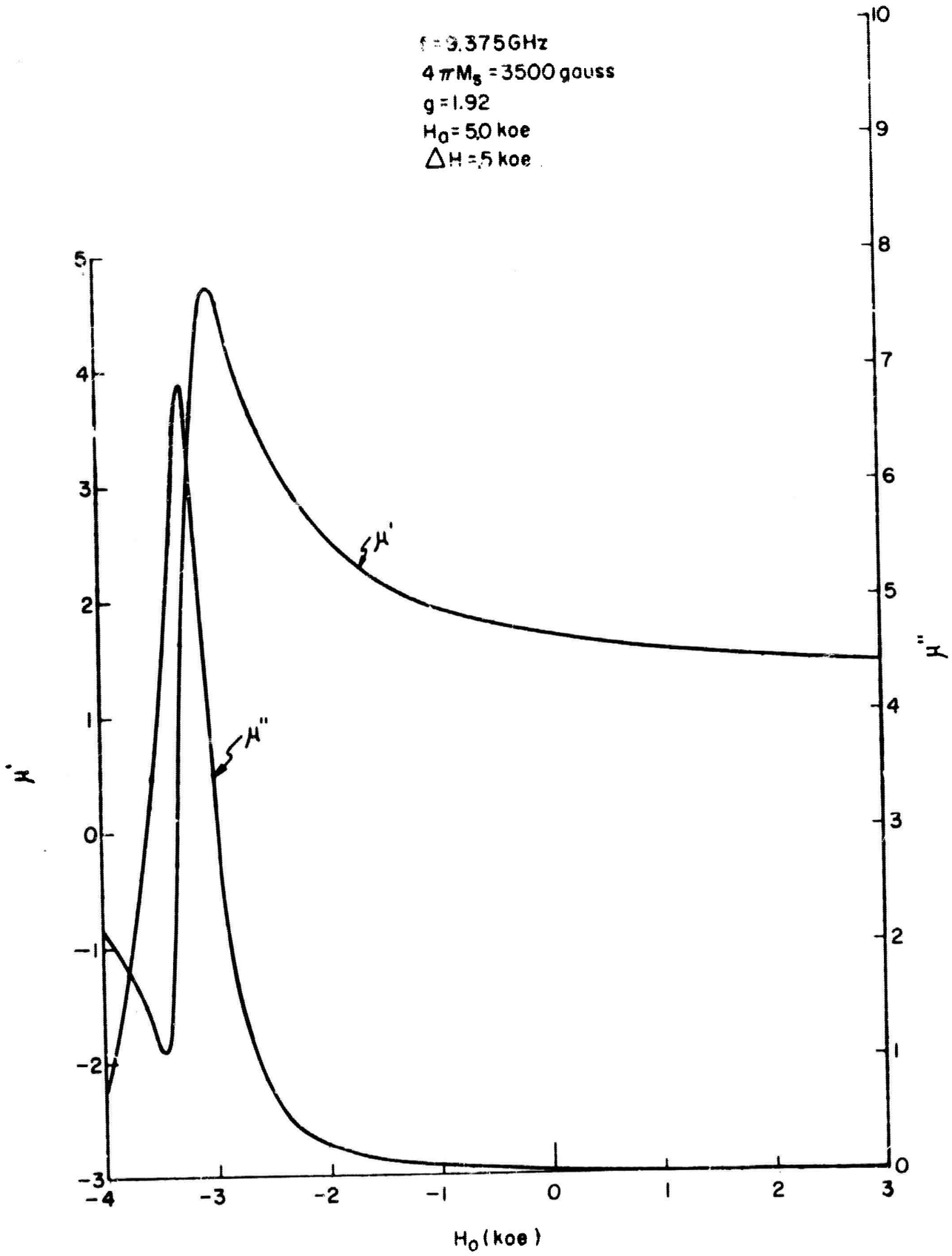

FIG. 9 $-\mu'$ AND μ'' vs APPLIED FIELD, $H_0 = 5.0$ koe AND $\Delta H = .5$ koe

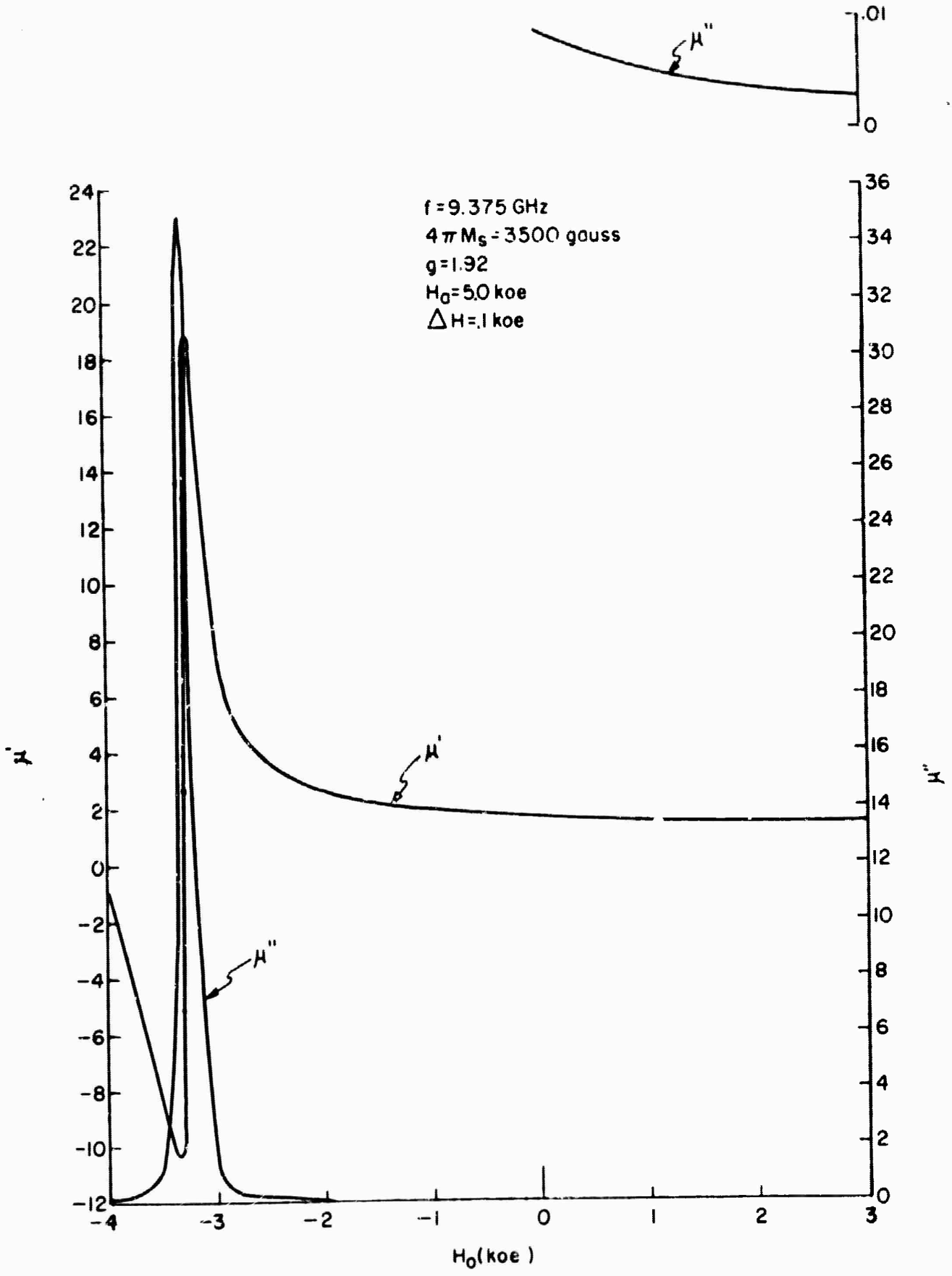

FIG. 10 $-\mu'$ AND μ'' vs APPLIED FIELD, $H_0 = 5.0$ koe AND $\Delta H = .10$ koe

Figures 2 and 3 show that for the same region χ'' is inversely proportional to ωT and, by Equation 36, directly proportional to ΔH; therefore, by Equation 33, the figure of merit increases in the same ratio that the linewidth decreases.

The small perturbation model assumes a rectangular waveguide containing a very small ferrite cross section, and propagating the dominant mode. At the other extreme, one can consider the parallel plane waveguide fully ferrite loaded. This behaves like a fully filled rectangular waveguide whose side walls have been moved out to infinity. In practice, this would be a fully filled guide many wavelengths wide. If the gyromagnetic properties of the ferrite were neglected, this structure could propagate the TEM mode. Suhl and Walker have shown[3] that the structure can be analyzed such that in the limit of zero magnetization it does propagate the TEM mode. One can therefore assume that $E_x = E_z = 0$. The geometry of the structure is such that the waveguide dimension in the x-direction goes to infinity (many wavelengths), and hence there is no spatial variation of the fields in this direction and therefore $\frac{\partial}{\partial x} = 0$. Assuming that all fields vary as exp $[kz + ay - \omega t]$ one can solve Maxwell's equations:

$$\nabla \times \vec{E} = -\frac{1}{c}\frac{\partial \vec{B}}{\partial t} \tag{37}$$

gives

$$\frac{\partial E_y}{\partial z} = \frac{1}{c}\frac{\partial B_x}{\partial t} \tag{38}$$

$$B_y = B_z = 0 \tag{39}$$

$$\nabla \times \vec{H} = \frac{\epsilon}{c}\frac{\partial \vec{E}}{\partial t}$$

gives

$$\frac{\partial H_x}{\partial z} = \frac{\epsilon}{c}\frac{\partial H_y}{\partial t} \; . \tag{40}$$

---

3. H. Suhl and L.R. Walker, "Topics in Guided Wave Propagation Through Gyromagnetic Media," Bell Telephone System, Monograph 2322, Part III, p. 166; 1954.

Differentiation of Equation 38 with respect to time and Equation 40 with respect to z allows them to be solved simultaneously for the wave equation in H_x

$$\frac{\partial^2 H_x}{\partial z^2} = -\epsilon \frac{\omega^2}{c^2} B_x. \tag{41}$$

Expressing $\vec{B}$ in terms of $\vec{H}$ through the permeability tensor of Equation 21 one may reduce Equation 41 to

$$k^2 H_x = \epsilon \frac{\omega^2}{c^2} [\mu H_x - j\kappa H_y]. \tag{42}$$

With the condition that $B_y = 0$, H_x and H_y are related through the permeability tensor:

$$j\kappa H_x = -\mu H_y \tag{43}$$

and Equation 42 can be written in terms of H_x alone,

$$k^2 H_x = \epsilon \frac{\omega^2}{c^2} \left[\mu H_x - j\kappa \left(\frac{-j\kappa}{\mu} H_x\right) \right], \tag{44}$$

which can be solved for the propagation constant,

$$k = \frac{\omega}{c} \sqrt{\epsilon} \left[\frac{\mu^2 - \kappa^2}{\mu}\right]^{\frac{1}{2}}. \tag{45}$$

The expression for propagation in the gyromagnetic medium is like that for an isotropic medium where the effective permeability is

$$\mu_e = \frac{\mu^2 - \kappa^2}{\mu} \tag{46}$$

and therefore

$$k = \frac{\omega}{c} \sqrt{\epsilon \mu_e}. \tag{47}$$

Phase shift and material loss can be found by considering the form of the complex propagation constant,

$$jk = \alpha + \beta. \tag{48}$$

Both electric and magnetic effects are considered by allowing,

$$\mu_e = \mu'_e - j\mu''_e \tag{49}$$

and

$$\epsilon = \epsilon' - j\epsilon''. \tag{50}$$

When Equations 48 and 47 are solved simultaneously under the condition

$$(\mu''_e)^2 << (\mu'_e)^2$$

and

$$(\epsilon'')^2 << (\epsilon')^2$$

one can show that

$$\beta = \frac{\omega}{c} \sqrt{\epsilon' \mu'_e} \tag{51}$$

and

$$\alpha = \frac{\omega}{2c} \sqrt{\epsilon' \mu'_e} (\tan \delta_e + \tan \delta_m), \tag{52}$$

where

$$\tan \delta_e = \frac{\epsilon''}{\epsilon'},$$

$$\tan \delta_m = \frac{\mu''_e}{\mu'_e}.$$

The differential phase shift is given by

$$\Delta\phi = \ell \, \Delta\beta = \ell \, \frac{\partial \beta}{\partial \mu'_e} \, \Delta\mu'_e, \tag{53}$$

where ℓ is the length of the ferrite, and the total material loss is given by $\alpha\ell$. The figure of merit is by definition $\frac{\Delta\phi}{\alpha\ell}$ where

$$\frac{\Delta\phi}{\alpha\ell} = \frac{\Delta\mu'_e}{\mu'_e (\tan \delta_e + \tan \delta_m)}. \tag{54}$$

In regions where magnetic losses are much greater than dielectric loss,

$$\tan \delta_m >> \tan \delta_e,$$

Equation 54 reduces to

$$\frac{\Delta\phi}{a\ell} = \frac{\Delta\mu'_e}{\mu''_e} . \tag{55}$$

Equation 55 is the same form used for figure of merit in the small perturbation model in which μ has been replaced by μ_e to include the effect of the off-diagonal tensor components. The dispersive and dissipative parts of μ_e are found by substituting into Equation 46

$$\mu_e = \frac{\mu^2 - \kappa^2}{\mu},$$

$$\mu'_e - j\mu''_e = \frac{(\mu' - j\mu'')^2 - (\kappa' - j\kappa'')^2}{(\mu' - j\mu'')} \tag{56}$$

which, after rationalization, gives

$$\mu'_e = \mu' - \frac{(\kappa'^2\mu' - \kappa''^2\mu' + 2\kappa'\kappa''\mu'')}{\mu'^2 + \mu''^2} \tag{57}$$

and

$$\mu''_e = \mu'' + \frac{(\kappa'^2\mu'' - \kappa''^2\mu'' - 2\kappa'\kappa''\mu')}{\mu'^2 + \mu''^2} \tag{58}$$

Generalized curves of κ were not generated; however, several specific cases were studied. It was found that the figure of merit, $\Delta\mu'_e/\mu''_e$, is still dependent on linewidth as in the small perturbation model. The figure of merit for the parallel plane model also increases in direct proportion to the decrease in linewidth through a proportiona decrease in the μ''_e term. The behavior of μ''_e is shown for several cases of narrow linewidth single crystal lithium ferrite in Figure 11.

In order to compare figures of merit for the two models proposed, some curves have been generated which show both μ and μ_e (curves of κ have also been included in order to show how κ varies with applied field)

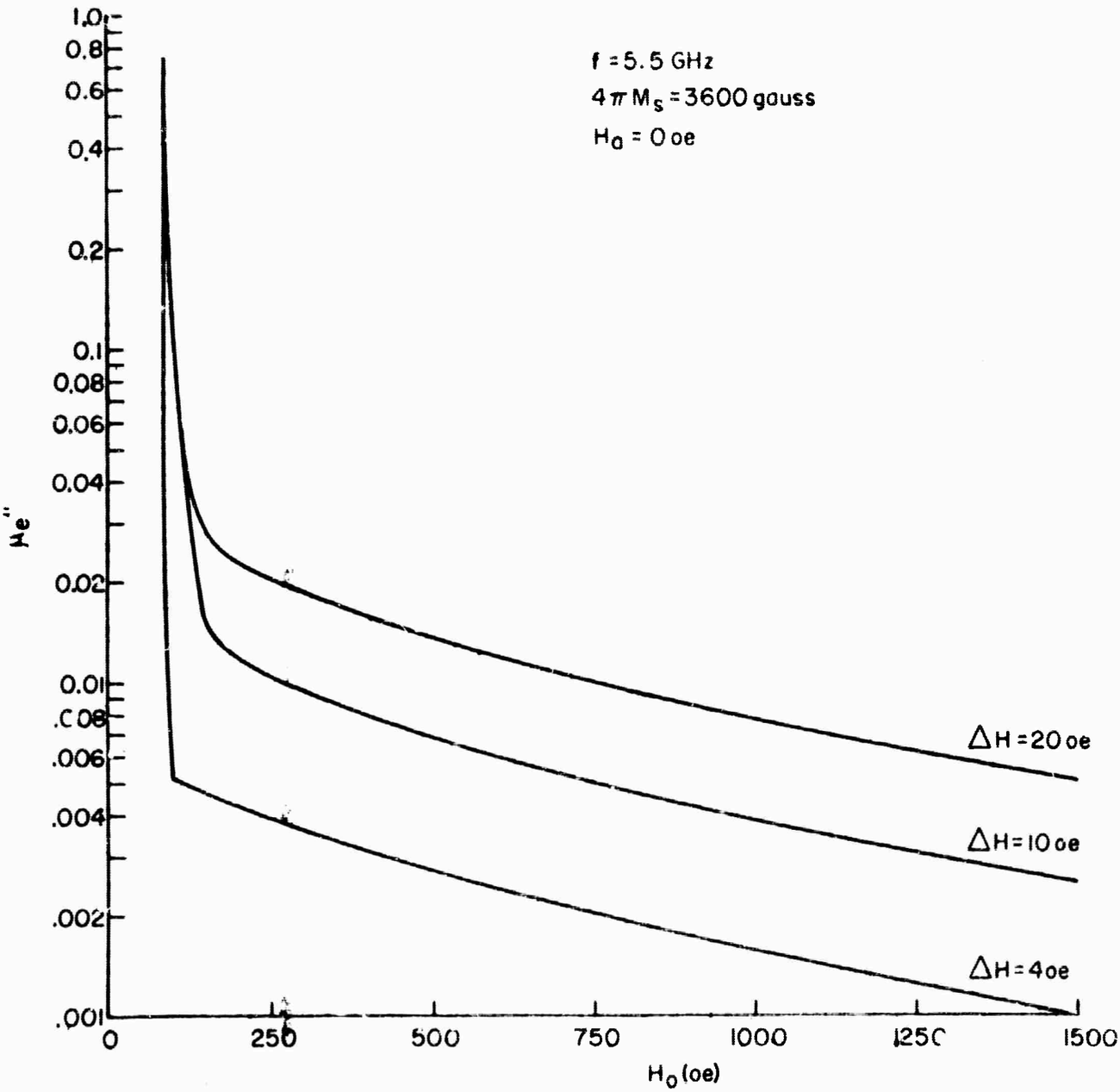

FIG. 11 - μ_e'' vs LINEWIDTH FOR LITHIUM FERRITE

for a single crystal lithium ferrite and a polycrystalline nickel ferrite (Trans-Tech TT2-111). These are given in Figures 12 and 13, respectively. Comparison of figure of merit for the small perturbation model ($\Delta\mu'/\mu''$) to that for the parallel plane model ($\Delta\mu'_e/\mu''_e$) shows that, for any range of applied field the parallel plane model has the larger figure of merit. Examination on a term by term basis shows that although the actual phase shift is much less (based on the $\Delta\mu'_e$ term) in the parallel plane model, the material loss is substantially smaller (the μ''_e term). This is most evident near resonance as can be seen in Figure 12. It is in this region that the greatest change in the dispersive terms, $\Delta\mu'$ and $\Delta\mu'_e$, takes place. However, the large dissipative term, μ'', close to resonance accounts for low figures of merit in the small perturbation approximation.

The effect of including the off-diagonal terms (κ) in the permeability tensor is to lower the dissipative term; thus, a ferrite in the parallel plane waveguide could be operated considerably closer to resonance to take advantage of the large phase shift per unit of dynamic field.

Although neither the small perturbation model nor the parallel plane waveguide model correspond to the actual structures investigated, they have served to show that linewidth is the most important material parameter affecting the figure merit.

Further considerations in the selection of ferrite materials for high power operation are taken from Fletcher and Silence.[4] In an extension of Suhls' theory on nonlinear effects at high power, they have shown that coupling between the uniform precision (dominant spin wave) and higher order spin waves, with the accompanying flow of power into the higher order modes, may occur at magnetic fields above ferrimagnetic resonance under certain conditions of frequency, material characteristics and configuration.

---

4. P.C. Fletcher and N. Silence, "Subsidiary Absorption above Ferrimagnetic Resonance," J. Appl. Phys, Vol. 32, p. 706; April, 1961.

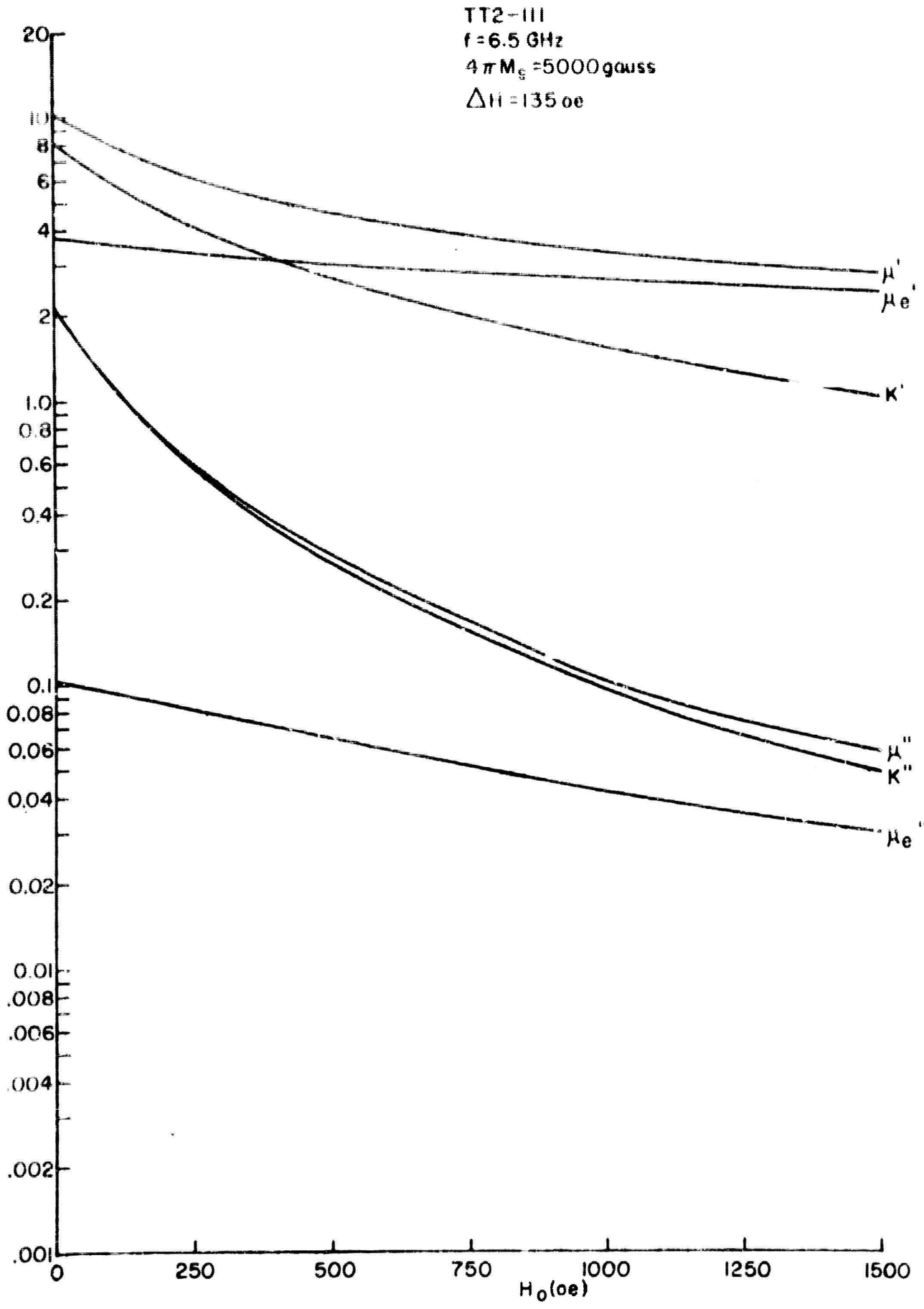

FIG. 12 - DISSIPATIVE AND DISPERSIVE PARTS OF μ, K, AND μ_e FOR NICKEL FERRITE (TT2-III).

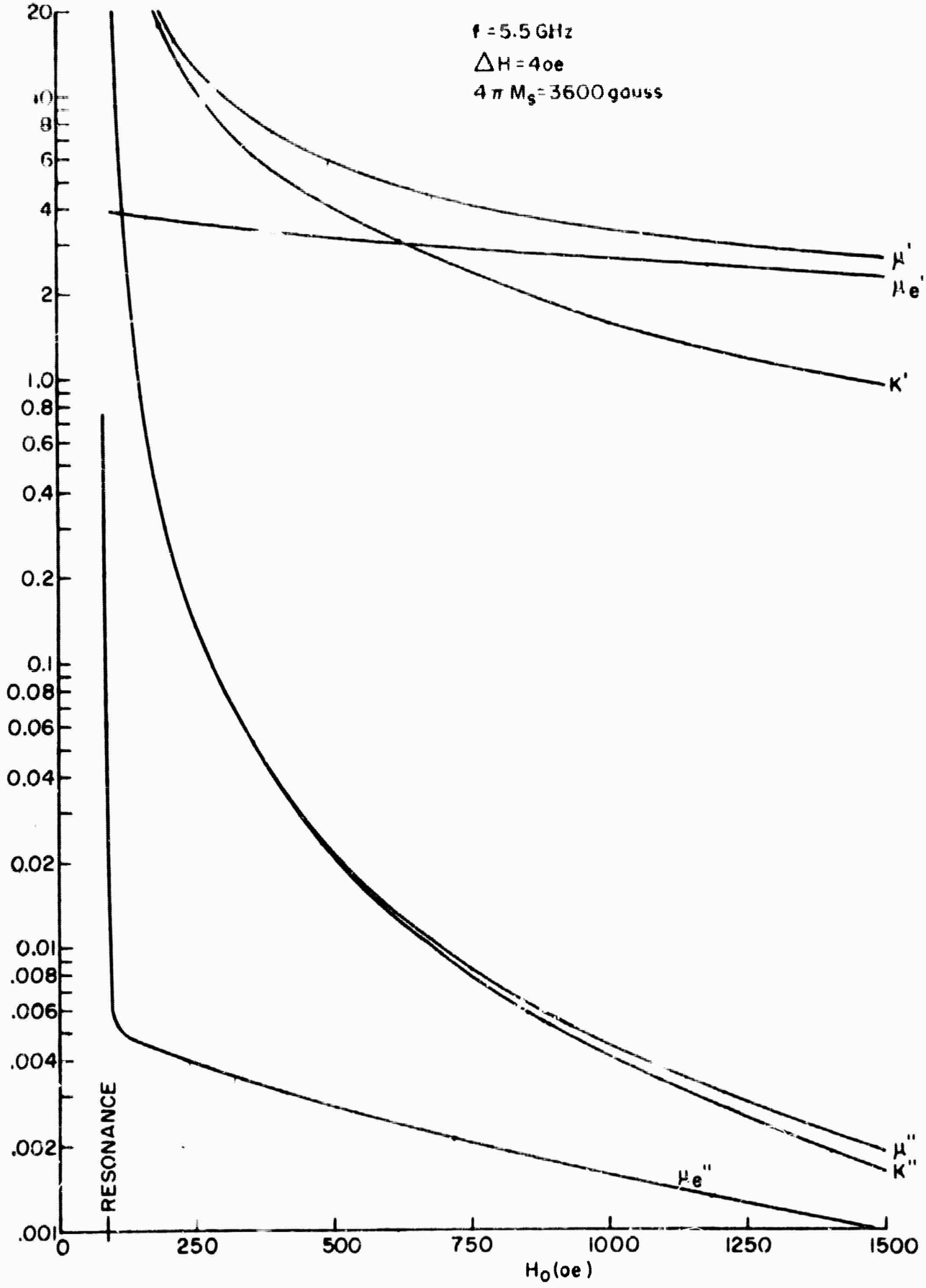

FIG. 13 – DISSIPATIVE AND DISPERSIVE PARTS OF μ, K, AND μ_e FOR LITHIUM FERRITE.

The conditions for the threshold of critical field (h_{crit}) for a rod configuration are expressed in the family of curves, Figure 14. For each curve, $\frac{\omega}{\omega_m}$, a value of magnetic field expressed as $\frac{\omega_r}{\omega}$ can be found where $h_{crit}/\Delta H$ rises sharply and beyond which subsidiary resonance is avoided.

The relationship of Figure 14 implies certain restrictions on the choice of saturation moment. One may not arbitrarily choose a material with the largest M_s for the sole purpose of relieving the magnetic field requirements because as the value $\frac{\omega}{\omega_m}$ decreases it is seen that a larger value of magnetic field is needed to avoid subsidiary resonance. As the operating region moves farther above resonance, phase shift activity decreases as shown in Figure 4. Nevertheless the figure of merit continues to rise because the magnetic losses diminish at an even greater rate. The rise in figure of merit, however, will eventually reach a limit and begin to fall when the magnetic losses become small with respect to the fixed dielectric and conductor wall losses.

In a phase shifter the disadvantage to operating far above resonance is that due to the reduced activity per unit length, a longer structure is required for the desired phase shift which, in turn, requires a longer magnetic driver coil and thus more power from the driver.

If one extracts from Figure 14 the pertinent information for the avoidance of subsidiary resonance the resulting relationship of $\frac{\omega}{\omega_m}$ vs $\frac{\omega_r}{\omega}$ is that given in Figure 15 (we have arbitrarily chosen to draw the relation at $h_{crit}/\Delta H = 2.5$).

From the definition of ω_r it may be easily shown that

$$H_o + H_a = \frac{\omega}{\gamma}\left(\frac{\omega_r}{\omega} - \frac{\omega_m}{2\omega}\right) . \qquad (59)$$

Choosing corresponding values from Figure 15 one finds that the term within the parenthesis does not vary greatly from 1/2. Thus, in the avoidance of high power subsidiary resonance a primary restriction is the minimum field

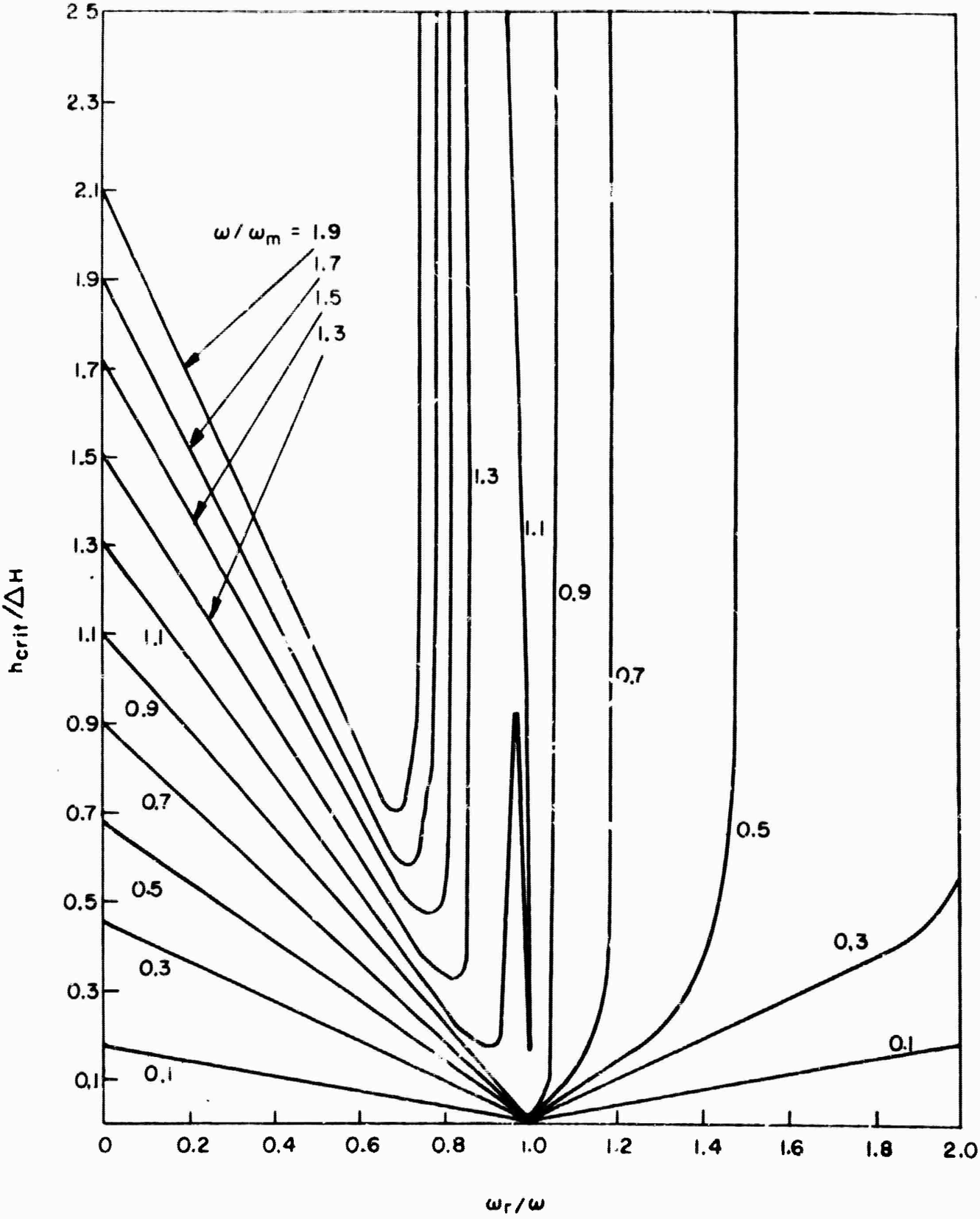

FIG. 14 -- THRESHOLD FOR SUBSIDIARY RESONANCE IN A ROD FOR THE UNIFORM PRECESSION. ($\Delta H/4\pi M = 0.003$). REF. 4.

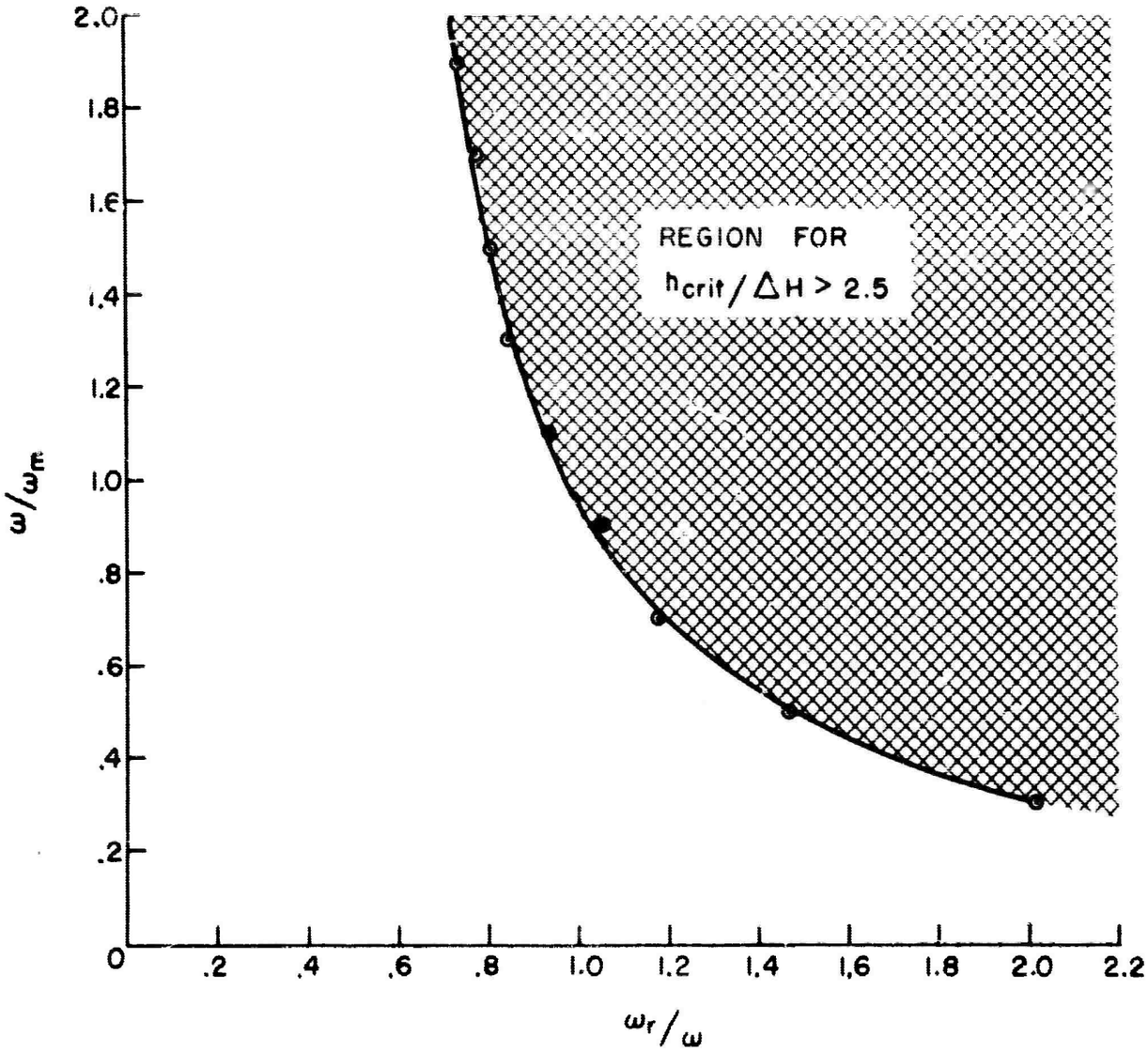

FIG. 15 -CRITICAL RELATIONSHIP OF SATURATION MOMENT AND MAGNETIC FIELD FOR THE AVOIDANCE OF HIGH POWER SUBSIDIARY RESONANCE.

$$H_o + H_a = \frac{\omega}{2\gamma} , \qquad (60)$$

and we note that this relationship is independent of the saturation moment.

For low loss operation we have estimated[5] that a magnetic field at least two linewidths above the value for resonance is required to reach the low loss region above resonance; thus,

$$H_o = \frac{\omega}{\gamma} - 2\pi M_s - H_a + 2\Delta H$$

and

$$H_o + H_a = \frac{\omega}{\gamma} - 2\pi M_s + 2\Delta H.$$

The optimum design will simultaneously satisfy both of the above expressions; thus, the optimum value for saturation moment is defined.

$$4\pi M_s = \frac{\omega}{\gamma} + 4\Delta H . \qquad (61)$$

For example, at C-band (6.5 GHz) with ferrites having zero anisotropy field and a relatively narrow linewidth (70 oe) the saturation moment should be at least 2600 gauss with an applied magnetic field in the region above 1160 oersted.

At X-band (10 GHz) with ferrites having zero anisotropy field and the same linewidth, the saturation moment should be at least 3850 oe with an applied magnetic field greater than 1785 oe.

The above appraisal of material requirements for the high power phase shifter indicates that the presently available ferrite materials would be satisfactory if one were willing to operate at high magnetic fields Equation 60 shows that the addition of a small anisotropy field (500-1500 oe) to the above material characteristics would relieve the

---

5. Progress Report, First Quarter, Contract No. AF 30(602)-3495, June 23 - September 23, 1964.

problem of high operating fields. Unfortunately, the combination of desired material characteristics has not been available; consequently, a number of apparent deviations from the scope of the program have been made during the experimental phase to compensate for the ideal material characteristics.

III. FERRITES WITH HEXAGONAL CRYSTAL STRUCTURE

1. Polycrystalline Ferrites

It was pointed out in the theoretical consideration of ferrite material parameters that for operation on some portions of the material's μ' and μ'' curves, it is desirable to have a properly oriented anisotropy field in order to reduce the magnitude of the required external field. Ferrites having hexagonal crystal structures have large anisotropy fields, which are oriented either along the hexagonal axis or in the basal plane of the crystal. These are referred to as uniaxial or planar ferrites, respectively.

Uniaxial ferrites contain very large linewidths, typically on the order of 2000 oersteds. A sample of nickel-"W" uniaxial material (Sperry Microwave Electronics Company - A-127) was tested, and the results were reported in the Semiannual Technical Report on this contract.

Unfortunately, it was necessary to fabricate the experimental rod of A-127 from six small pieces cut from elliptical discs approximately 1" x 0.6" x 0.2" thick because this was the only shape available at the time. Another undesirable feature of A-127 was that its anisotropy field was so large (9500 oersteds) that the lowest applied magnetic field placed the operating region far above ferrimagnetic resonance, where the phase shift activity is consequently very low.

To remedy these difficulties a new ferrite material was ordered from Sperry. The anisotropy of A-127 was reduced by the addition of cobalt to the mix. The new material, which was designated A-130, has a composition of $BaO \cdot 2(NiO)_{.62} \cdot 2(CoO)_{.38} \cdot 7.5\ (Fe_2O_3)$ and the following characteristics:

$4\pi M_s$ = 3200-3500 gauss

ΔH = 1900 oersteds

H_a = 4500 oersteds

ϵ_r = 13.25

tan δ	=	.0028
T_c		450°C
g		1.92
crystalographic alignment	>	0.8

A special tool was made for pressing the powdered ferrite and orienting the magnetic anisotropy parallel to the long dimension of the bar. The dimensions of the rough bar were 2.3" x 0.8" x 0.4".

Two test specimens were cut 0.160" square and 2.3" long and centered on the bottom wall of RG 50/U waveguide making a rod 4.6" long. Insertion loss and phase shift for five frequencies from [illegible]-7 GHz were made. The data is given in Figure 16. The increase in both phase shift and loss with increasing frequency is indicative of increasing binding of energy to the ferrite rod. At 6.5 GHz phase shift activity reaches a maximum, and at 7.0 GHz loss has continued to increase whereas phase shift has decreased. This effect is observed when the ferrite-waveguide configuration is too large for the operating frequency, and energy is coupled into higher order modes. The best figure of merit, at 6.5 GHz, is 25 for a magnetic field swing from 800 to 1800 oersteds.

Further experiments with position of A-130 ferrite in the waveguide were conducted. Figure 17 presents the data taken at 6.5 GHz. The curves show that doubling the volume while halving the length produces approximately half the effect in both phase shift and loss. It is concluded that the addition of a second rod to the configuration in Figure 16 would not increase the phase shift at 6.5 GHz. When a single rod is positioned in the center of the waveguide, the activity is greatly reduced. It is felt that the loss of activity is due to reduced coupling to the ferrite and that full activity could be restored with a larger diameter ferrite rod.

A series of measurements were made on a phase shifter which consisted of a stripline loaded with A-130 ferrite. This

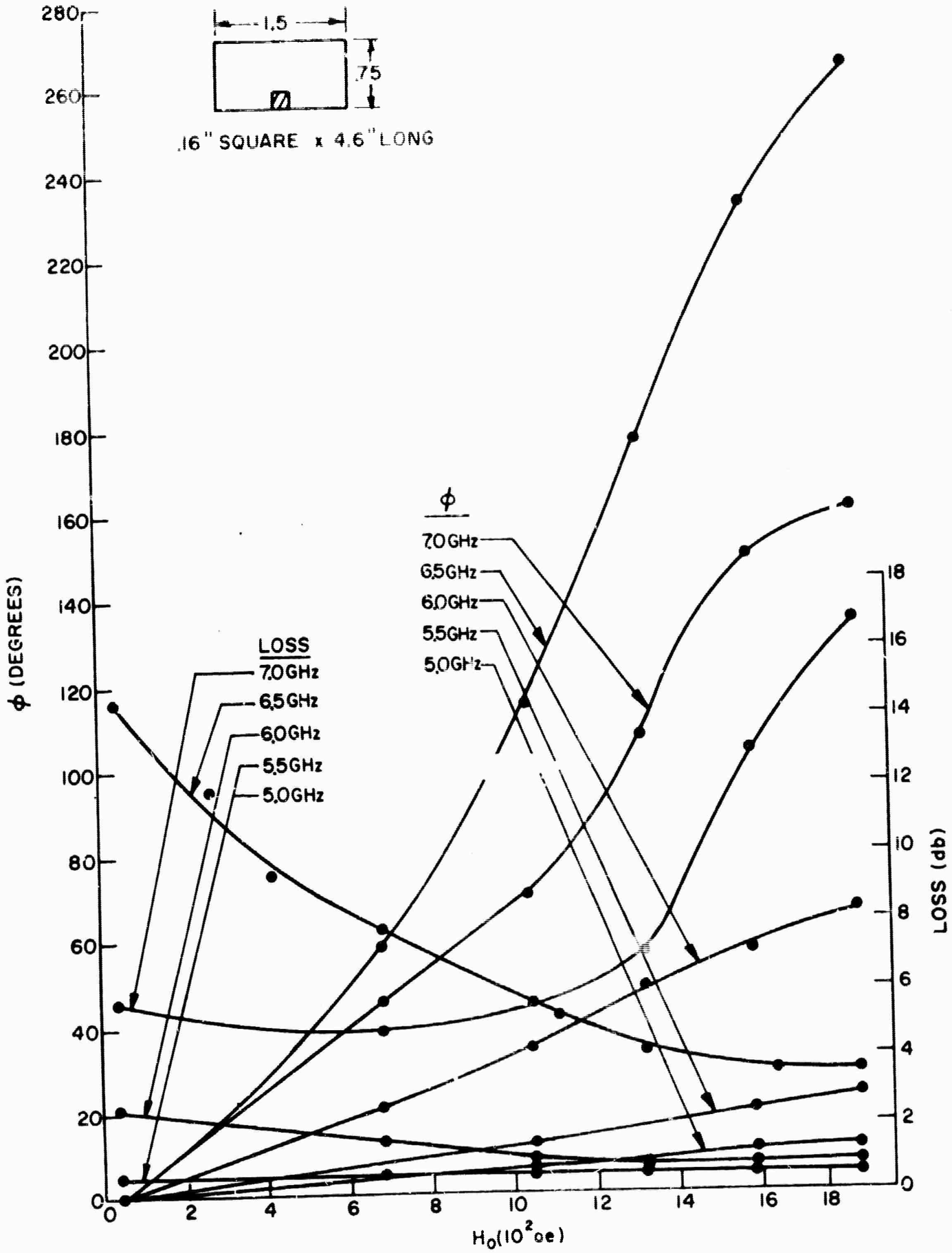

FIG. 16 -LOSS AND PHASE SHIFT OF A-130 FERRITE, AS A FUNCTION OF FREQUENCY.

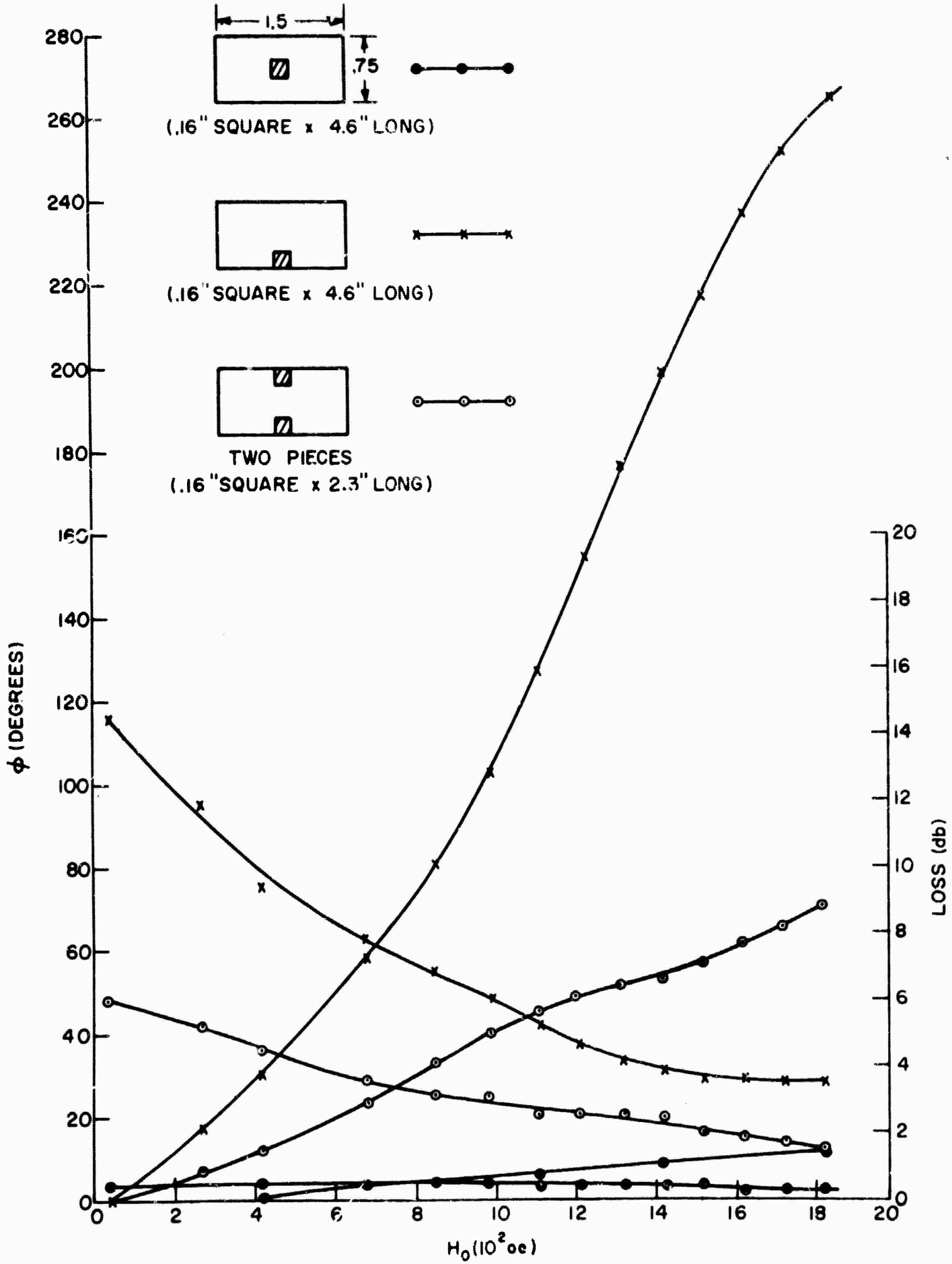

FIG. 17 – LOSS AND PHASE SHIFT OF A-130 FERRITE, AS A FUNCTION OF ROD POSITION AT 6.5 GHz

configuration was chosen in order to study the effects of a high-anisotropy material in a TEM mode of propagation. Two ferrite slabs which measured 3.25" x 0.160" x 0.048" were used to load a 4" stripline structure. The center conductor dimensions were 0.001" x 0.010", which gave an output impedance of 25 ohms for the line.

Figure 18 shows the phase shift and loss characteristics of the stripline phase shifter at 6.5, 6.0, and 3.0 GHz. The maximum figure of merit obtained was 16°/db at 6.0 GHz for a magnetic field variation of 1000 oersteds. The measured figures of merit were poor in all the experiments with uniaxial ferrites. This result is in agreement with the theoretical consideration that narrow linewidths are necessary for good figures of merit. It was therefore concluded that the uniaxial class of hexagonal ferrites would not be satisfactory for operation on the high magnetic field side of resonance unless their linewidth could be reduced at least an order of magnitude.

Planar anisotropic ferrites have linewidths substantially smaller than uniaxial ferrites; however, their anisotropy field is considerably larger than desired for "C" or "X" band operation. Nevertheless, a sample of planar material was obtained from Sperry Microwave Electronics Company to demonstrate the advantages of narrow linewidth materials having an anisotropy field to reduce the requirement for large external magnetic fields. In order to be able to operate close to resonance, the experiment was made at 21.75 GHz. This material, designated HP-42A, has the following characteristics:

$4\pi M_s \approx 3500$ gauss

$\Delta H \approx 324$ oersteds

$H_a \approx 7000$ oersteds

$g = 1.92$

The sample had a rectangular cross section which was small compared to the sample length. In the experiment the length was fixed at 1.5" while the cross section was varied. The results of the phase shift and

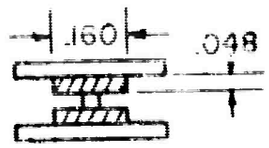

FERRITE, TWO PIECES – .160" x .048" x 3.25" LONG
CENTER CONDUCTOR – .001" x .010"

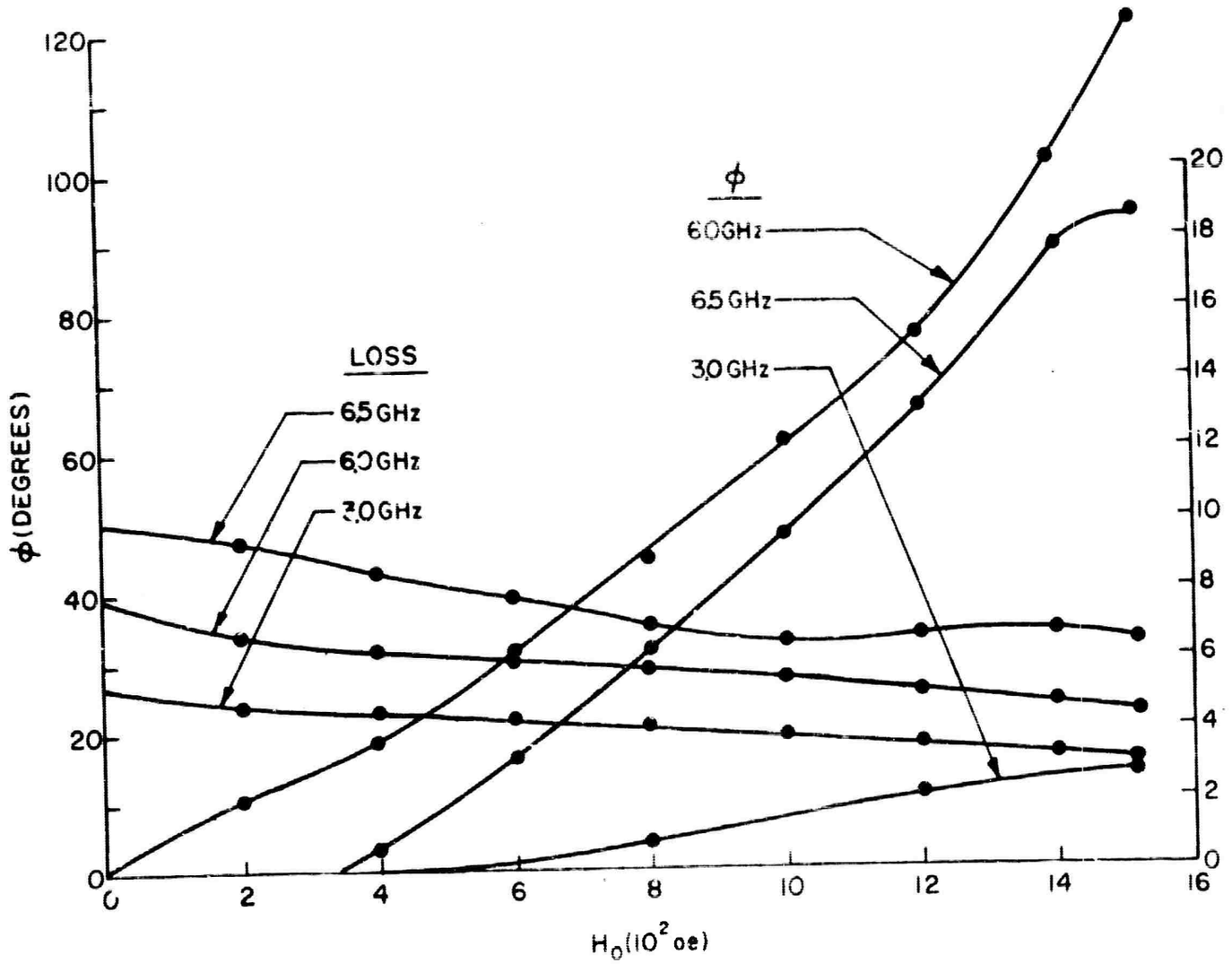

FIG. 18 – LOSS AND PHASE SHIFT OF A – 130 FERRITE IN STRIPLINE.

loss measurements are given in Figures 19, 20, and 21. Because of an observed hysteresis effect, the measurements were made starting above magnetic saturation at the maximum available magnetic field (designated as the + direction). Data was taken as the field was decreased through zero, reversed, and increased to maximum in the negative direction. The sample was longitudinally magnetized and positioned on the axis of RG 53/U waveguide (0.420" x 0.170"). The ferrite was oriented so that the easy plane of magnetization was the plane of the electric vector and the direction of propagation; thus, the externally applied field was in the easy plane and could induce the large anisotropy field in the sample.

From Figures 19, 20, and 21 it can be shown that as the thickness of the ferrite varied from 0.0945" to 0.075" to 0.055" the figure of merit maximizes at 0.075". The figure of merit is the total observed phase shift divided by the maximum observed value of the insertion loss in the range from 0 to +1000 oersteds. The peaking in the figure of merit is due to several effects which cannot be separated, but is explained as follows: If one considers that a pure TE type mode is propagated in the presence of the ferrite, then as the ferrite cross sectional dimensions are reduced the binding of the electromagnetic energy, and hence the interaction, is reduced. The results are a decrease in both phase shift and insertion loss. Their rate of decrease, therefore, affects the figure of merit. However, the simple case of a pure TE mode does not hold for this experimental configuration. It was pointed out in the theoretical discussion that as the ferrite dimensions increase, one no longer has pure TE or TM type modes, but rather some more complicated mode containing both electric and magnetic components in the direction of propagation. Therefore, as the dimensions are varied, one has the combined effect of a change in binding and a change in the field structure within the ferrite.

The best figure of merit for HP-42A was 125.7 degrees per db of insertion loss which occurred for a cross section of 0.1435" x 0.075" centered in 0.420" x 0.170" waveguide. A direct

INS. LOSS (db)

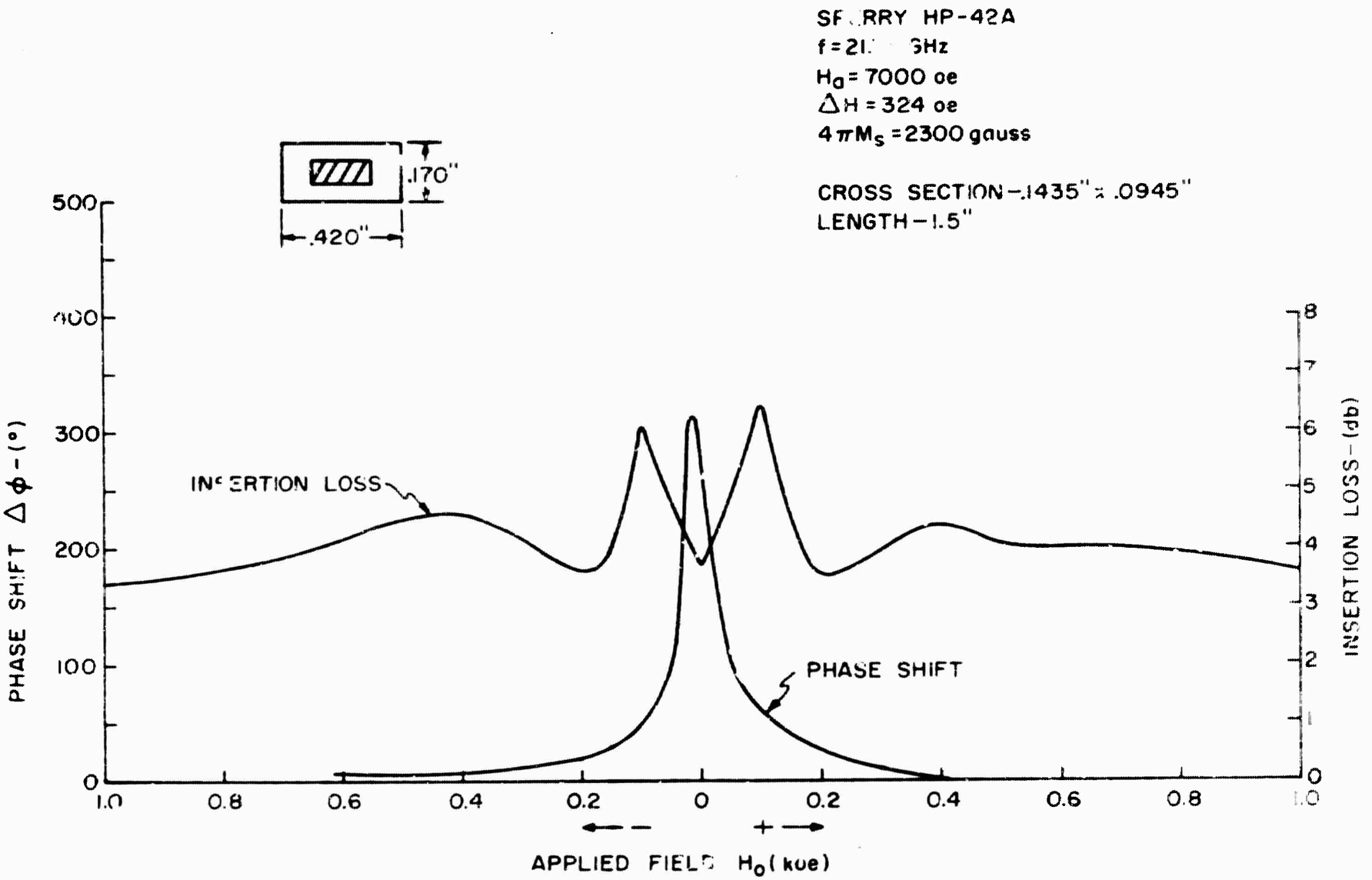

FIG. 19 – PHASE SHIFT AND INSERTION LOSS OF A PLANAR HEXAGONAL FERRITE – CROSS SECTION .1435" x .0945".

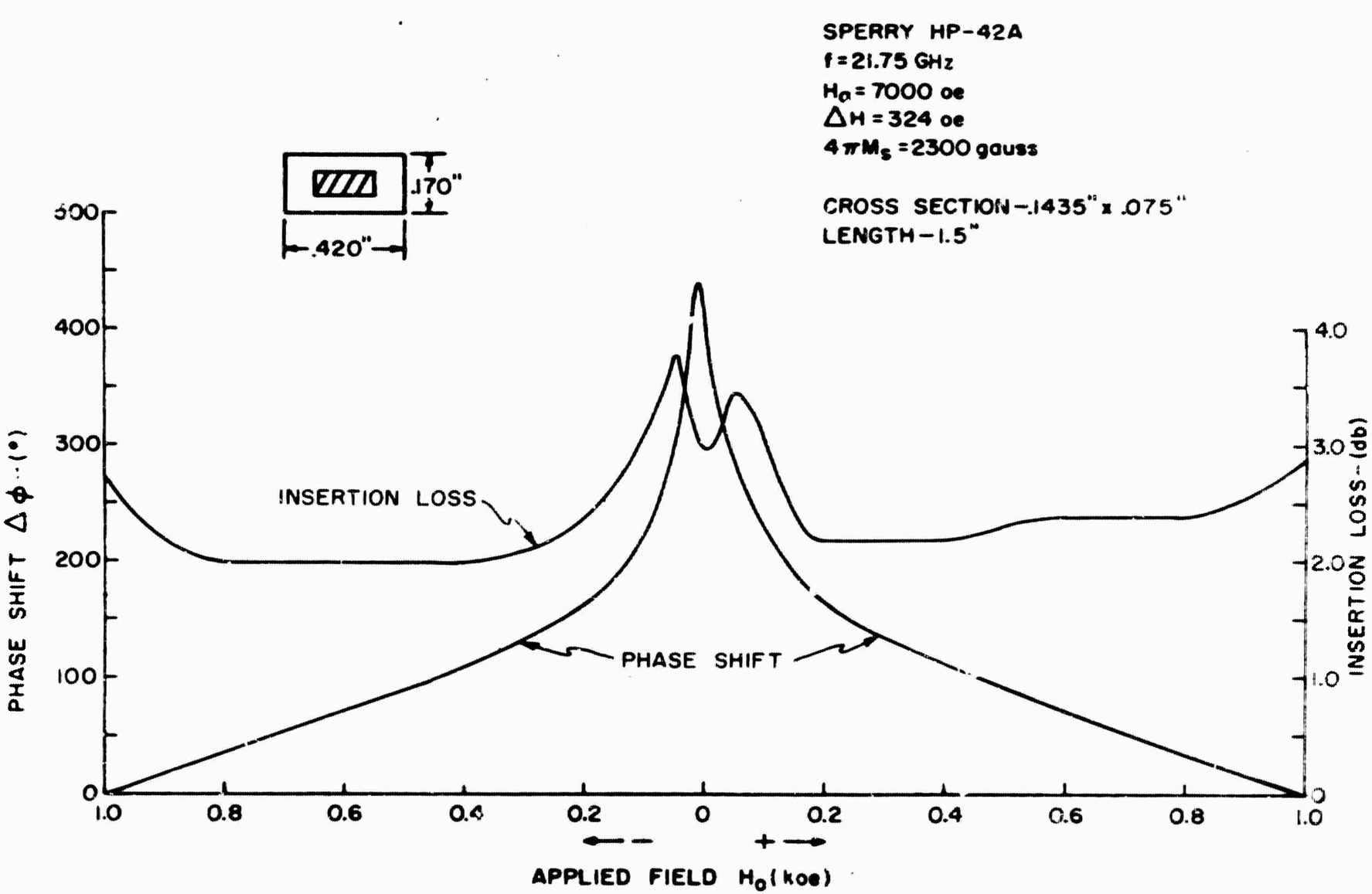

FIG. 20 – PHASE SHIFT AND INSERTION LOSS OF A PLANAR HEXAGONAL FERRITE – CROSS SECTION .1435" x .075"

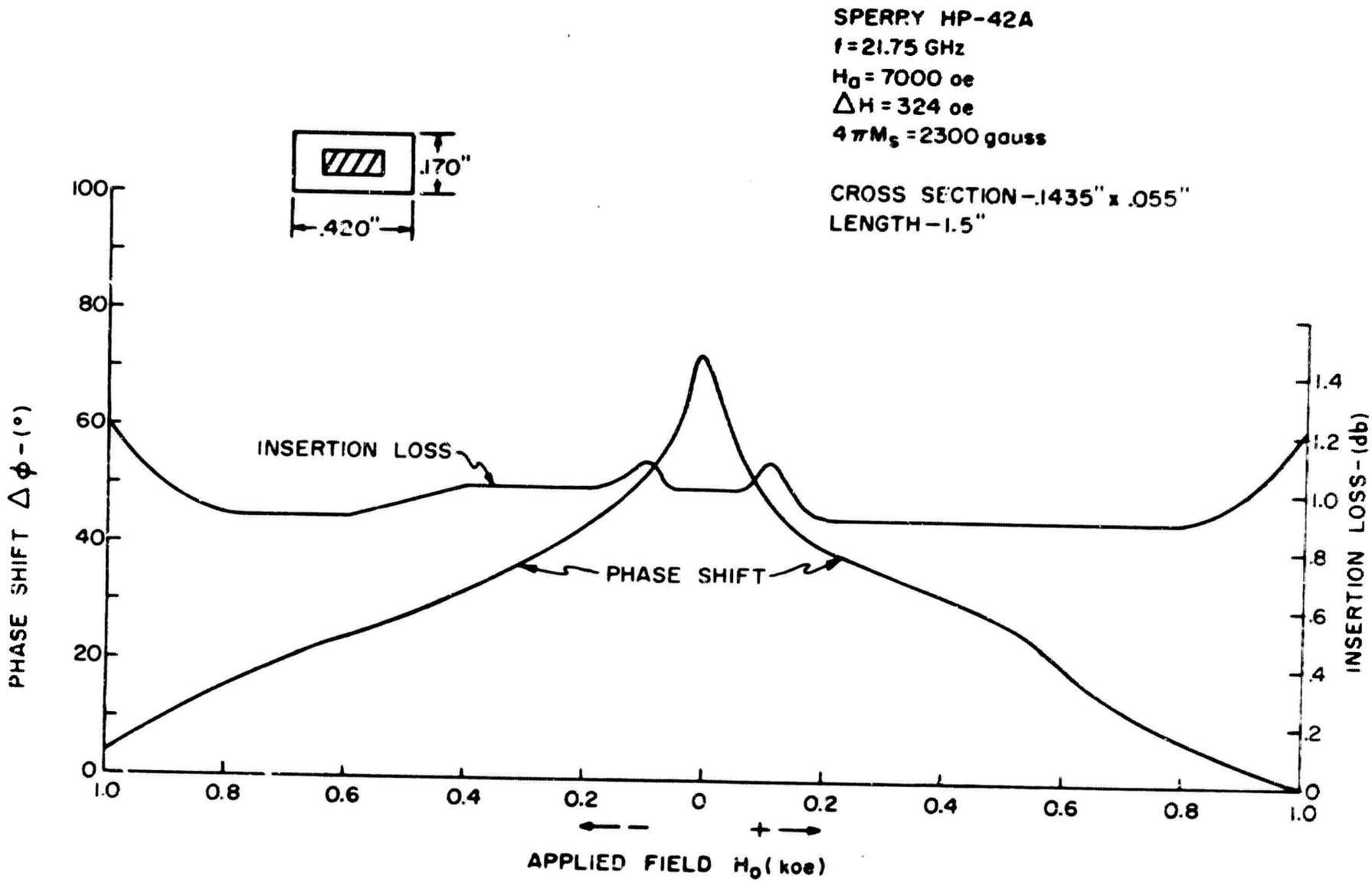

FIG. 21 – PHASE SHIFT AND INSERTION LOSS OF A PLANAR HEXAGONAL FERRITE – CROSS SECTION .1435" x .055"

comparison, based on a decrease in linewidth, between the planar ferrite and the uniaxial ferrite cannot be made because of the variation in the other material properties ($4\pi M_s$, H_a and hence ω_r). The largest observed figure of merit for the uniaxial ferrite was of the order of 25 degrees per db of insertion loss. With this criteria the planar material appears substantially better. A further decrease in linewidth would be expected to increase the figure of merit. The inverse proportionality relationship between linewidth and figure of merit predicts that a linewidth of 100 oersteds in a ferrite with material characteristics of HP-42A could yield a figure of merit as large as 375 degrees per db of insertion loss. It is noted that planar anisotropic ferrites have been reported with linewidths of 150 oersteds.[6,7] When further reduction in linewidth is realized in these materials, consideration should be given to their application in K-band, high power phase shifters.

2. Single Crystal Ferrites

The largest reduction in linewidth, and hence largest increases in figure of merit, can be achieved through the use of single crystals. Several samples of Zn-Y, a planar anisotropic ferrite with hexagonal crystal structure, were obtained from Mr. Arthur Tauber of the U.S. Army Electronics Research and Development Laboratories, Fort Monmouth. The magnetic properties of this material are:

$4\pi M_s$ = 2500 gauss

H_a = 10,000 oersteds

ΔH = 10 oersteds.

---

6. I. Bady and G. McCall, "Ferromagnetic Line Width of Nonoriented Polycrystalline Hexagonal Ferrites With Large Magnetic Anisotropy Fields," IEEE Trans., Vol. MTT-1, No. 5, pp. 442-443; September, 1963.

7. R. Harvey, I. Garden and R. Braden, "Hexagonal Magnetic Compounds," RCA Laboratories, Princeton, N.J., Quarterly Report No. 6, Contract DA 36-034 sc-87533; December, 1962.

Since the size of the available single crystals were so small, it was decided to test this material in a configuration which would afford the maximum interaction between the ferrite and the electromagnetic field. Such a structure is the fully filled rectangular waveguide. Propagation in the structure was initially analyzed on the assumption that the dimensions of the waveguide could be reduced such that only the dominant, TE_{10}, mode could propagate. For this type of operation the y- component of the RF magnetic field is zero, and hence elements of the permeability tensor are the diagonal components given by Equations 25 and 26. Because of the large value of H_a the experiment to measure the figure of merit of single crystal Zn-Y ferrite was designed to operate at 31.5 GHz in order to operate in the low loss region just above resonance. The waveguide consisted of one inch long tapers from RG 96/U (0.280" x 0.140") to a cross section of 0.046" x 0.023". The total length of the reduced section was 0.385". The taper sections were appropriately loaded with stycast to effect the transition to the ferrite. The experiment was unsuccessful because energy would not propagate through the structure. It was concluded that the assumed value of permeability was too high and that the reduced size waveguide was beyond cutoff. Further theoretical analysis with the parallel plane waveguide model outlined in Section II points out that regardless of the waveguide dimensions a fully filled waveguide cannot propagate a pure TE type mode and that propagation is also a function of the off diagonal terms of the permeability tensor (κ). An exact form of the propagation constant is not known since the field configuration in such a medium is quite complicated. However, if the height of the guide is reduced to a point where rotation is prohibited, it is felt that the form of the propagation constant will be very similar to that of the fully filled parallel plane waveguide. The effective permeability will then be given by Equation 46.

$$\mu_e = \frac{\mu^2 - \kappa^2}{\mu} \quad . \tag{46}$$

Examination of the form of μ and κ indicates that, on the high magnetic field side of resonance, both μ and κ are positive quantities and hence $\mu_e < \mu$. This accounts for our structure being cutoff, since the scale factor used in reducing the guide dimensions was based on μ rather than the more correct permeability, μ_e.

There was not sufficient material left to construct another device using Zn-Y ferrite and since the operating frequency for this material was considerably above the range of interest on this contract, no further work was performed on Zn-Y. The initial interest in Zn-Y stemmed from its availability and the fact that the performance at 31.5 GHz could be related to the performance at the frequencies of interest of very narrow linewidth materials with zero anisotropy fields. In the initial incorrect model figures of merit (based on $\Delta\mu_e'/\mu_e''$) is expected to be even larger because, as seen in Figures 12 and 13 for TT2-111 and lithium ferrite, respectively, $\Delta\mu_e'/\mu_e''$ is larger than $\Delta\mu'/\mu''$.

The high value of H_a and narrow linewidth of Zn-Y suggests that it may be profitable to examine its application to K-band high power phase shifters when large pieces of Zn-Y become available.

IV. FERRITES WITH CUBIC CRYSTAL STRUCTURE

1. Polycrystalline Ferrites

One of the major problems encountered with ferrite in waveguide has been the appearance of a second resonant peak at values of applied magnetic field above ferromagnetic resonance. These secondary peaks are believed to be caused by the existence of a cavity mode within the ferrite. The physical size of the ferrite is such that at certain values of μ' there is a loss of transmitted energy as a result of energy being coupled into the ferrite cavity. This so-called "body resonance" can be eliminated by simply reducing the size of the ferrite until the second resonance disappears. A necessary consequence of the ferrite reduction is the loss of "activity", or phase shift. This was certainly to be expected because of the dependence of phase shift on ferrite volume within the waveguide. However, once the maximum size of the ferrite (which could be used without supporting a "body resonance") was determined, the volume of ferrite within the waveguide could be increased by using multiple loading of identical ferrite pieces.

A long thin rod of TT2-111 ferrite, which has a $4\pi M_s$ of 5000 and a linewidth (ΔH) of 135, was measured for insertion loss as a function of magnetic field at 7.5 GHz in RG 50/U waveguide. The initial size of the ferrite rod was chosen to be 4.75" long by 0.125" in diameter. This diameter was chosen to be small enough to prevent Faraday rotation of the plane of polarization and large enough to support a cavity mode. The data on the measurements taken for this ferrite rod is shown in Figure 22. The effect of the body resonance can be seen as a second resonance curve which has its peak value at 1540 oersteds; while the main or ferromagnetic resonance occurs at 610 oersteds. A calculation of the field required for ferromagnetic resonance at 7.5 GHz for TT2-111 shows that resonance should occur at 180 oersteds. This discrepancy in the measured and calculated values of magnetic field required for resonance can be accounted for by the demagnetizing factor of the

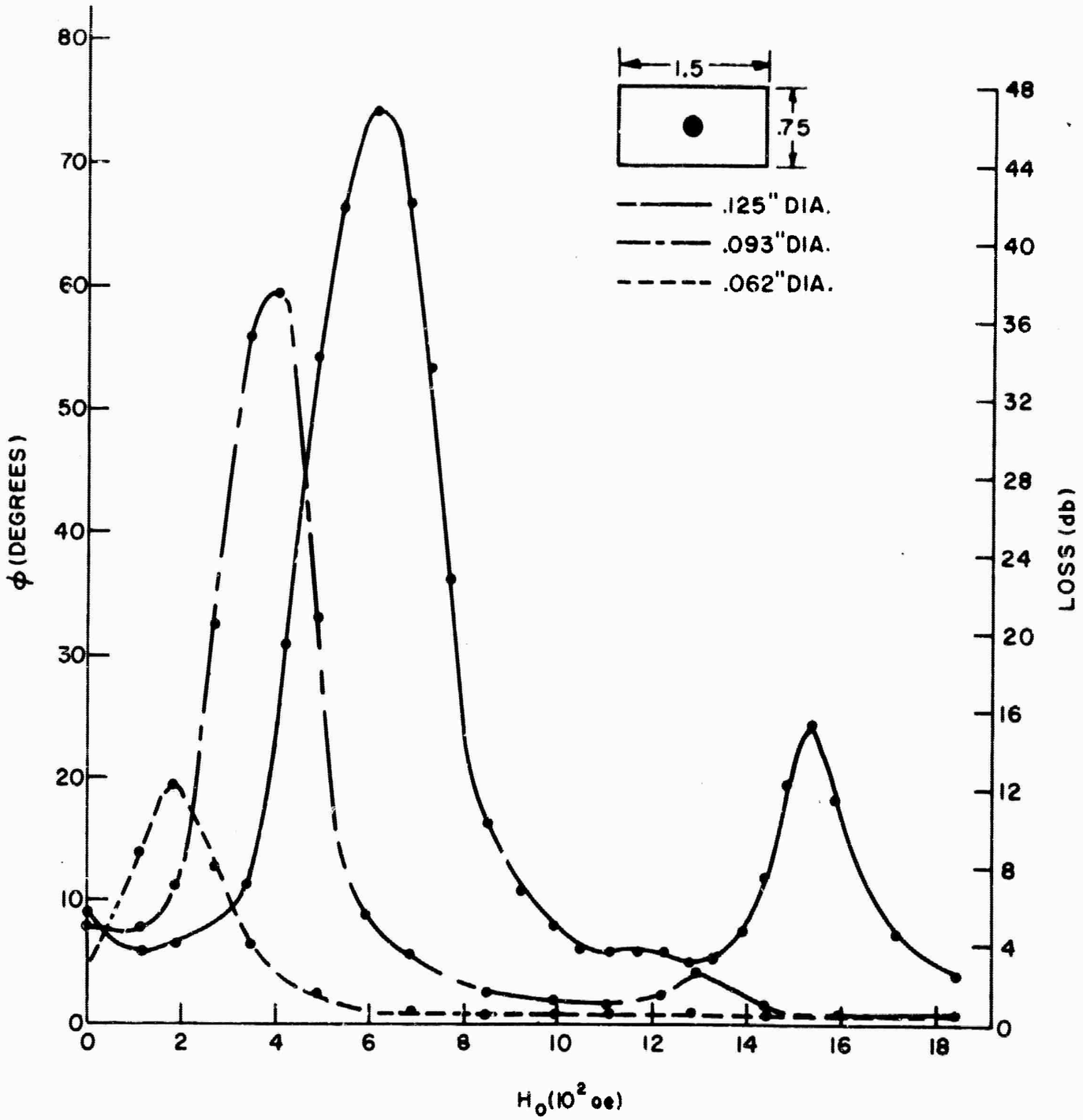

FIG. 22 – EFFECT OF ROD DIAMETER ON RESONANCE CHARACTERISTICS OF TT2-111 AT 7.5 GHz

ferrite rod. Apparently, the length to diameter ratio is not large enough to give a demagnetizing factor equal to 0.5. The demagnetizing factor computed from the measured data for the 0.125" rod is 0.41.

Reducing the diameter of the ferrite rod had a twofold effect on the measured characteristics of the phase shifter. The body resonance disappeared, and ferromagnetic resonance occurred at decreasing values of applied magnetic field. These effects can be seen in Figure 22. With a rod of 0.062" diameter there is no sign of a body resonance and the field for ferromagnetic resonance is that predicted with a demagnetizing factor of 0.5. One might question by looking at the data of Figure 22, whether the second resonance disappeared because the volume of ferrite within the waveguide was reduced or because of the anti-resonant dimensions of the ferrite. The explanation is the latter, and this is demonstrated by increasing the volume of ferrite loading in the waveguide with three 0.062" diameter ferrite rods. These results are shown in Figure 23. It is seen that the ferromagnetic absorption increased from 12 db with a single rod to 35.6 db with the three rods, and that there is no evidence of a body resonant peak. Phase shift has increased more than threefold, from 13.5° to 50°.

A second increase in ferrite loading, in this case doubling the volume with six identical 0.062" diameter ferrite rods, produced the loss and phase shift characteristics shown in Figure 24. Although the loss increased only 50%, the phase shift increased 260%; however, the effect of body resonance began to appear at 1170 oersteds. The figure of merit is approximately 33° per db of insertion loss.

Measurements of phase shift and loss were also made at 7.0 GHz on the phase shifter loaded with six ferrite rods. At the lower frequency less energy is coupled into the body resonance as can be seen in Figure 25 and the figure of merit has increased to 54° per db.

Reducing the frequency to 6.5 GHz produces the loss and phase shift characteristics shown in Figure 26. At this frequency

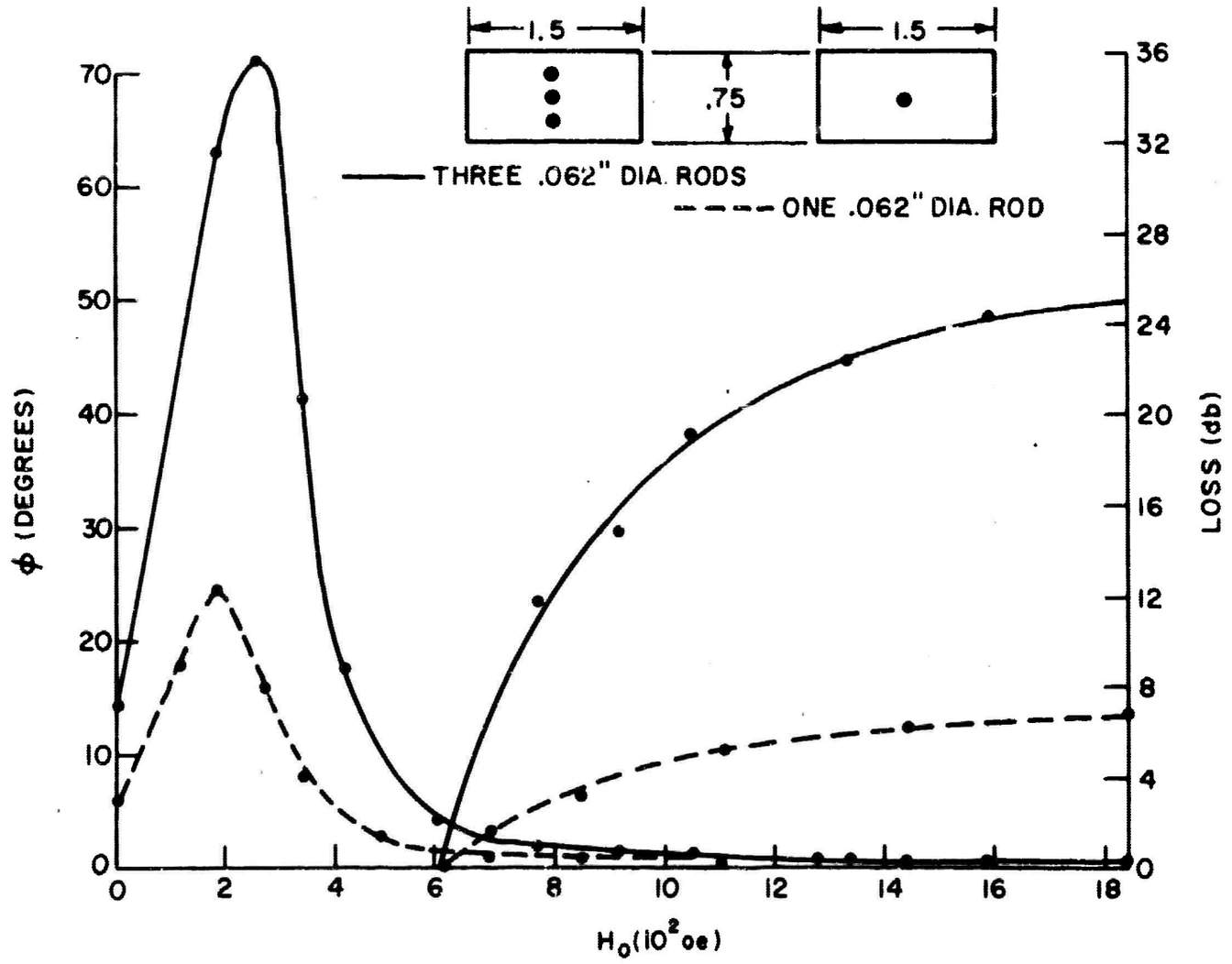

FIG. 23 - LOSS AND PHASE SHIFT FOR THREE RODS vs ONE ROD OF TT2-111 AT 7.5 GHz

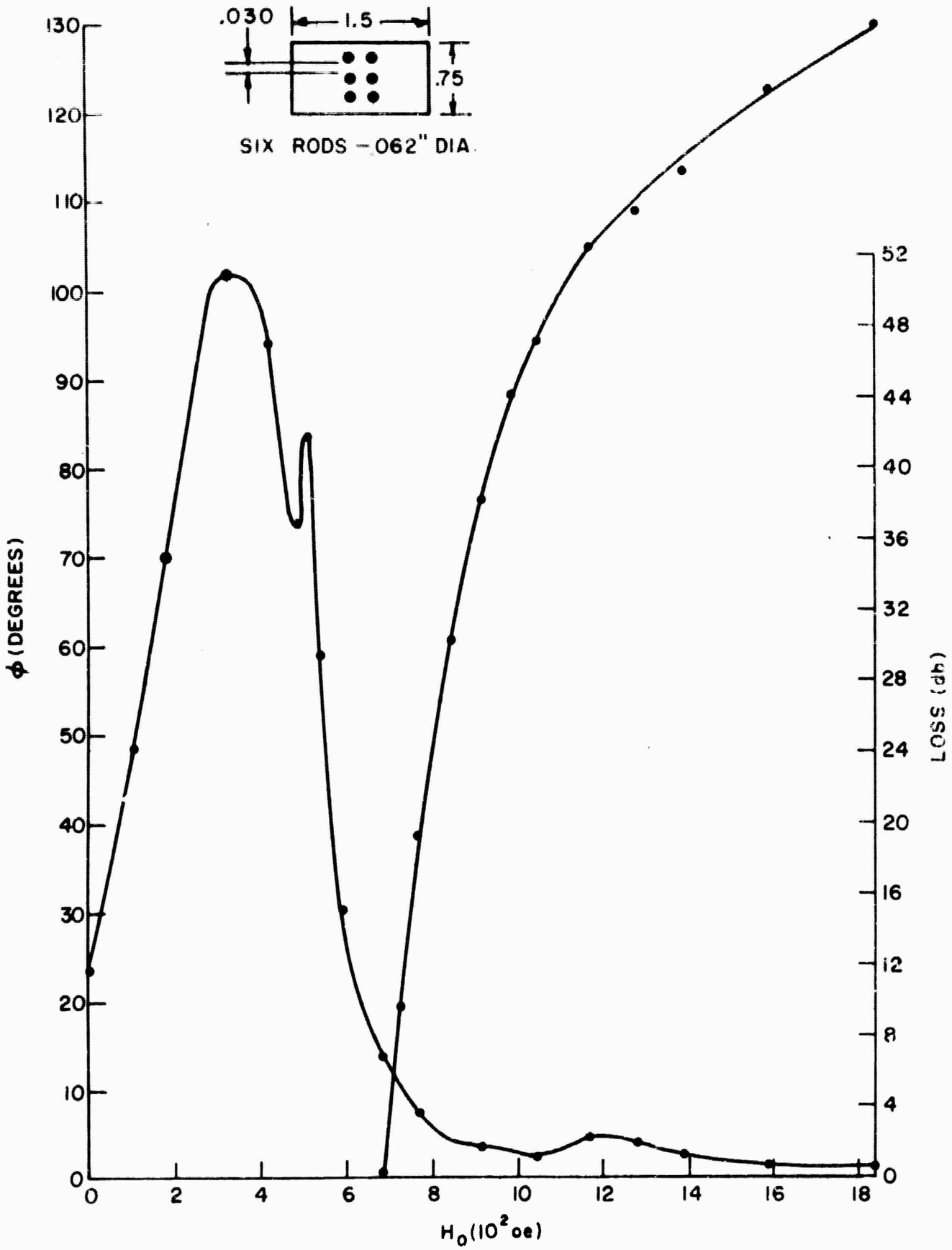

FIG. 24 – LOSS AND PHASE SHIFT FOR SIX RODS OF TT2–111 AT 7.5 GHz

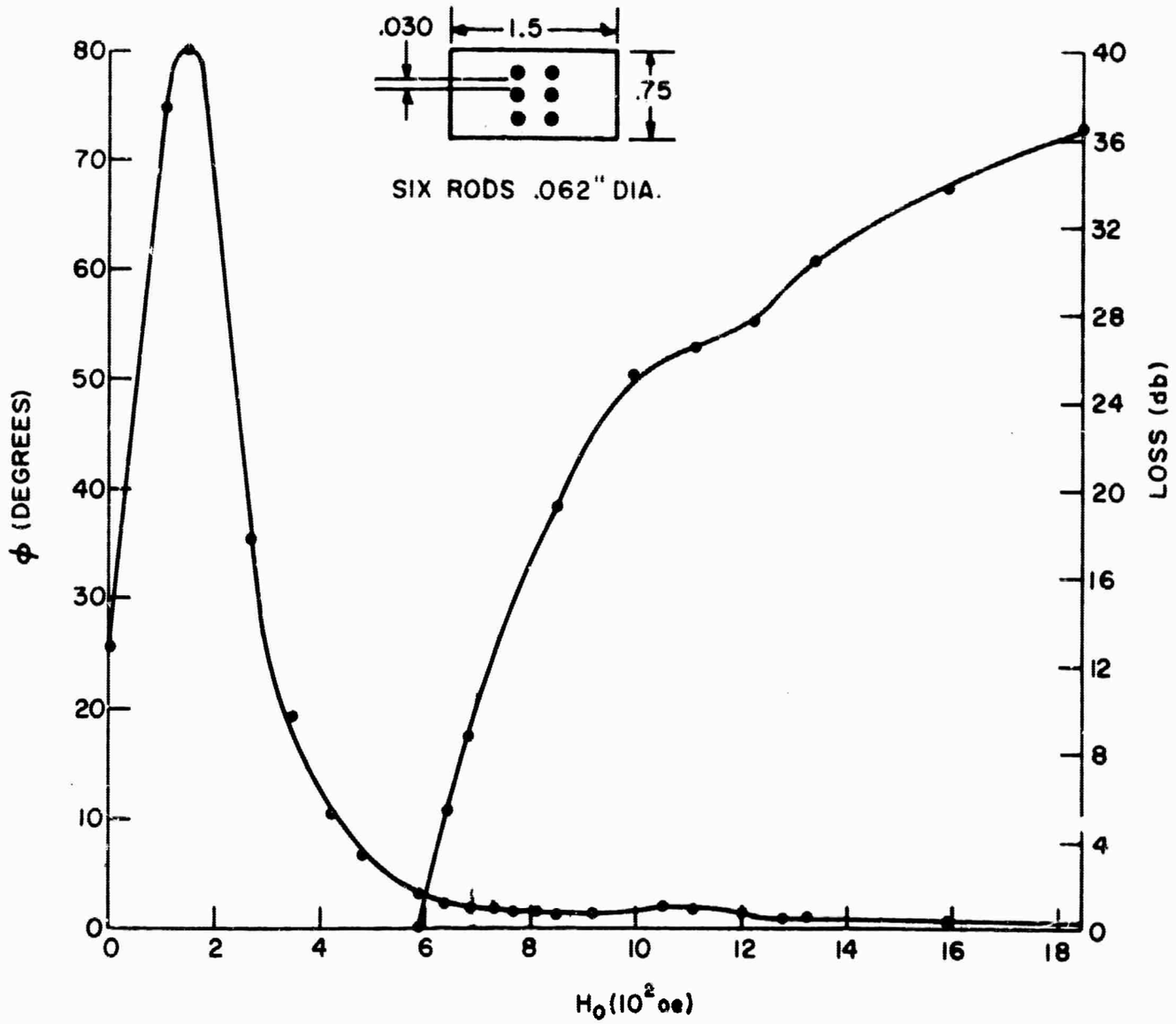

FIG. 25 – LOSS AND PHASE SHIFT FOR SIX RODS OF TT2-111 AT 7.0 GHz

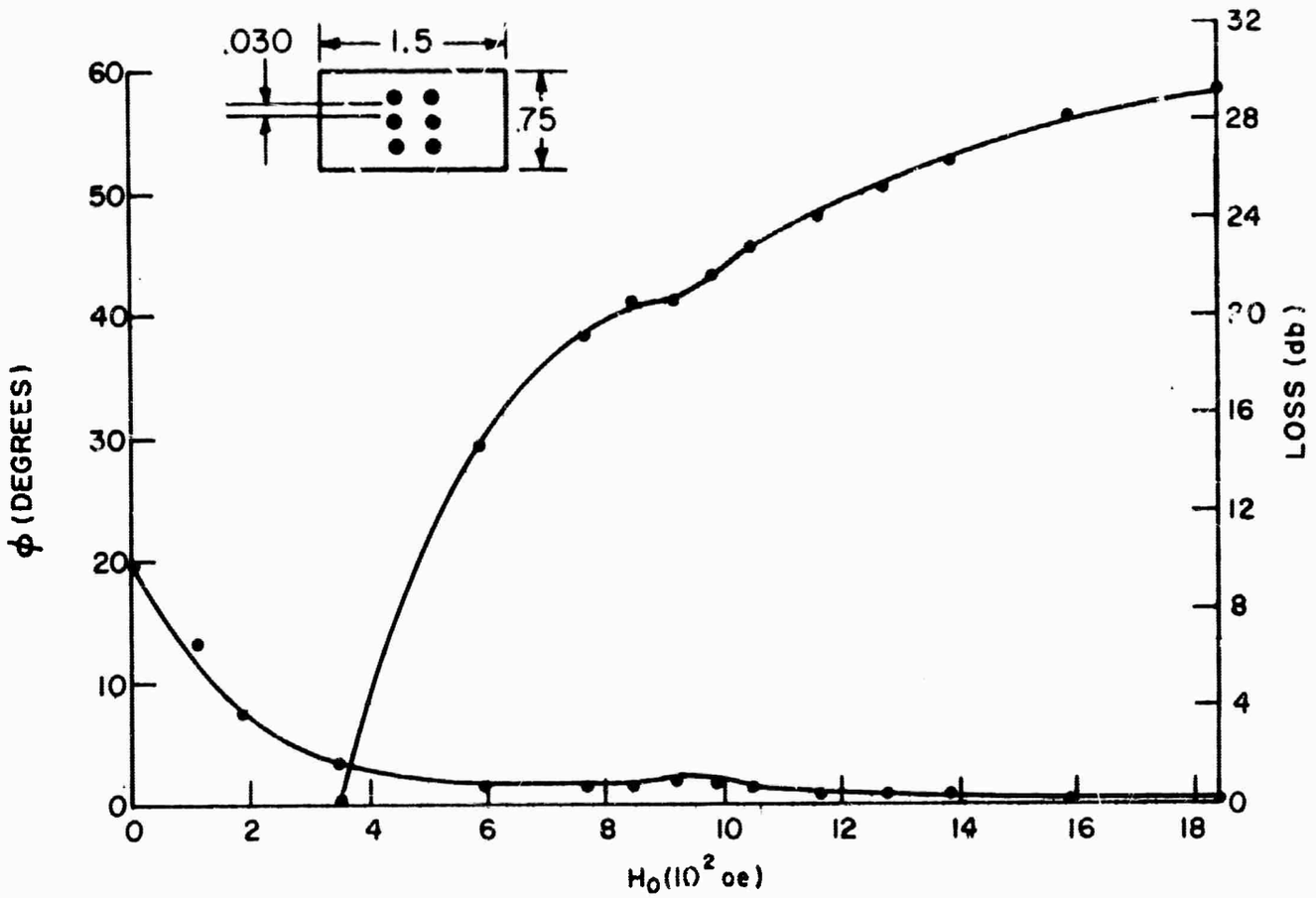

FIG. 26 – LOSS AND PHASE SHIFT FOR SIX RODS OF TT2-111 AT 6.5 GHz

ferromagnetic resonance occurs at a negative value of applied magnetic field; therefore, the peak does not appear in the data. There is still evidence, even at this lower frequency of a body resonance. The figure of merit at this frequency is 45° per db of loss. It should be noted here that all of the figures of merit above were calculated for applied magnetic fields variation of 1000 oersteds.

An alternate approach to thin ferrite rod loading is thin ferrite slab loading. The results of a considerable number of experiments on this geometry where all of the slabs were positioned on the broad wall of the waveguide were presented in the Semiannual Report. When the slab was positioned in the center of the waveguide, body resonance vanished as shown in Figure 27. It was then decided to place three ferrite slabs in the center of the waveguide. Figure 28 gives the characteristics of a phase shifter with three slabs of yttrium iron garnet, each measuring 4.0" x 0.400" x 0.050"; and Figure 29 shows the results using garnet slabs which are 4.0" x 0.400" x 0.040". The reduction in slab thickness from 0.050" to 0.040" removed the subsidiary loss peak on the upper skirt of the main resonance curve. The best figure of merit for the garnet slabs is 21 (see Figures 28 and 29). The value was computed for the region 1200 to 1800 oersteds.

During the first half of this program all of the potentially acceptable polycrystalline ferrites were examined for use in the high power phase shifter. The results of this work have been reported in the Semiannual Technical Report, January 15, 1965. It was then concluded that none of the presently available polycrystalline ferrites would be satisfactory because of their high loss and low phase shift characteristic. The theory in Section II has specified that a narrow linewidth is the principal requirement for a good phase shifter figure of merit, and calculations indicate that linewidths on the order of 10 oersteds would be needed. It was found that the narrow linewidth characteristic is available only in single crystal ferrites.

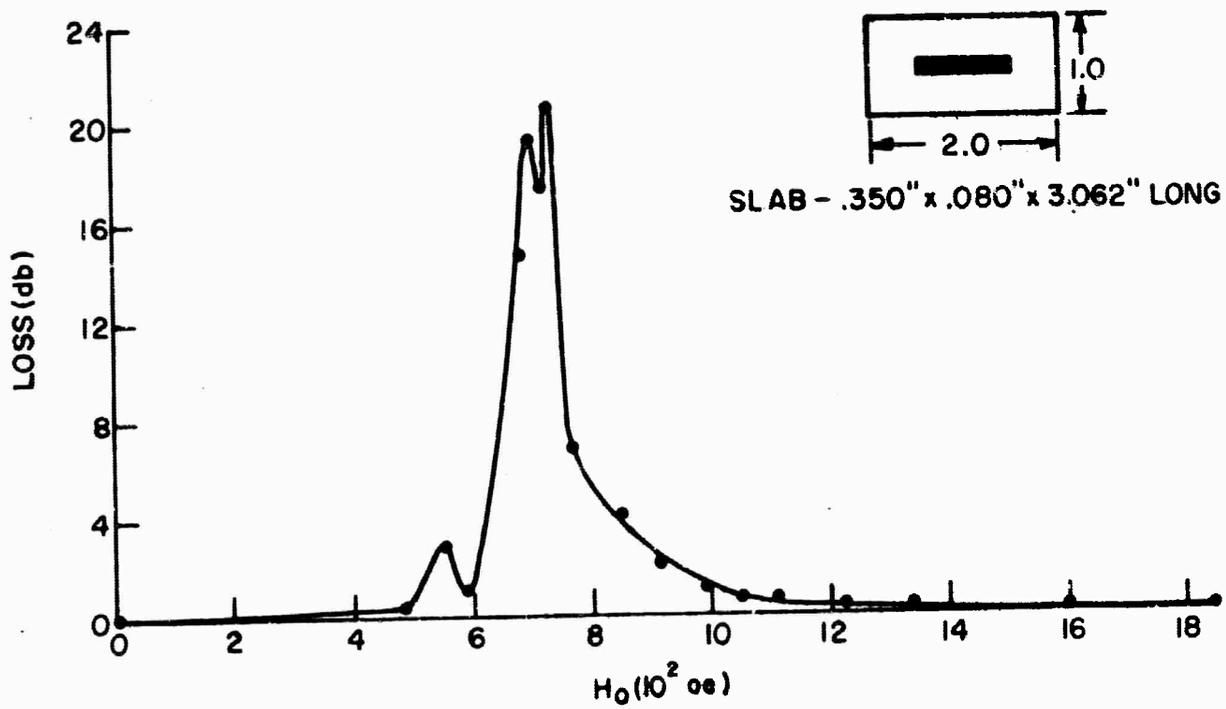

FIG.27 - LOSS CHARACTERISTIC FOR ONE SLAB OF LITHIUM IRON GARNET AT 4 GHz

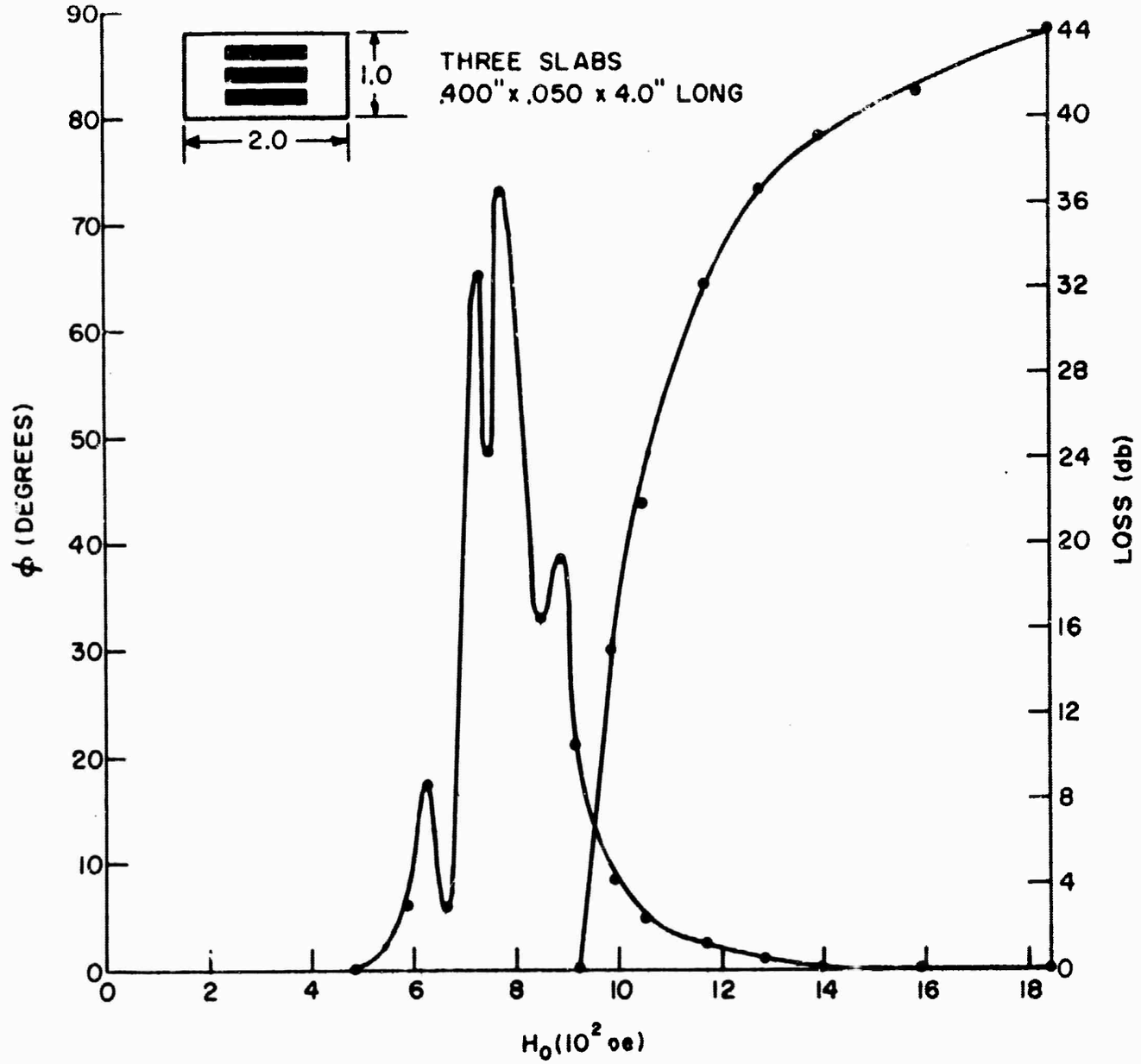

FIG. 28 – LOSS AND PHASE SHIFT FOR THREE SLABS OF TTG-113 AT 4 GHz

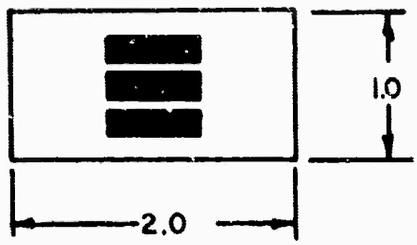

THREE SLABS - .400"x.040"x4.0" LONG

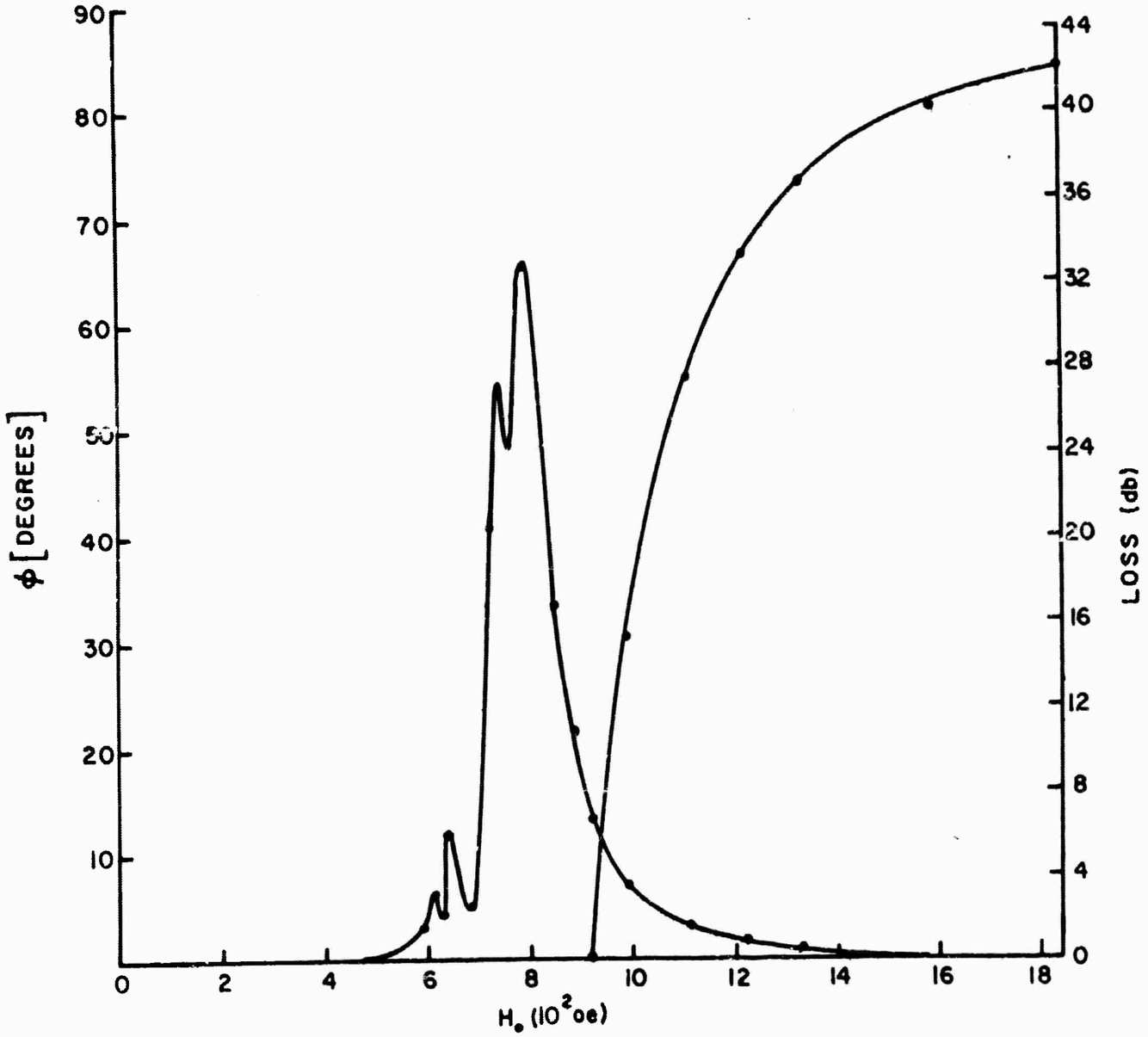

FIG. 29 - LOSS AND PHASE SHIFT FOR THREE SLABS OF TTG-113 AT 4 GHz

2. Single Crystal Ferrites

The most readily available single crystal ferrite is yttrium iron garnet. It has exhibited linewidths as low as 0.5 oersteds in small spheres; however, garnet is not wholly acceptable because its saturation moment is only 1780 oersteds, making resonance occur at 1420 oersteds at 6.5 GHz. To reach the low loss region the operating magnetic field would have to be above 1500 oersteds which was judged to be excessive for a practical phase shifter.

A hitherto unexplored material is lithium ferrite. In single crystal form it appears to possess all the desired characteristics for a C-band high power phase shifter. Linewidths of 3-5 oersteds at C-band have been reported, the saturation moment is 3600 gauss, and the Curie temperature is 670°C. A search for a source of large single crystals of lithium ferrite, fortunately, located several pieces in stock at Airtron.* These crystals which were grown during some earlier work done at Airtron were purchased for study in this program.

---

* Airtron Division, Litton Industries, Morristown, New Jersey.

V. LITHIUM FERRITE

The first test specimens of single crystal lithium ferrite designated Li"F"-1 were in the form of thin plates 0.050-.100 inch thick and 0.5 to 1 inch on a side. (See Figure 30.) Preliminary measurement of phase shift and insertion loss at C-band was made with the crystal in its original uncut state positioned in the center of the waveguide. The data showed that the saturation moment was approximately 3500 oersteds. The measured linewidth was approximately 100 oersteds, which was an order of magnitude larger than anticipated. A measurement of the dc resistivity between parallel conducting fac s deposited on the test specimen gave 447 ohm-cm; the loss tangent measured at 5.5 GHz was 0.08. This test was made in a waveguide cavity with a small rod of lithium ferrite positioned at a point of minimum RF magnetic field. The dielectric constant obtained from the same test was 17.5.

In the process of grinding the crystals prior to slicing, it was found that the interiors contained large flux inclusions and voids as shown in the photograph, Figure 31. Further grinding to salvage a usable specimen was not successful due to crumbling and parting at already existing cracks, one of which can be clearly seen in Figure 30.

In the pursuit of higher quality lithium ferrite Airtron again was contacted and Mr. D.A. Lepore, who is an authority on the subject of single crystal growth, was able to undertake the task of growing large single crystals.

In the past lithium ferrite had been available only in very small specimens and because of its limited use, the technology for the production of large pieces with high purity had not been developed. In preparation for growing large crystals four small (250 ml) experimental batches, with iron to lithium weight ratios ranging from 0.5 to 2, were made to determine the recipe which would produce crystals with the highest resistivity. These batches were designated Li"F"-2 through Li"F"-5. From each batch selected specimens were chosen to be ground on

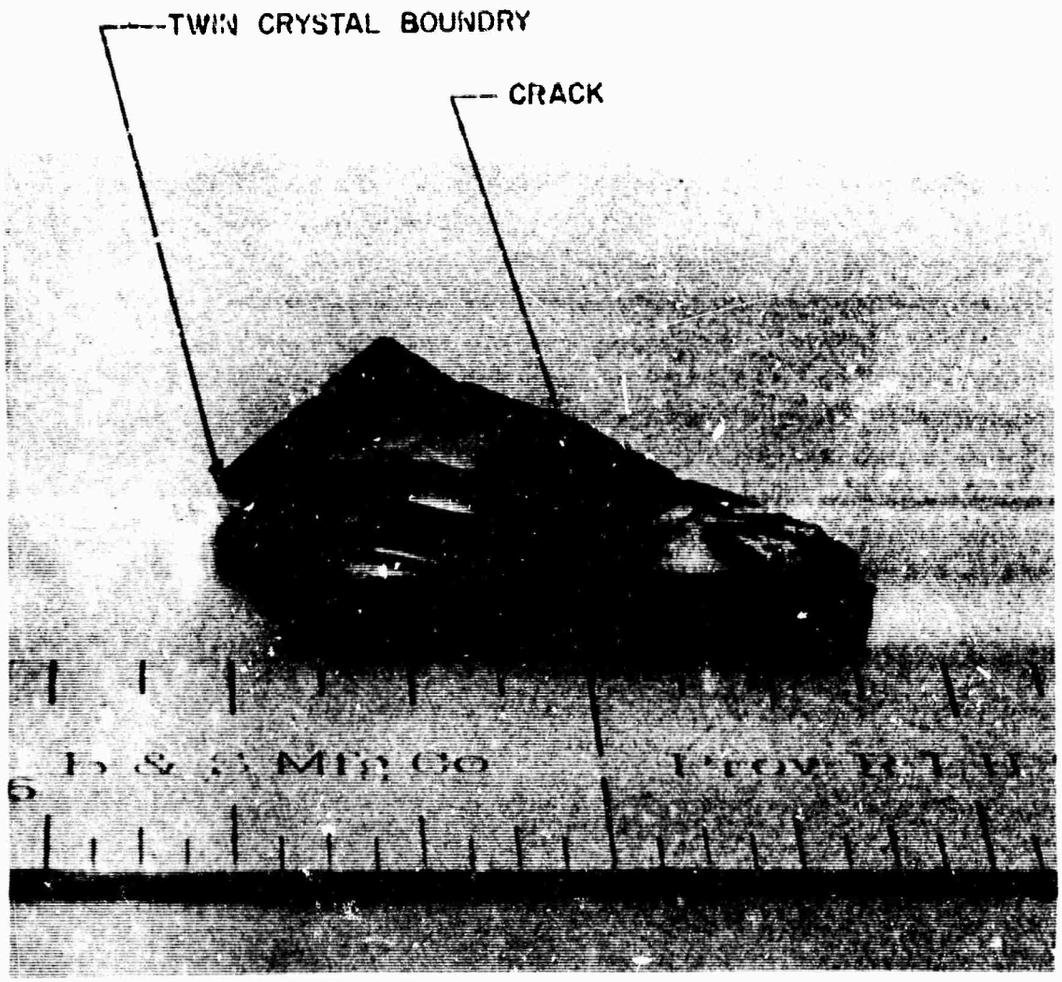

FIG. 30 - PHOTOGRAPH OF LITHIUM FERRITE CRYSTAL PLATE, UNCUT.

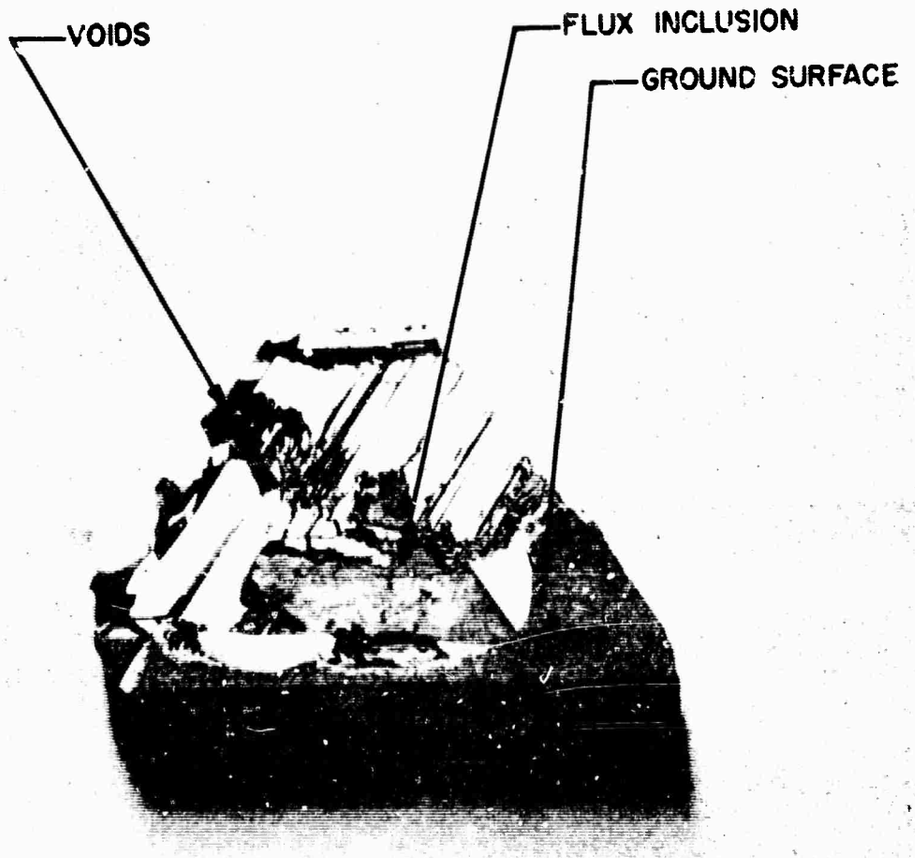

FIG. 31 – PHOTOGRAPH OF PARTIALLY GROUND LITHIUM FERRITE PLATE WHICH CRUMBLED ALONG GROWTH STRIATIONS EXPOSING FAULTY INTERIOR.

opposing parallel faces. Conducting surfaces of gold were deposited on these faces and a measure of the dc resistance taken. The following table is a summary of the results:

Batch No.	Iron/Lithium	Sample No.	Resistivity - Ohm/Cm
Li"F"-1	1.5	1	54. k
		2	9.3 k
		3	12 k - 8.5 k
		4	0.8 k
Li"F"-2	1.0	1	23.8 k
		2	40.2 k
		3	0.5 k - 0.78 k
Li"F"-3	2.0		No Yield
Li"F"-4	0.5	1	2.2 k
Li"F"-5	1.75	1	1.3 k

It should be noted that the resistivity measurements do not give conclusive indication of the best recipe; however, it appears that a value between 1.5 and 1 would be satisfactory. Using this information and other considerations such as crystal size and appearance, Mr. Lepore chose an intermediate ratio of 1.25 for the 7.5-10 kg batch. The final yield, designated Li"F"-6, weighed 250 mg and is shown in the photograph, Figure 32. Some of the larger octahedrons measured as much as 2 cm on an edge.

Two large crystals were sliced on planes normal to a pair of crystal faces ($\{111\}$ planes); however, the remaining large crystals were sliced parallel to the crystal faces because as it was learned the centers are usually of poor quality having flux inclusions and voids. The dc resistivity of these slices was measured by two methods. (1) between points on the same surface[8] and (2) between plane conductors deposited on opposite parallel surfaces. The resistivity from the first method varied, depending upon the position of the probes on the surface of the crystal, and is therefore reported by a range of values. The

8. L.B. Valdes, "Resistivity Measurements on Germanium for Transistors," Proc. IRE, Vol. 42, pp. 420-427; February, 1954.

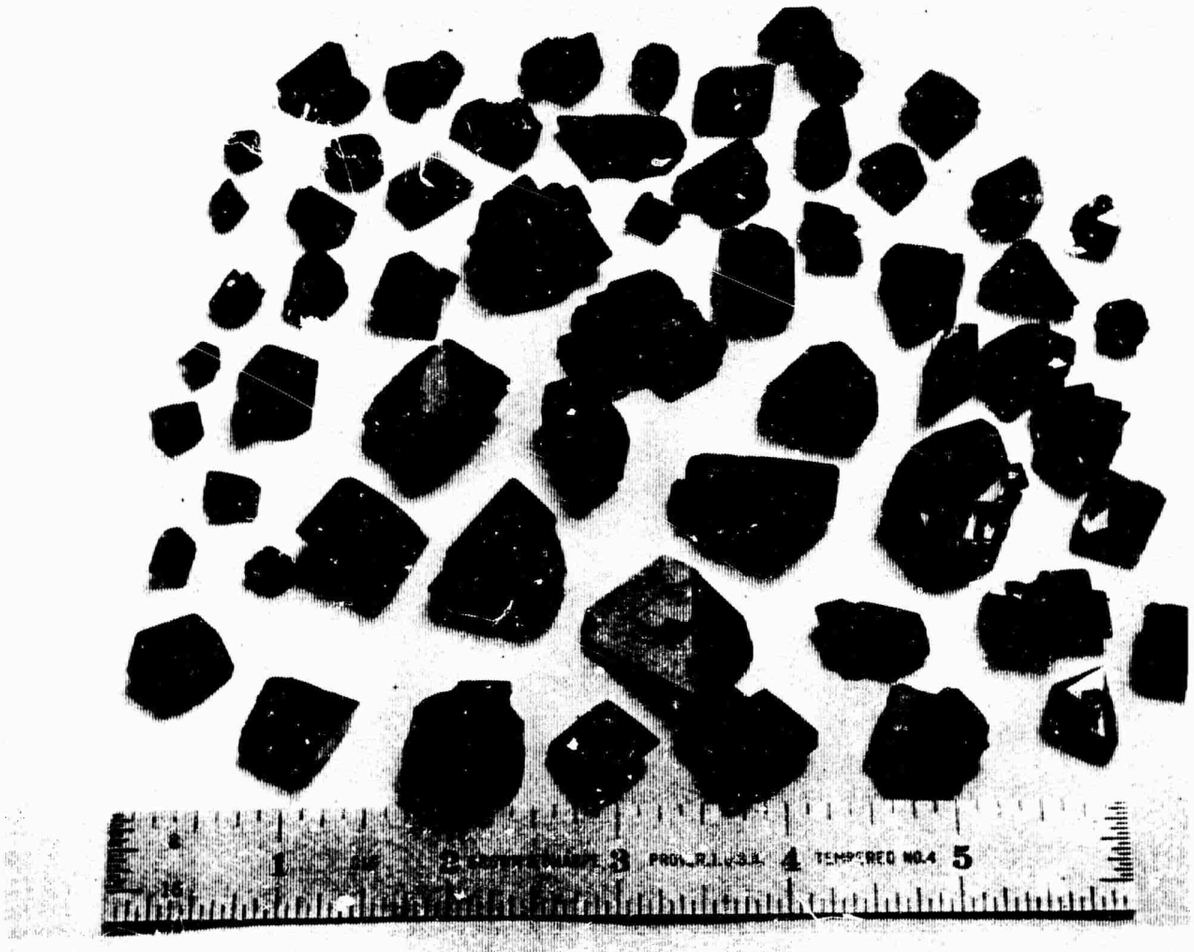

FIG. 32 – PHOTOGRAPH OF UNCUT LITHIUM FERRITE – OCTAHEDRON CRYSTALS

resistivity from he second method which measures through the total volume of the sample depends upon the specimen being sound and hon.ogeneous for reliability. On several samples it was found that a thin strata of flux produced a very low value of resistivity. These data were not used. The following table summarizes the dc resistivity measurements on Li"F"-6:

Sample No.	Resistivity Ohm-cm	Measurement Method
1	1330-2000	Between Points
2	220- 330	Between Points
3	386	Between Planes
4	1524	Between Planes
5	310	Between Planes

The dc resistivity of Li"F"-6 has proved to be an order of magnitude smaller than expected after the measurements on the crystals from the small experimental batches #2 through #5. These values of resistivity predict a high RF loss tangent which was verified by cavity measurements of several samples at C-band. The measurements were made at 5.5 GHz and gave loss tangents of 0.13 to 0.14 and dielectric constants of 15.4 to 16.7.

The need for additional study in the growth of single crystal lithium ferrite was obviously indicated; however, since we were not in a position to support such a program it was decided to go ahead with the planned experiments to demonstrate, if possible, the applicability of lithium ferrite to the high power phase shifter.

Experiments to reduce the linewidth and loss characteristics of lithium ferrite, using the various methods outlined by Nielsen[9] et al,

---

9. J.W. Nielsen, D.A. Lepore, J. Zneimer and G.B. Townsend, "Effect of Mechanical, Thermal and Chemical Treatment of the Ferrimagnetic Resonance Line Width on Lithium Ferrite Crystals," J. Appl. Phys., Vol. 33, p. 1379; March (Supplement) 1962.

have met with some measure of success as will be described. Although the improvements are relatively minor with regard to phase shifter operation an important benefit of this work is to indicate the reason Li"F"-6 failed to exhibit the expected narrow linewidth and the approach which might be taken in growing higher quality lithium ferrite. It also shows the importance of highly polished surfaces in reducing the linewidth of ferrite components.

A sample of Li"F"-6, 0.090" square and 0.418" long was subjected to four operations to reduce its linewidth and loss tangent. After each test the sample was centered in a test section of C-band waveguide on which insertion loss measurements were made. The results of these data are given in Figure 33(a) through (e). The curves (a) and (b) show that polishing all surfaces of the rough cut sample improves linewidth from 130 oersteds to 110 oersteds. To test the possibility that lattice disorder was contributing to the linewidth, the sample was heated to 710°C in air for two hours followed by controlled cooling for 4 hours to 580°C, at which time the oven was cut off and allowed to cool over night. Curves (b) and (c) show that an increase in linewidth resulted which may be explained by (1) the roughened surface observed after the heat treatment or (2) too rapid cooling from 580°C after the oven was turned off. The third test was a heat treatment in an oxygen atmosphere at 1000°C to oxidize the residual free iron in the ferrite. The oven was held at a temperature slightly above 1000°C for 2-1/2 hours and then was permitted to cool rapidly (30 minutes) to 750°C followed by controlled cooling for 5 hours to 470°C, at which time the oven was turned off to cool over night. Curves (c) and (d) show a subsequent improvement in linewidth from 125 to 90 oersteds.

The final operation was a heat treatment of the lithium ferrite in a boat filled with lithium carbonate to test the possibility of lithium deficiency in the crystal. The oven was held at temperatures above 750°C for two hours followed by controlled cooling for 5-1/2 hours to

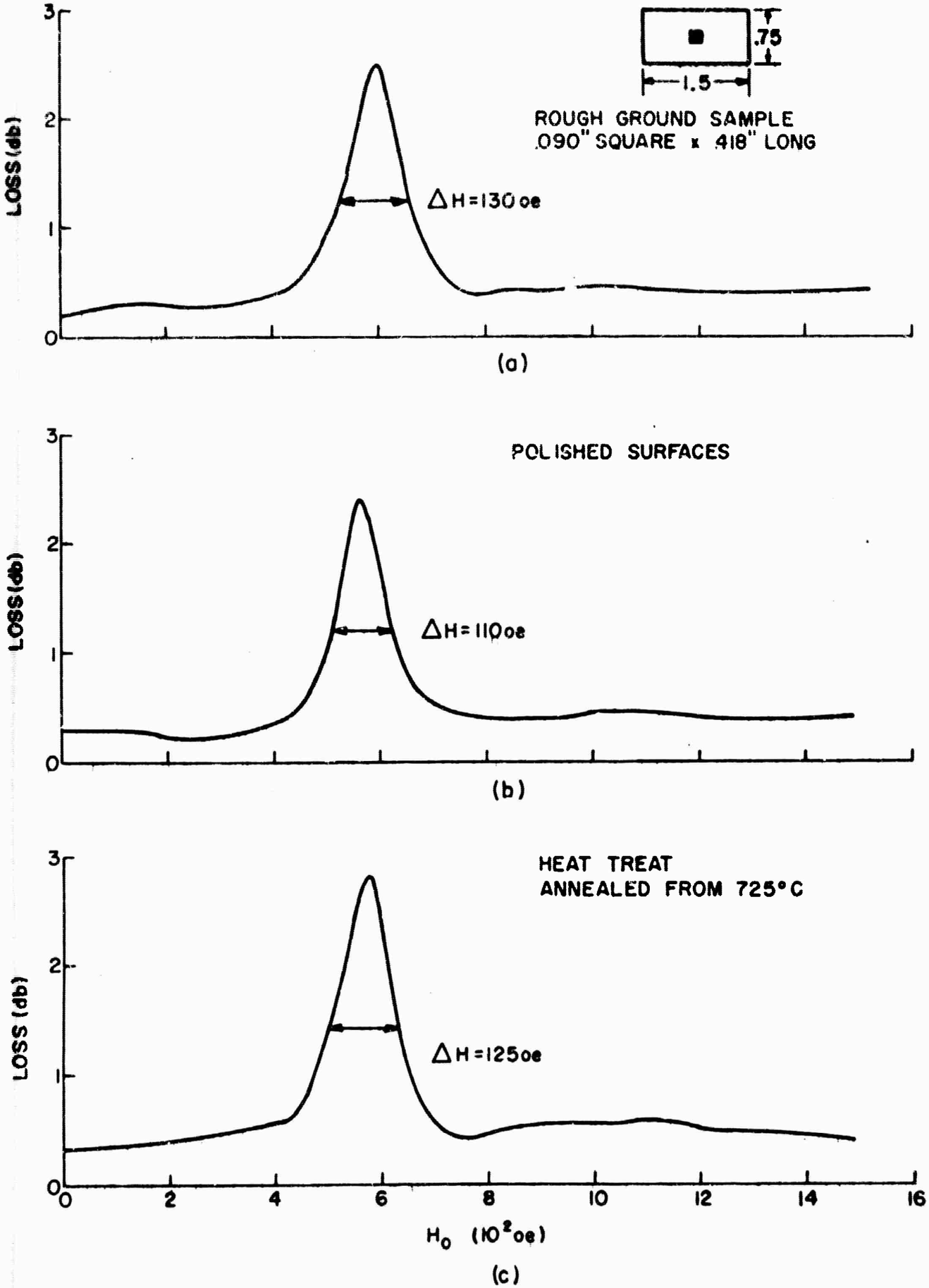

FIG.33 a,b,c – INSERTION LOSS AT 6.5 GHz OF LiF-6 SHOWING THE EFFECT OF SUCCESSIVE OPERATIONS ON LINE WIDTH.

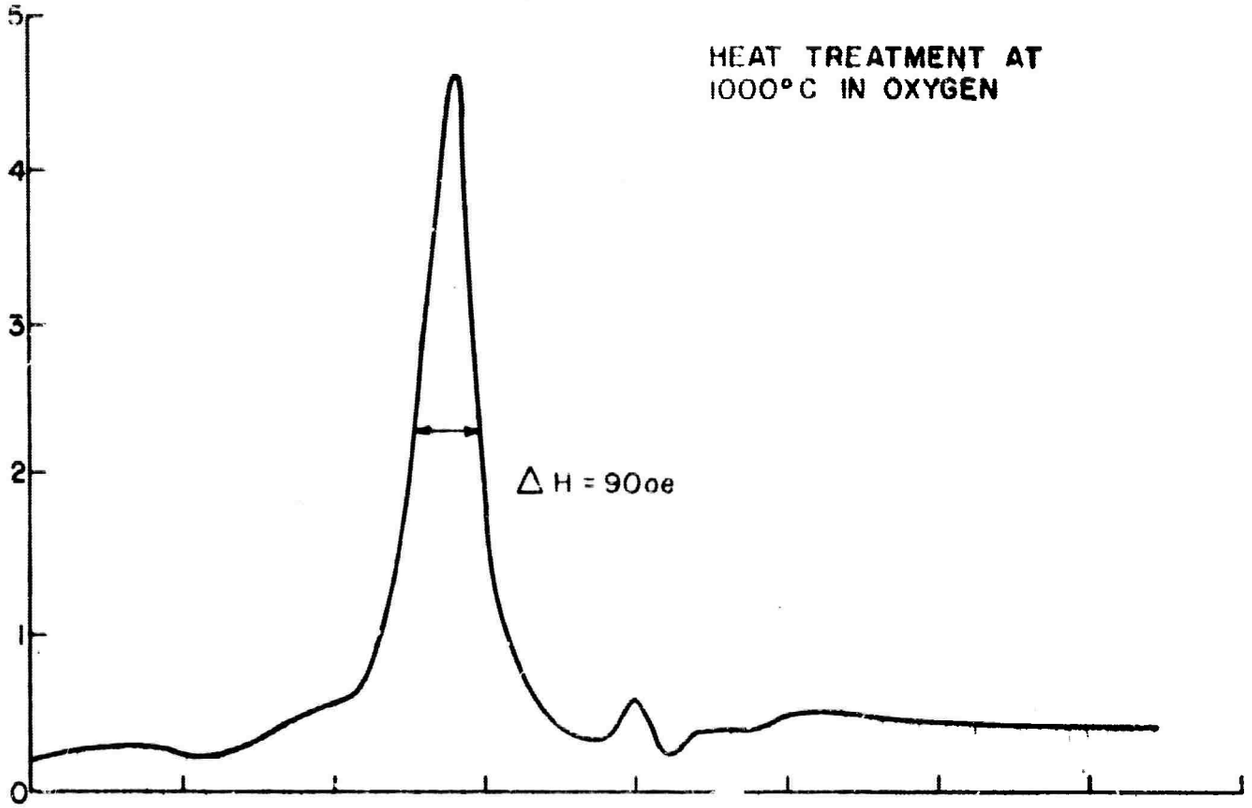

(d)

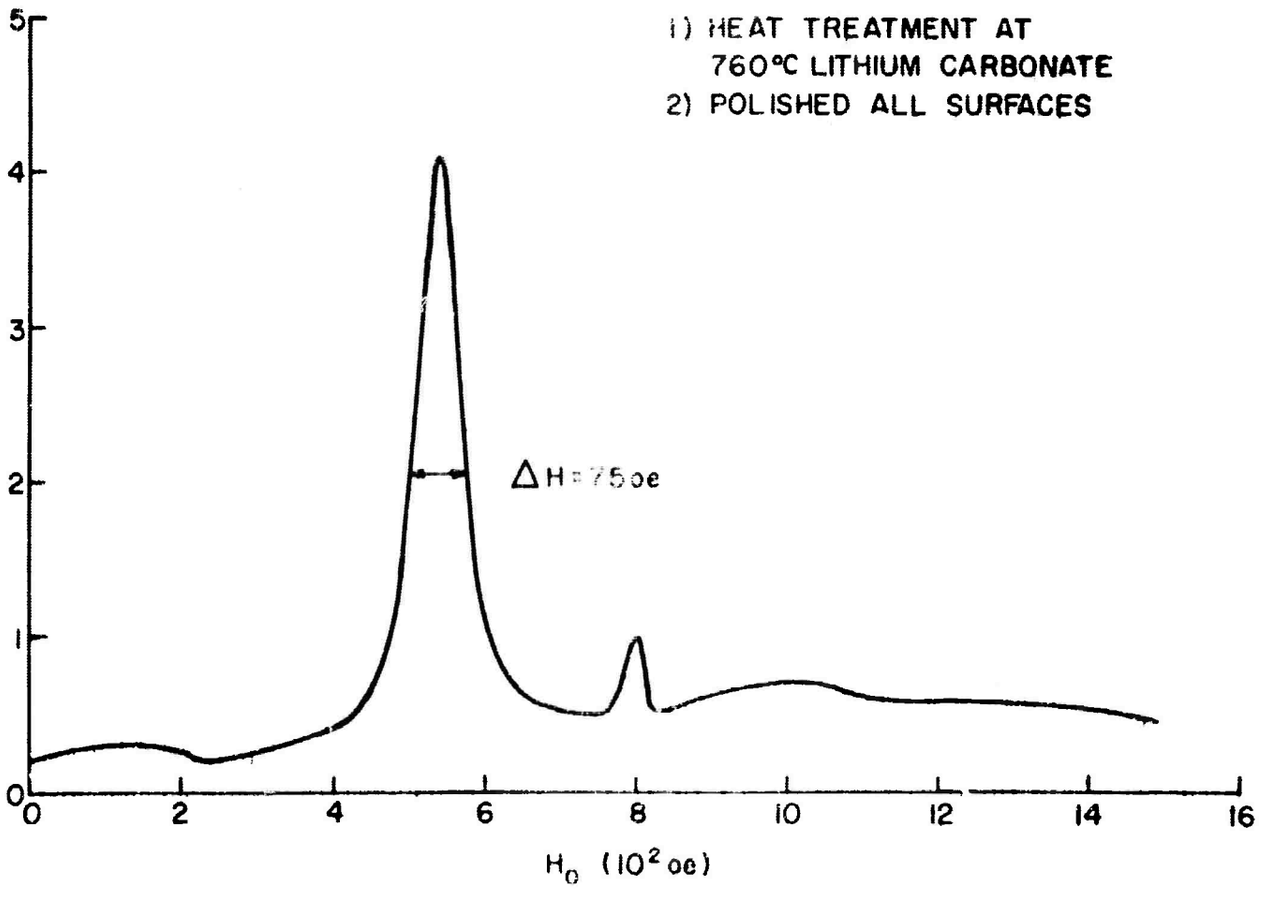

(e)

FIG.33d,e – INSERTION LOSS AT 6.5 GHz OF LiF–6 SHOWING THE EFFECT OF SUCCESSIVE OPERATIONS ON LINE WIDTH

515°C at which time it was turned off to cool over night. Since the surface was quite rough after this treatment, the specimen was polished with Linde A 0.3 micron* alumina abrasive. Curves (d) and (e) show a reduction in linewidth from 90 to 75 oersteds. It is felt that the improvement in this last test is principally attributable to polishing. In reviewing the sequence of the above experiments it is felt that polishing of the crystal surfaces should have been performed last in which case the several operations could have been appraised independently. The conclusions which are suggested by these tests are that oxidation of divalent iron coupled with strain relief and ordering of the crystal lattice by annealing plus surface polishing of the crystal has resulted in reducing the linewidth from 130 oersteds to 75 oersteds. In the region of interest above ferrimagnetic resonance it was observed that no reduction of insertion loss was realized indicating that the dielectric loss tangent was unchanged by the various operations; therefore, continued pursuit along this course was considered unproductive and was discontinued.

Insertion loss measurements were made on 12 samples with 0.090" square cross section and from 0.328" to 0.500" long. The linewidths of the rough cut samples ranged from 40 to 130 oersteds. Measurements at Airtron on 17 small spheres from the same batch gave linewidths from 3 to 50 oersteds; the linewidth of 12 of these was less than 15 oersteds. It is not the intent here to show a disagreement in the linewidth measurements but to report the values observed since it is known that linewidth measured on a rod sample is several times larger than that measured on a small sphere as pointed out by Dillon.[10]

The loss and phase shift characteristics at RF peak powers ranging from 1 mw to 1 kw are given in Figure 34 for a rod of

---

* Trademark, Union Carbide Corporation

10. J. F. Dillon, Jr., "Magnetostatic Modes in Discs and Rods," J. Appl. Phys , Vol. 31, p. 1605; September 1960 (see pp. 1612-1613)

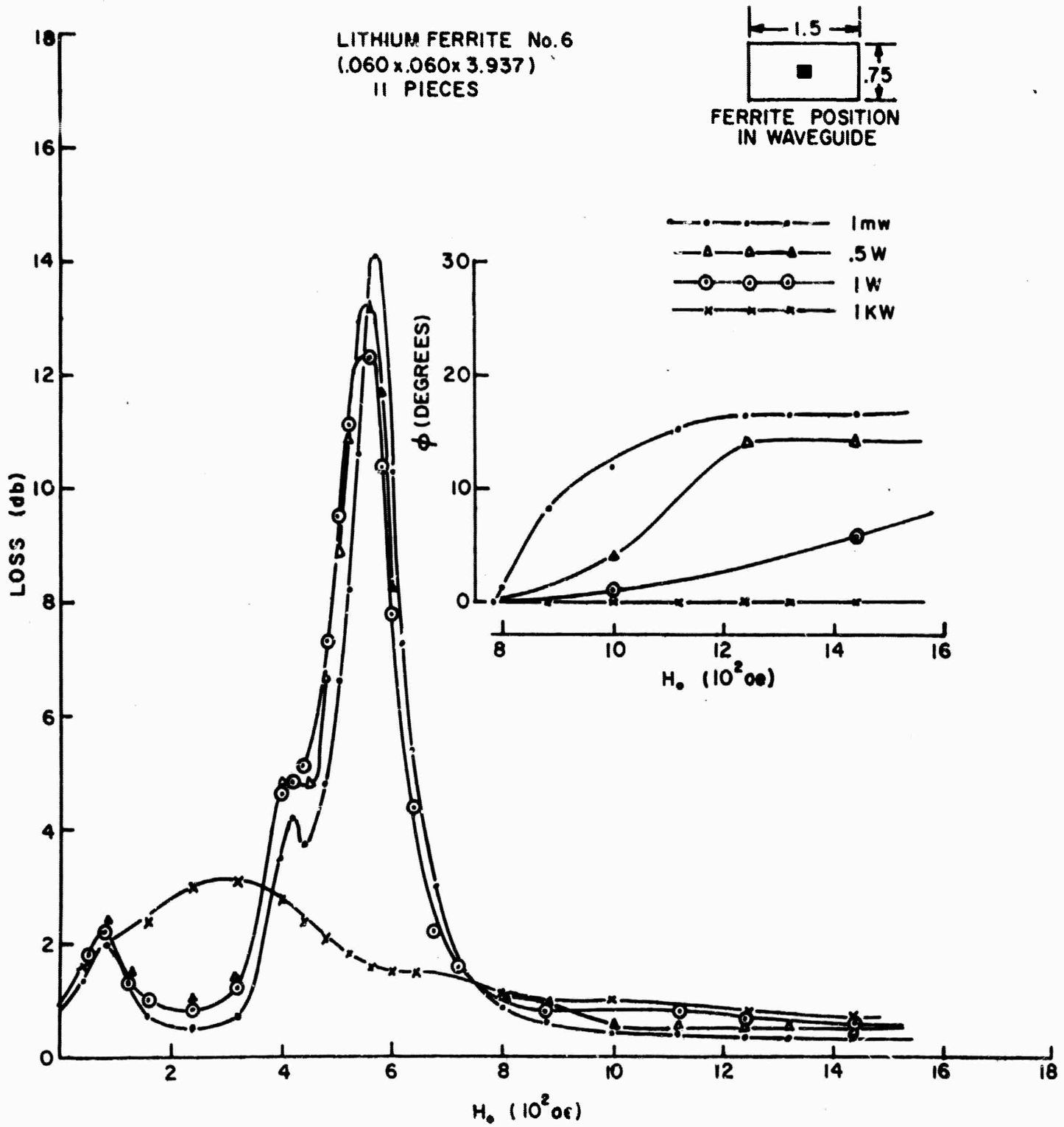

FIG.34-LOSS AND PHASE SHIFT AS A FUNCTION OF R.F. PEAK POWER AT 6.5 GHz

0.060" x 0.060" cross section and 3.937" long. The rod was fabricated from 11 pieces of single crystal lithium ferrite. The effect of increasing power is seen to decrease the ferrimagnetic resonance peak and to diminish the phase shift activity to zero at 1 kw peak power. These results are explained in the work by Fletcher and Silence cited in Section II. Applying the appropriate parameters to the curves, Figure 15, one finds that operation with lithium ferrite should be restricted to magnetic fields above 1050 oersteds to avoid the unwanted high-power effects. These calculations are based upon a zero magnetic anisotropy for lithium ferrite; however, experimental data to be discussed next indicates that the anisotropy field is at least 235 oersteds. If the rods of lithium ferrite used in the experiment could be sliced through the center of the crystal normal to the $\{111\}$ plane, then the existence of the anisotropy field would be an advantage because it would be oriented in the phase shifter parallel to the applied dc magnetic field. Since the rods had to be cut parallel to the $\{111\}$ plane, the anisotropy was a disadvantage; therefore, it is estimated that the operating region of magnetic field should be greater than 1200 oersteds to avoid the unwanted high-power effects.

An examination of the low power phase shift in Figure 34 shows that the activity has ceased for magnetic fields above 1200 oersteds. According to the generalized curves, phase shift activity at low RF power should not vanish as indicated by the experiment. The observed loss in activity is at least partially explainable by the reduction in binding of energy to the ferrite due to the normal decrease in permeability with increased magnetic fields in the region above resonance. It is, however, the relatively small cross sectional dimensions which make the decrease in permeability so critical to binding. Intuitively, this problem could be dealt with by using a larger ferrite cross section. Experimental proof of such a solution was attempted using a rod 0.180" square which was assembled with fourteen pieces of the 0.090" square rods described earlier in this section. Phase shift could not be measured because the insertion loss on the high side of resonance was too

high (8 db) as seen in Figure 35. It was not possible to slice 0.180" square rods because the remaining lithium ferrite was too small.

An examination of the insertion loss measurements of the 12 individual samples revealed that ferrimagnetic resonance for the two samples cut on planes normal to the crystal faces occurred at magnetic fields approximately 350 oersteds smaller than that of the remaining 10 samples, which were sliced parallel to the crystal faces. The effect of the magnetic anisotropy of lithium ferrite is thus demonstrated where in the first two samples the external magnetic field was applied in the easy direction, parallel to the anisotropy field and in the hard direction for the remaining 10 samples. In lithium ferrite the direction of the anisotropy field is more complex than in uniaxial anisotropy materials because the easy direction of magnetization is normal to every face and consequently, the hard direction cannot be orthogonal to the easy direction. Nevertheless, in order to estimate the magnitude of the anisotropy field we have chosen to use the following uniaxial relationship to solve for H_a:

$$H_a = -\frac{2H_E + H_H}{2} + \sqrt{\left(\frac{2H_E + H_H}{2}\right)^2 + H_H^2 - H_E^2} \quad .$$

Thus, H_a = 235 oersteds at 6.5 GHz when H_E = 540 oersteds is the magnetic field required for resonance when applied in the easy direction, and H_H = 902 oersteds is the magnetic field required for resonance when applied in the hard direction.

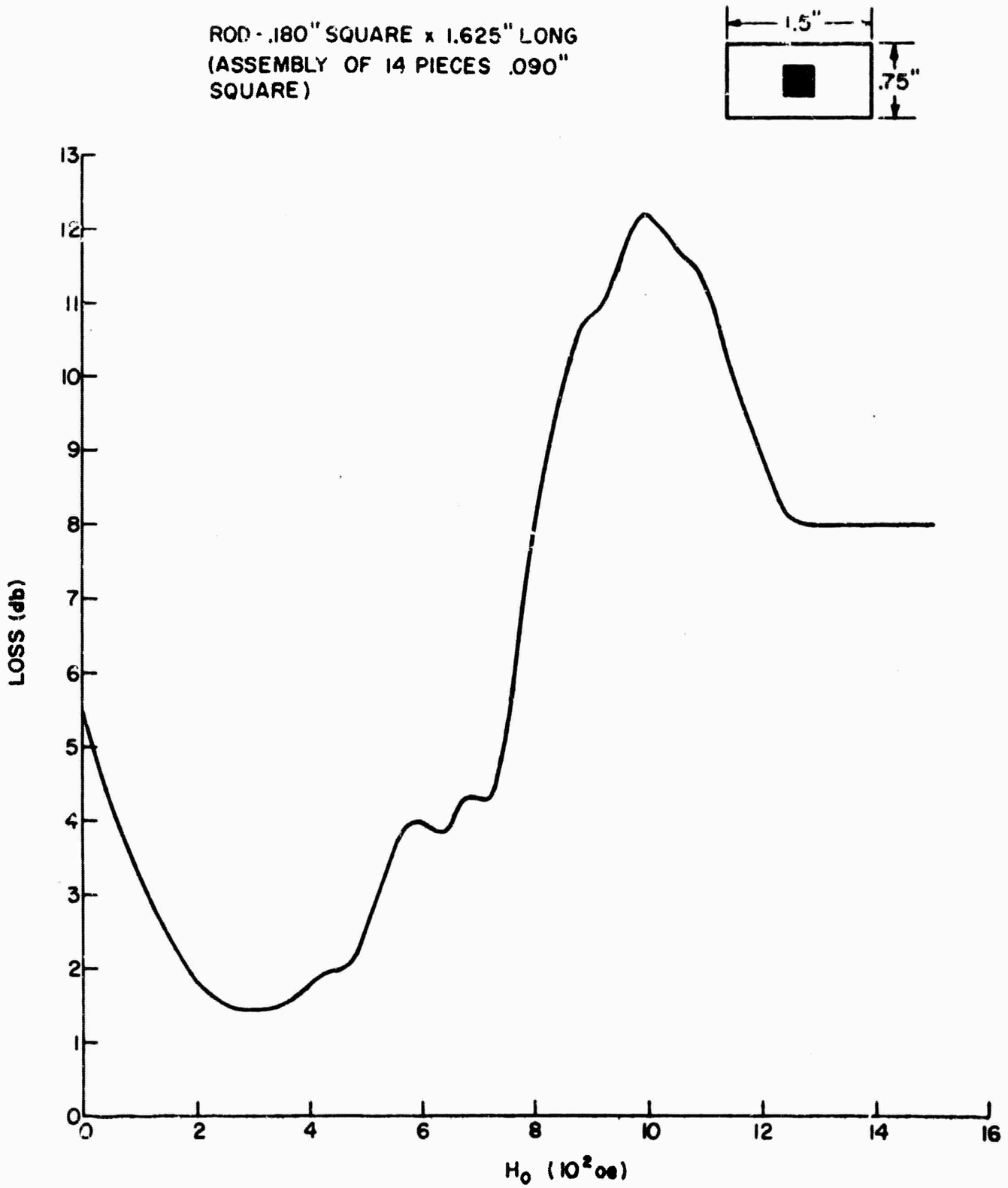

FIG.35 —INSERTION LOSS AT 6.5 GHz OF LiF—6

VI. HIGH POWER TESTS

The ability to maintain phase shift and loss characteristics at high power levels by operating at magnetic fields specified by Fletcher and Silence[4] was tested with three ferrite materials: single crystal lithium ferrite, nickel ferrite (TT2 111), and nickel-cobalt "W" (A-130). A block diagram of the test apparatus is shown in Figure 36. The peak power obtainable with this setup was 25 kw to 100 kw. To prevent heating of the ferrite during the test, the average power was limited to a maximum of 2 watts by using a 20 Hz repetition rate and a 1 μs pulse width. In the setup phase shift was measured by noting the shift of the null on the slotted line. The difference in signal amplitude between the input and output of the phase shifter provided a measure of the loss characteristics.

The variation of loss and phase shift with increasing power in lithium ferrite has been given in Figure 34, where it was observed that phase shift vanished for power above 1 kw. A discussion of these results has been given in Section V.

The configuration of six parallel rods discussed in Section IV was tested at peak power levels, 1 mw to 100 kw at 6.5 GHz. The results of loss and phase shift are given in Figure 37. It may be observed that phase shift appears to level off between 800 and 1000 oersteds; however, at 1000-1100 oersteds phase shift resumes at a relatively uniform rate. Referring to Figure 15 one may calculate that the magnetic field above which high power effects are avoided is approximately 1120 oersteds which coincides with the field where phase shift is resumed in Figure 37.

The third ferrite tested at high power was A-130. Again using Figure 15 one may calculate that the field required to avoid high power effects is 1090 oersteds; however, this value includes the anisotropy field which is 4500 oersteds for A-130. The implication is that high power effects should not be observed in A-130 at 6.5 GHz. These

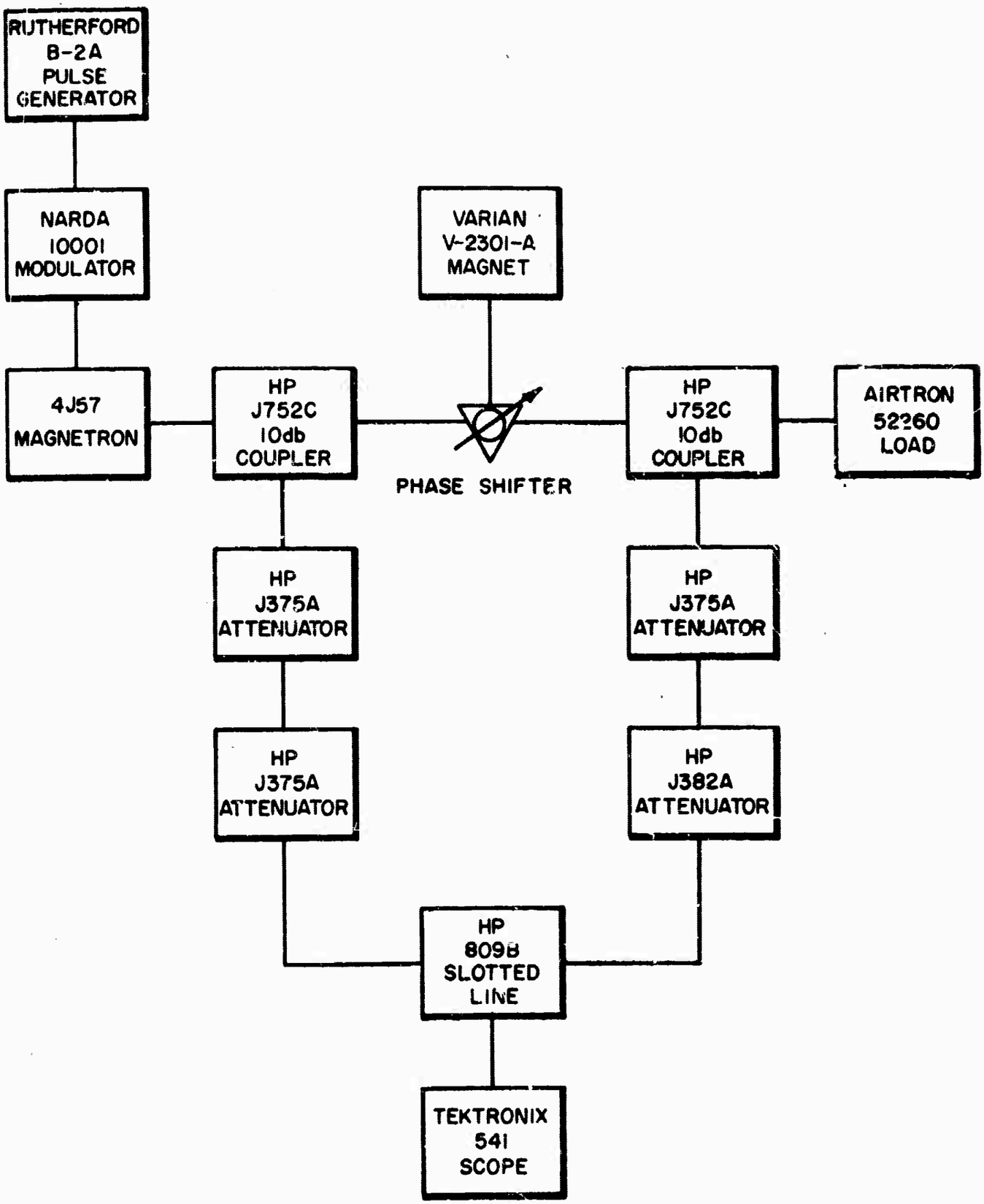

FIG. 36 – BLOCK DIAGRAM OF HIGH POWER PHASE SHIFT TEST SETUP

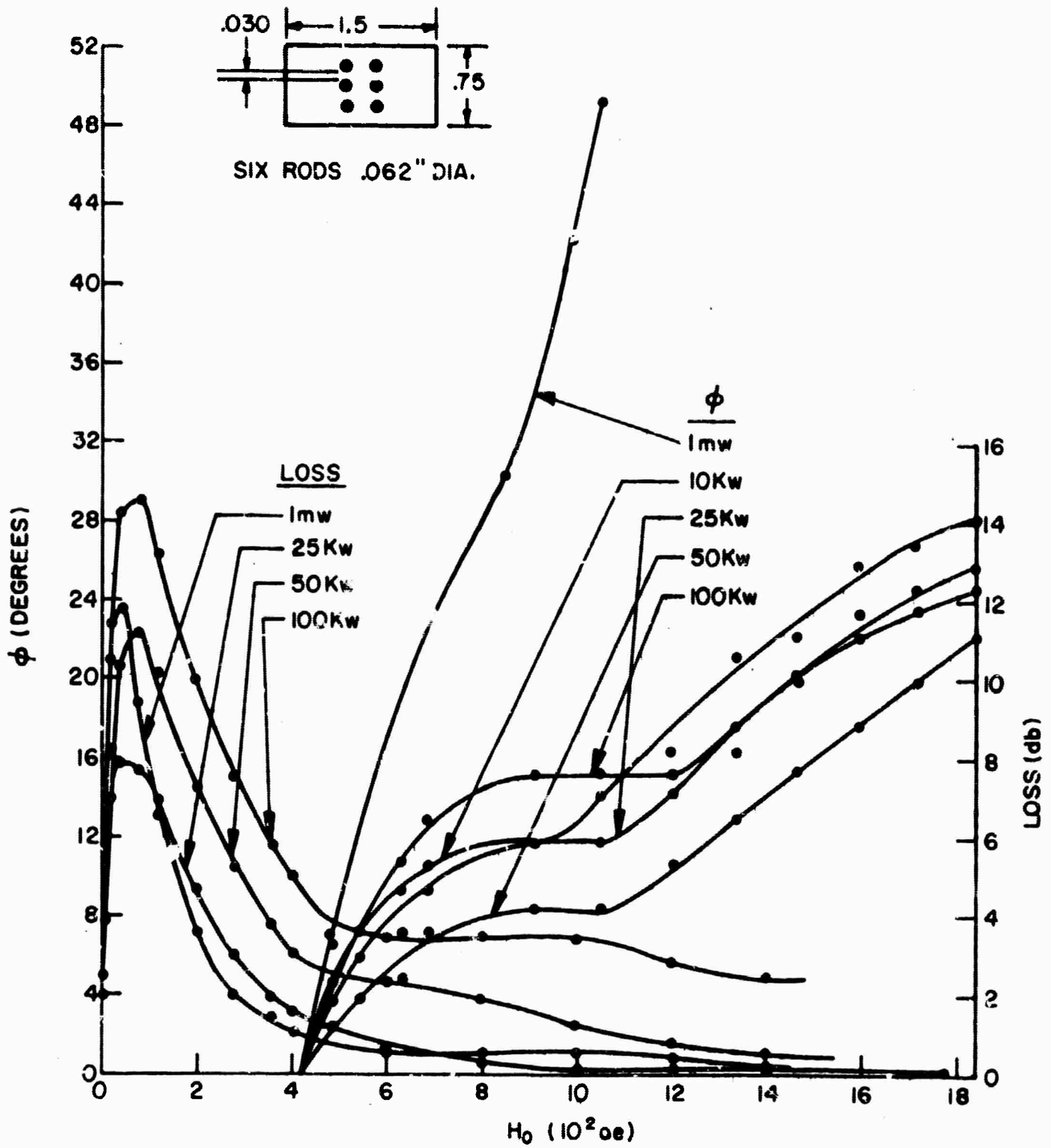

FIG. 37 – LOSS AND PHASE SHIFT FOR SIX RODS OF TT-211 AT 6.5 GHz AS A FUNCTION OF RF PEAK POWER

predictions are verified by the measured data presented in Figure 38. With the exception of the very low power (1 mw) measurements both loss and phase shift show only minor changes with increased power. Unfortunately the loss for A-130 is so large that it would not be acceptable for a practical phase shifter. In the test on A-130 it was found necessary to place a 0.005 inch thick mylar tape between the ferrite rod and the bottom wall of the waveguide to prevent voltage breakdown at high power.

An alternative to using the mylar tape is to deposit gold on the bottom side of the ferrite and then solder the ferrite to the waveguide. The particular advantages to this technique are that soldering provides a means of permanently mounting the ferrite and a good thermal path for cooling.

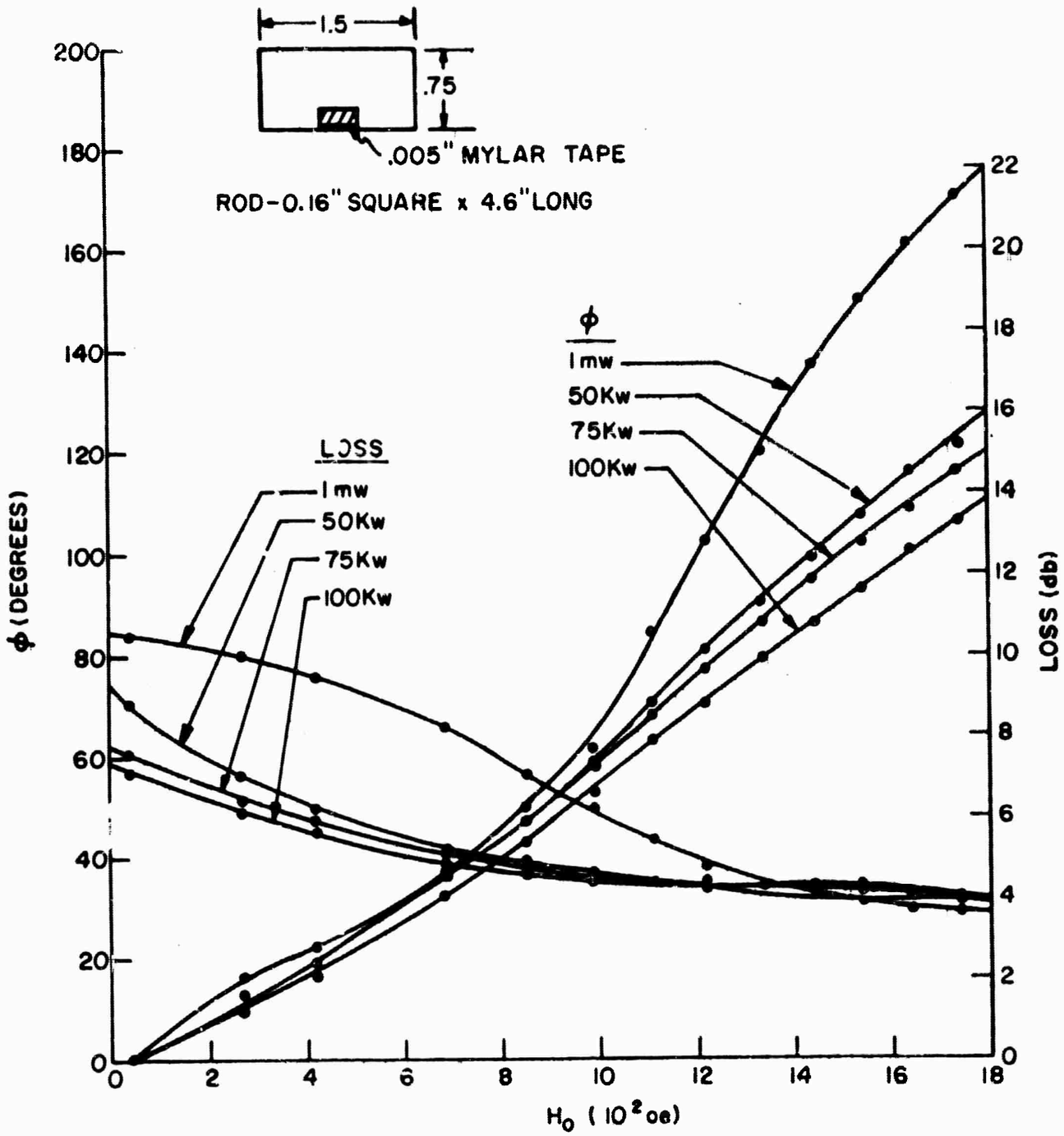

FIG. 38 - LOSS AND PHASE SHIFT OF ONE ROD OF A-130 AT 6.5 GHz AS A FUNCTION OF RF PEAK POWER

VII. CONCLUSIONS AND RECOMMENDATIONS

The experimental phases of this program which are reported here and in the Semiannual Technical Report have shown that reciprocal phase shift is achievable at C- and X-band in a waveguide configuration using longitudinal magnetic fields in the region above ferrimagnetic resonance. The tests at RF peak powers from 25 kw to 100 kw have demonstrated that the nonlinear losses which may occur at high power can be avoided by operating at magnetic fields above a prescribed value which is determined by the saturation moment and linewidth of the ferrite and the frequency of operation. As a general rule, the applied magnetic field cannot be less than $\frac{\omega}{2\gamma}$, where ω is the operating frequency and γ is the gyromagnetic ratio; thus, at 6.5 GHz and 10 GHz the applied fields must be greater than 1160 oersteds and 1785 oersteds, respectively. There then exists a practical upper limit on the frequency of operation determined by the maximum bias field achievable with permanent magnets.

The maximum applied field as defined above may, however, be reduced by the amount of anisotropy field in the ferrite provided that the two fields are parallel. Care must be taken to choose a ferrite that does not have an excessively large anisotropy field; otherwise, there will be the handicap of reduced activity per unit length, and hence a longer structure would be needed for the desired phase shift.

During this program the most practical ferrites were polycrystalline hexagonal materials. With present technology these materials can be produced in pieces sufficiently large for phase shifter application. Unfortunately not all of the desired material characteristics are found in a single ferrite type. The planar ferrite, HP-42A, proved to have the highest figure of merit as predicted by its narrow linewidth; however, it had to be operated at 21.75 GHz because its anisotropy field was so large. The uniaxial ferrite, A-130, was operated at 6.5 GHz as proposed and demonstrated satisfactory

phase shift characteristics at 25 to 100 kw peak power, but its figure of merit was too low because of excessive insertion loss. The high loss is attributable to both high dielectric loss and high magnetic loss. Because of the large linewidth of A-130 (2000 oersteds) the operating region had to be far above resonance; thus, the usable phase shift activity was considerably reduced from its maximum value.

The foregoing discussion indicates two approaches which might be taken to develop the desired ferrite. The first is to reduce the dielectric loss, the magnetic loss and the linewidth of A-130. The second approach is to modify HP-42A to achieve similar planar ferrites having an anisotropy field of 2000 oersteds for C-band operation and 2700 oersteds for X-band operation. A reduction in the linewidth of HP-42A without reducing the anisotropy field would make that material suitable for application to a high power K-band phase shifter.

The work with single crystal ferrites has pointed out several shortcomings which preclude their application to phase shifters in the near future. In particular, their small size introduces a difficult assembly job which is made more complex by the fact that the anisotropy fields of the numerous pieces must be in close alignment; otherwise, the linewidth of the ensenble is greatly increased. Although the art of growing large single crystals of lithium ferrite was extended by this program, most of the crystals were of poor quality and all of the samples tested showed a high loss tangent due to a low bulk resistivity.

The work with single crystal Zn-Y was restricted by the small quantity available and by the same poor quality exhibited by lithium ferrite. It should be noted, however, that a significant amount of development is presently being done with Zn-Y by A. Tauber* and the progress of this work merits attention. In the event that large pieces of high quality Zn-Y are produced, its application to K-band high power phase shifters should be examined.

---

*U.S. Army Electronics Laboratories, Fort Monmouth, New Jersey.

DOCUMENT CONTROL DATA - R&D

(Security classification of title, body of abstract and indexing annotation must be entered when the overall report is classified)

1. ORIGINATING ACTIVITY *(Corporate author)*
Advanced Technology Corporation, 1830 York Road
Timonium, Maryland

2a. REPORT SECURITY CLASSIFICATION
Unclassified

2b. GROUP

3. REPORT TITLE
HIGH POWER FERRITE PHASE SHIFTER

4. DESCRIPTIVE NOTES *(Type of report and inclusive dates)*
Final Technical Report

5. AUTHOR(S) *(Last name, first name, initial)*
Wentworth, Frederick L.

6. REPORT DATE
October, 1965

7a. TOTAL NO. OF PAGES
78

7b. NO. OF REFS
10

8a. CONTRACT OR GRANT NO.
AF 30(602)-3495

b. PROJECT NO.
ARPA Order No. 550

c. TASK
Program Code No. 4730

d.

9a. ORIGINATOR'S REPORT NUMBER(S)

9b. OTHER REPORT NO(S) *(Any other numbers that may be assigned this report)*

10. AVAILABILITY/LIMITATION NOTICES

11. SUPPLEMENTARY NOTES

12. SPONSORING MILITARY ACTIVITY
Rome Air Development Center,
Air Force Systems Command
Griffiss AFB, New York

13. ABSTRACT

Theoretical estimates of phase shifter performance as a function of material parameters are presented by examining the results obtained from the small perturbation model used by Button and Lax and from the fully ferrite loaded, parallel plane waveguide model used by Suhl and Walker. The extension of Suhl's theory on nonlinear effects at high power by Fletcher and Silence is applied to relate the material parameters and operating frequency to the magnetic field required to avoid high power subisidiary resonance effects. Experiments designed to demonstrate the relationship of phase shift and loss characteristics to material parameters and configuration for longitudinally magnetized ferrites in rectangular waveguide are described. Polycrystalline ferrites with both cubic and hexagonal structures are examined. Of the hexagonal materials, both uniaxial and planar types with oriented anisotropy fields are discussed. The experimental work leading to the growth of extremely large single crystals of lithium ferrite and their electrical and magnetic properties are reported Experiments which reduced the linewidth of lithium ferrite samples by heat treatment and polishing are described. High power tests to 100 kw peak are reported for waveguide configurations containing (1, single crystal lithium ferrite; (2) polycrystalline cubic structure, nickel ferrite; and (3) polycrystalline hexagonal structure nickel-cobalt "W" ferrite with its magnetic anisotropy oriented parallel to the applied magnetic field. These high power tests demonstrate that the nonlinear high power effects can be avoided by operating at magnetic fields above ferrimagnetic resonance as prescribed by Fletcher and Silence.

DD FORM 1 JAN 6[illegible] 1473

14. KEY WORDS	LINK A		LINK B		LINK C	
	ROLE	WT	ROLE	WT	ROLE	WT
Phase Shifters - Development						
Ferrites - Electromagnetic properties						

INSTRUCTIONS

1. ORIGINATING ACTIVITY: Enter the name and address of the contractor, subcontractor, grantee, Department of Defense activity or other organization *(corporate author)* issuing the report.

2a. REPORT SECURITY CLASSIFICATION: Enter the overall security classification of the report. Indicate whether "Restricted Data" is included. Marking is to be in accordance with appropriate security regulations.

2b. GROUP: Automatic downgrading is specified in DoD Directive 5200.10 and Armed Forces Industrial Manual. Enter the group number. Also, when applicable, show that optional markings have been used for Group 3 and Group 4 as authorized.

3. REPORT TITLE: Enter the complete report title in all capital letters. Titles in all cases should be unclassified. If a meaningful title cannot be selected without classification, show title classification in all capitals in parenthesis immediately following the title.

4. DESCRIPTIVE NOTES: If appropriate, enter the type of report, e.g., interim, progress, summary, annual, or final. Give the inclusive dates when a specific reporting period is covered.

5. AUTHOR(S): Enter the name(s) of author(s) as shown on or in the report. Enter last name, first name, middle initial. If military, show rank and branch of service. The name of the principal author is an absolute minimum requirement.

6. REPORT DATE: Enter the date of the report as day, month, year, or month, year. If more than one date appears on the report, use date of publication.

7a. TOTAL NUMBER OF PAGES: The total page count should follow normal pagination procedures, i.e., enter the number of pages containing information.

7b. NUMBER OF REFERENCES: Enter the total number of references cited in the report.

8a. CONTRACT OR GRANT NUMBER: If appropriate, enter the applicable number of the contract or grant under which the report was written.

8b, 8c, & 8d. PROJECT NUMBER: Enter the appropriate military department identification, such as project number, subproject number, system numbers, task number, etc.

9a. ORIGINATOR'S REPORT NUMBER(S): Enter the official report number by which the document will be identified and controlled by the originating activity. This number must be unique to this report.

9b. OTHER REPORT NUMBER(S): If the report has been assigned any other report numbers *(either by the originator or by the sponsor)*, also enter this number(s).

10. AVAILABILITY/LIMITATION NOTICES: Enter any limitations on further dissemination of the report, other than those imposed by security classification, using standard statements such as:

(1) "Qualified requesters may obtain copies of this report from DDC."

(2) "Foreign announcement and dissemination of this report by DDC is not authorized."

(3) "U. S. Government agencies may obtain copies of this report directly from DDC. Other qualified DDC users shall request through _____."

(4) "U. S. military agencies may obtain copies of this report directly from DDC. Other qualified users shall request through _____."

(5) "All distribution of this report is controlled. Qualified DDC users shall request through _____."

If the report has been furnished to the Office of Technical Services, Department of Commerce, for sale to the public, indicate this fact and enter the price, if known.

11. SUPPLEMENTARY NOTES: Use for additional explanatory notes.

12. SPONSORING MILITARY ACTIVITY: Enter the name of the departmental project office or laboratory sponsoring *(paying for)* the research and development. Include address.

13. ABSTRACT: Enter an abstract giving a brief and factual summary of the document indicative of the report, even though it may also appear elsewhere in the body of the technical report. If additional space is required, a continuation sheet shall be attached.

It is highly desirable that the abstract of classified reports be unclassified. Each paragraph of the abstract shall end with an indication of the military security classification of the information in the paragraph, represented as *(TS), (S), (C), or (U).*

There is no limitation on the length of the abstract. However, the suggested length is from 150 to 225 words.

14. KEY WORDS: Key words are technically meaningful terms or short phrases that characterize a report and may be used as index entries for cataloging the report. Key words must be selected so that no security classification is required. Identifiers, such as equipment model designation, trade name, military project code name, geographic location, may be used as key words but will be followed by an indication of technical context. The assignment of links, rules, and weights is optional.